MTOR COMPLEX 1: ACTIVATION AND THE NEUROPATHOLOGICAL CONSEQUENCES OF PERSISTENT ACTIVITY

By
Po Yu (Jeff) Chen

A dissertation submitted to
Johns Hopkins University
in conformity with the requirements for
the degree of Doctor of Philosophy

Baltimore, Maryland
September 2013

ABSTRACT

Mammalian Target of Rapamycin (mTOR) forms two distinct protein kinase complexes termed mTOR complex 1 (mTORC1) and mTOR complex 2 (mTORC2) and reside in the center of complex cellular signaling networks that integrates extracellular stimuli and intracellular status to maintain cellular integrity and function. Proper regulation of mTORC1 signaling is required for organism development, function and aging. Persistent increases in mTORC1 activity are associated with diseases such as cancer, diabetes and neurodegeneration. Here we examine how mTORC1 is activated in neurons, and the neuropathological consequences of persistent increase of mTORC1 signaling.

Ras homology enriched in brain 1 (Rheb1) is an immediate early gene and a small GTPase that contributes to mTORC1 signaling. Characterization of a conditional Rheb1 knockout (KO) mouse line, demonstrates Rheb1 is essential for mTORC1 signaling. Biochemical studies show Rheb1 is enriched in synaptic vesicle fractions. myc-Rheb1 (S16H) immunoprecipitation from the forebrains of conditional over-expresser mice show enrichment for ubiquitinylated proteins, selective synaptic proteins and synaptic vesicle associated proteins. Pharmacological modulation studies in cultured neurons provide a model of Rheb1's contribution to mTORC1 activation through group I metabotropic glutamate receptors (mGluR1/5) and proteosomes.

Conditional expression of myc-Rheb1 (S16H) provides a mouse model to examine the consequences of persistent activation of mTORC1 in brain. Behavioral studies reveal prominent reduction of social motivation and reduced locomotor activity in response to amphetamine treatment. Pharmacological and biochemical analysis of the mTORC1 signaling cascade in the striatum of the mutant mice reveals inhibition of dopamine D1 receptor signaling in combination with altered activities in Protein phosphatase 1 (PP1), Protein phosphatase 2A (PP2A) and dopamine- and cyclic AMP- regulated phosphoprotein (DARPP-32). Preliminary electrophysiological studies support the hypothesis that persistent mTORC1 signaling inhibits D1 dopamine receptor effects on corticostriatal plasticity. As D1 dopamine receptors provide an important reward signal in brain, these studies suggest that reduced social motivation may be linked to failure of this behavior to evoke reward.

These results provide molecular insights to mTORC1 activation with relevance for neurological diseases.

Thesis Advisor: Dr. Paul F. Worley

Second Reader: Dr. Richard L. Huganir

ACKNOWLEDGMENTS

First and foremost I would like to thank Paul Worley for welcoming me into his laboratory and entrusting me with such interesting and challenging projects. His generous support for my research and passion for science are genuinely inspiring. I am grateful for his mentorship and guidance in science and life.

I would like to thank my thesis committee members, Richard Huganir, David Linden and Rajini Rao, for their support and encouragements. Their positive outlook, curiosity for science and willingness to help are exemplary of their characters and leadership in science. I would like to emphasize the great environment that Richard Huganir, the Director of the Neuroscience Department, has established for the students.

I would also like to acknowledge many talented expert collaborators that I have had the fortunate opportunity to work with. Alena Savonenko, David Linden, Joo Min Park, Rachel Green, Karen Wehner, Seyun Kim and Solomon Snyder at Johns Hopkins University. Ron Petralia and Shmuel Muallem at NIH. Karen Szumlinski at UCSB. They have contributed significantly to my growth scientifically and personally.

I would like to thank all the members of the Worley who supported me and made my thesis work possible. Especially Jia Hua Hu, Meifang Xiao and Wenchi Zhang, their work ethic and scientific integrity are truly exceptional. I would also like to thank the CMM graduate program, and Neuroscience office staff for their support and help making JHU a wonderful place to be.

I would also like to thank Thomas Tuschl for his mentorship and all of the contributions to my scientific career.

Lastly, I would like to thank my family and friends who supported me. I would like to acknowledge my friends at JHU for making the tough days easier and making the good days even more enjoyable. I would like to thank my friends outside of JHU for their support. I would like to especially thank my mom and dad, my parents in-law and brothers and sisters in-law for their love and support. Most importantly I would like to thank my wife, Gloria, for her unconditional love, support and understanding throughout the years. All of my achievements are possible because of her.

TABLE OF CONTENTS

LIST OF FIGURES

CHAPTER 3:

CHAPTER 1:

General Introduction

Importance of understanding the cellular mechanisms underlying mTOR signaling.

The ability to adapt to environmental changes has contributed to the success of living organisms in evolution. Factors that influence anabolism and catabolism in cells include the abundance of oxygen, availability of nutrients, changes in stress and energy levels. These influences ultimately determine the survival, and proliferation of the organism. Cellular mechanisms that integrate environmental cues and controls cellular functions accordingly ensure the cell's survival, function and proliferation. Mammalian Target of Rapamycin (mTOR) is a protein kinase that resides in a complex signaling network, and integrates extra-cellular and intra-cellular cues to regulate cellular functions. Thus, it is not surprising that genetic mutations of the components in the mTOR signaling network or deregulation of the network are associated with diseases such as diabetes, various forms of cancer, lysosomal disease, Alzheimer's Disease (AD), Autism Spectrum Disorder (ASD), Schizophrenia, Fragile X syndrome, Huntington's Disease (HD) among others (Hoeffer and Klann). Studying the functions and the impact of alterations to the mTOR signaling network will facilitate the advancement in fundamental biology and therapeutics development.

Discovery and characterization of mTOR

Rapamycin, an anti-proliferative compound, is a macrolide produced by Streptomyces Hygroscopicus. In studying the mechanisms of Rapamycin, *Target of Rapamycin -1 and -2 (TOR1, TOR2)* was identified through a genetic screen assay in yeast (Cafferkey, Young et al.). A single gene *FRAP1* encodes the ortholog of *TOR* in mammals termed mammalian Target of Rapamycin (mTOR) and is ubiquitously expressed throughout the body including nervous, vascular and immune systems (Maiese, Chong et al.) (Sabatini, Erdjument-Bromage et al.). Characterization studies of mTOR revealed that it is a 2549 amino acid serine/threonine kinase that belongs to the phosphoinosidite 3-kinase protein (PI3K) kinase family (Hoeffer and Klann). More than 20 Huntington, Elongation Factor 3, A subunit of P2A, TOR1 (HEAT) domain repeats are located in the N-terminal domain of the protein and mediate protein-protein interactions to form distinctive protein complexes. Biochemical and genetic studies have shown that mTOR exists in two distinct protein complexes. mTOR complex 1 (mTORC1) associates with a protein termed Raptor, while mTOR complex 2 (mTORC2) associates with Rictor protein. In addition to these two protein partners of mTOR, many other proteins identified are shared between the complexes (Laplante and Sabatini). The C-terminal portion of mTOR contains several functional domains. FKBP12-rapamycin binding domain (FRB) is bound by the FKBP-rapamycin complex and represents the rapamycin dependent site for mTOR activity (Hoeffer and Klann). Two Transactivation/transformation domain-associated protein (TRRAP) domains that are conserved with PIKK family members are necessary for mTOR catalytic function. The catalytic or kinase (KIN) domain encodes the serine/threonine kinase activity of mTOR (Hoeffer and Klann). The

aforementioned domains are integral for mTOR to function in an ever-expanding complex signaling network (Laplante and Sabatini).

Rheb and its role in mTOR signaling

Ras homology enriched in brain 1 (Rheb1) was identified as an immediate early gene induced by neuronal activity in the brain (Yamagata, Sanders et al.). Characterization studies demonstrated Rheb is a small GTPase that is a member of the Ras superfamily, and most highly conserved with hRas (Yamagata, Sanders et al.). Sequence analysis identified a CAAX box at the carboxylterminal sequence allowing for post-translational farnesylation modification (Yamagata, Sanders et al.). While studies have shown Tuberous sclerosis complex (Tsc) coupling to mTOR activity, the mechanism remained elusive until through a genetic epistasis screens in Drosophila melanogaster revealed that Rheb1 was positioned down-stream of Tsc and up-stream of mTOR (Saucedo, Gao et al.). Follow up studies indicated Tsc complex is comprised of Tsc1 and Tsc2 proteins and possesses GTP Activating Protein (GAP) activity that inactivates mTOR through Rheb1 (Zhang, Gao et al.). Tsc negatively regulates mTOR by increasing the intrinsic GTPase rate of Rheb1 yielding a GDP bound Rheb1 that is incapable of stimulating mTOR kinase activity. Through an alanine mutagenesis screen approach it was revealed that serine 16 mutation to histidine reduces the GAP activity of Tsc on Rheb1, thus resulting in an increase in mTOR kinase activity (Tabancay, Gau et al.).

mTOR signaling pathway

mTOR signaling has been a focus for investigators encompassing all biological research as it is involved in many aspect of cellular functions. The initiation of the signaling cascade can be triggered by intra- and extra-cellular stimuli. However, the canonical signaling usually starts from a cell surface receptor such as receptor tyrosine kinase (RTK) or insulin receptor. Ligand binding triggers dimerization of the RTK and activates Phosphoinositide 3-kinase (PI3K). PI3K phosphorylates Phosphatidylinositol 4,5-bisphosphate (PIP2) to Phosphatidylinositol 3,4,5-triphosphate (PIP3), and thus activates Phosphoinisitol dependent kinase 1 (PDK1). This step is also regulated by a phosphatase, Phosphatase and tensin homolog (Pten). PDK1 activates Akt, which in turn regulates targets that are involved in cell survival, metabolism and proliferation. Akt also inhibits Tsc, which is a negative regulator of Rheb1. GTP bound Rheb1 activates mTOR kinase that phosphorylates target proteins such as eukaryotic translation Initiation Factor 4E binding protein (eIF4E-BP) and s6 kinase (s6K) to increase protein translation and inhibit autophagy (Laplante and Sabatini). In addition to the extra-cellular stimuli, other cellular status changes can also influence mTOR activity through other proteins. Studies have shown hypoxia and energy depletion inhibits mTOR through Tsc by Hypoxia Induced Factor 1 (HIF1) and 5' adenosine monophosphate-activated protein kinase (AMPK) correspondingly. On the contrary, amino acids can elevate mTOR kinase activity through an alternate PI3 kinase, VPS34 (Gulati, Gaspers et al.).

One effecter of the mTORC1 signaling is the ribosomal subunit s6, which facilitates the scanning mechanism of the 40S subunit to mediate translation

initiation. Concomitantly, mTORC1 phosphorylation of eukaryotic Initiation 4E binding protein (eIF4E-BP) relieves its inhibition of the methyl-7-Guanosine (m7G) cap binding of eukaryotic Initiation Factor 4E. Once relieved of its inhibition, eIF4E interacts with eukaryotic initiation factor 4G (eIF4G) and Poly A Binding Protein (PABP) to form the initiation complex and allows for protein translation to take place (Laplante and Sabatini). Moreover, previous investigations have demonstrated that the activity of eukaryotic Elongation Factor 2 Kinase (eEF2K) to be inhibited by s6 kinase (s6K), a target of the mTORC1 pathway. As the result of the activation of mTORC1 enhancing translation initiation while inhibiting eEF2K to facilitate elongation, the global translation kinetics is enhanced. The canonical activation of mTOR pathway has been well established. Activation of receptors such as Insulin receptor or Trk B receptor leads to a kinase cascade activation of mTORC1 through PDK1, PI3K class I, Akt, Tsc1/2 and Rheb-1 (Han, Chen et al.) (Figure 1).

mTOR and synaptic plasticity

Neuronal networks established by the electrochemical communications between synapses of neurons provide a "platform" for memory storage and retrieval. The physiological responsiveness of the synaptic connections is plastic and can be modified through activity experiences. Plasticity is often defined temporally with observable alterations occurring from seconds to years. Long-term depression (LTD) is an activity-dependent reduction in the efficacy of the synapses, while Long-term potentiation (LTP) is an activity-dependent enhancement of the synaptic transmission (Malenka and Bear). LTP and LTD are influenced by neuronal

surface receptors and channels including N-methyl-D-aspartate receptors (NMDA-R), α–amino-3-hydroxy-5-methyl-4-isoxazolepropionic acid receptors (AMPA-R), brain-derived neurotrophic factors (BDNF) and dopaminergic and metabotropic glutamate receptors (mGluRs) (Malenka and Bear). The mTOR signaling pathway is coupled to these receptors to contribute to their signal output (Hoeffer and Klann). Rapamycin has been a key reagent for establishing evidences of mTOR signaling in synaptic plasticity. Seminal studies in *Aplysia* showed rapamycin blocked translation elongation and long-term facilitation (Yanow, Manseau et al.) (Carroll, Warren et al.). These findings provided a hint that TOR signaling participates in long-lasting plasticity changes. Studies in rats showed that rapamycin blocks late phase NMDA-R dependent hippocampal LTP (L-LTP) suggesting a requirement for protein translation mediated by mTOR to facilitate long lasting LTP (Tang and Schuman) (Cammalleri, Lutjens et al.). Rapamycin and pharmacological inhibition of PI3K upstream of mTOR is also reported to block mGluR-dependent-LTD (Banko, Hou et al.). Moreover depotentiation by activation of mGluR in the hippocampus is reported to be mTOR dependent (Zho, You et al.). These studies indicate that mTOR signaling participates in different physiological outcomes to contribute to synaptic plasticity in the brain.

mTOR and neuropathological diseases

mTOR is a key integrator that resides in the center of signaling networks that influence many aspects of cellular homeostasis, and crucial for cellular integrity (Maiese, Chong et al.). In the central nervous system, unregulated mTOR signaling is

highly correlated with devastating neurodegenerative diseases. An increase in the phosphorylation levels of mTOR and its substrates has been observed in AD, suggestive that these substrates may promote AD progression (Griffin, Moloney et al.). One exemplary substrate is p70S6K which associates with hyperphosphorylated tau and neurofibrillary accumulation in AD patients (Maiese, Chong et al.). Furthermore, mTOR inhibits autophagy, which mediates the degradation of amyloid beta (Aß) (Wu, Feng et al.). Thus elevated mTOR activity may lead to the accumulation of Aß in neurons. Increased accumulation of Aß is toxic to neurons, microglias and other lymphocytes and leads to neurodegeneration (Shang, Chong et al.). Mutations and functional disruptions in *TSC1/2*, *PTEN* and *EIF4E* result in over-activated mTOR signaling and have been demonstrated to lead to autism-relevant behaviors (Sawicka and Zukin) (Sharma, Hoeffer et al.) (Schellenberg, Dawson et al.). Studies in a mouse model of Fragile X syndrome (FXS), the most common heritable form of intellectual disability, also show elevated mTOR signaling at the synapse (Sharma, Hoeffer et al.). These findings suggest dysregulation of mTOR signaling as a unified pathological mechanism in FXS, Tsc1/2, and Pten associated autism syndromes.

Schizophrenia is another neuropsychiatric illness that is linked to altered signaling in the mTOR pathways. Schizophrenia is associated with multiple genetic mutations and leads to a complex trait disorder manifested by severe neurocognitive dysfunctions (Emamian). Genetic and biochemical studies have converged on disrupted Akt signaling as one of the most consistent correlates in humans and mouse models (Emamian). Since Akt resides upstream of mTOR in the

signaling pathway, reduction in Akt signaling results in reduced mTOR signaling. The reduction in mTOR signaling is in contrast to the other neurocognitive diseases where mTOR signaling is elevated. However, recent findings that elevated mTOR signaling leads to a negative feedback to Akt may reconcile the conflicting observations (Guertin, Stevens et al.).

CHAPTER 2:

Materials and Methods

Antibodies and drugs

The following antibodies previously described are commercially available from Cell Signaling: anti-ps6 (S240/244) (rabbit polyclonal), anti-s6 (rabbit polyclonal), anti-p4EBP (T37/46) (rabbit polyclonal), anti-4EBP (rabbit polyclonal), anti-pAkt (S308) (rabbit polyclonal), anti-pAkt (S473) (rabbit polyclonal), anti-pTsc2 (T1462) (rabbit polyclonal), anti-Tsc2 (rabbit polyclonal), anti-pmTOR (T1442) (rabbit polyclonal), anti-mTOR (rabbit polyclonal) anti-Actin (rabbit polyclonal), anti-pMek (S217/221) (rabbit polyclonal), anti-pMapk (T202/Y204) (rabbit polyclonal), anti-pDarpp32 (T34) (rabbit polyclonal), anti-Rag (rabbit polyclonal), anti-Rab7 (rabbit polyclonal), anti-Rab4 (rabbit polyclonal), anti-pGSKa/b (S21/9) (rabbit polyclonal), anti-PP2A (rabbit polyclonal), anti-pPP1a (T320) (rabbit polyclonal), anti-STIM1 (rabbit polyclonal), anti-STIM2 (rabbit polyclonal), anti-Pan Calcineurin A (rabbit polyclonal), anti-myc (rabbit polyclonal), anti-myc (mouse monoclonal), anti-HA (rabbit polyclonal), anti-DAT (rabbit polyclonal). The following antibodies previously described are commercially available from Santa Cruz: anti-Shank3 (rabbit polyclonal); from Sigma Aldrich: anti-DRD1 (rat monoclonal); from Abcam: anti Lamp2 (rat monoclonal), anti-pPP2A (Y307) (rabbit polyclonal); from Millipore: anti-FK1 (mouse monoclonal), anti-DRD2 (rabbit polyclonal); from ENZO life sciences: anti-RPT6 (rabbit polyclonal); GE healthcare: anti-rabbit IgG-HRP, anti-mouse IgG-HRP, anti-rat. IgG-HRP. Anti-

NR1 (rabbit polyclonal), anti-NR2A (rabbit polyclonal), anti-GluR1 (rabbit polyclonal), anti-GluR2 (mouse monoclonal) were kind gifts from Richard L. Huganir.

MK-801, Bay 36-7620, MPEP hydrochloride, AIDA, Bay K 8644 (R), Bay K 8644 (S), MG132 and Gadolinium chloride are commercially available through Tocris. Rapamycin was purchase from LC laboratories. BDNF was purchased from Invitrogen. Insulin and amino acids were from Sigma.

Constructs

The full-length and modified Orai, STIM1, Rheb1 constructs have been described previously (Yuan, Zeng et al.) (Zou, Zhou et al.). Full length Darpp32 construct was purchased from Addgene.

Cell Culture and Transfection

Cell culture and transfection techniques were carried out as previously described in (Park, Park et al.) (Zou, Zhou et al.). Neuronal cultures from embryonic day 18 (E18) pups were prepared as reported previously (Rumbaugh, Sia et al.), with minor alterations. For biochemistry experiments, 0.4 x 10^6 neurons were added to each well of a 6-well plate (Corning) coated with poly-L-lysine. Growth medium consisted of NeuroBasal (Invitrogen) supplemented with 1% fetal bovine serum (Hyclone), 2% B27, 1% Glutamax (Invitrogen), 100U/mL penicillin, and 100U/mL streptomycin (Invitrogen). Neurons were fed twice per week with glia conditioned growth medium. HEK293T cells were maintained in Dulbecco's

modified Eagle's medium (DMEM) with Glutamax, containing 10% heat-inactivated fetal bovine serum (Invitrogen), 100U/mL penicillin, and 100U/mL streptomycin at 37ºC and 5% CO2.

Over-expression of plasmids method utilized liposome vehicles with Fugene 6 from Roche. Sinbis virus expression was prepared and carried out according to manufacturer's protocol (Invitrogen Cat: K750-01).

Immunoprecipitation assays

Indicated brain regions were dissected and lysis was carried out in ice cold 1% Triton-X 100 IP buffer (1 X PBS, pH 7.4, with 5 mM EDTA, 5 mM EGTA, 1 mM Na3VO4, 10 mM sodium pyrophosphate, 50 mM NaF, and 1% Triton X-100 containing Complete™ EDTA-Free protease inhibitors was added and vigorously vortexed) or RIPA buffer + 0.1% SDS (150 mM NaCl 1% NP-40 0.5%DOC (deoxycholic acid) 0.1% SDS, 50mM Tris PH 8.0 1 mM Na3VO4, 10 mM sodium pyrophosphate, 50 mM NaF, and Complete™ EDTA-Free protease inhibitors was added and vigorously vortexed) with . Lysate was sonicated and cleared by centrifugation. 50 µl of anti-myc coupled magnetic bead slurry (antibody coupling procedure was carried out according to manufacturer's protocol (Invitrogen Cat: 143.11D)) was added to 10 ml of supernatant and rotated overnight at 4°C. The magnetic beads were washed three times with ice-cold IP buffer. The protein samples were eluted with 100 µl of SDS loading buffer and analyzed by SDS-PAGE followed Western blotting or silver staining (Invitrogen Cat: LC6070). Harvard Taplin Mass Spectrometry Core Facility carried out Mass spectrometry analysis.

Sub-cellular fractionation assays

Sub-cellular fractionation assays were carried out as described (Hallett, Collins et al.)

Western Blotting on Brain Lysates

Western blot procedures were carried out as previously described (Zou, Zhou et al.). Brain extracts were made from indicated brain regions of mice (4weeks – 6 months old) with lysis buffer (2% SDS with proteinase and phosphatase inhibitors unless indicated otherwise). After quantification of the total amount of proteins in each sample, the samples were loaded into SDS-PAGE gels and blotted with various antibodies, according to standard Western blotting procedures.

Animal behavioral assays

Mice were generated on a mixed 129s6; C57BL6/J background and backcrossed with littermates for at least 5 generations. Male littermate mice were used as controls in all behavior tests. All procedures involving animals were under the guidelines of Johns Hopkins University Institutional Animal Care and Use Committee.

Behaviors were recorded by computer-based tracking systems (HVS Image Analysis VP-200, HVS Image, Hampton, England; Any Maze 4.72, Stoelting Co, Wood Dale, IL; Noldus, Ethovision 2.3.19, SR-LAB, San-Diego Instruments, CA, USA) and

scored when necessary by trained observers blind to genotype using computer-assisted data system.

Acute Slice Preparation and Treatment

Acute slice preparations were carried out as previously described (Wu, Petralia et al.). 8- to 9-week-old mice were anesthetized with isoflourane and decapitated upon disappearance of tail withdrawal reflex. The brain was removed and immediately submerged in ice cold dissection buffer containing: 2.6 mM KCl, 1.25 mM NaH_2PO_4, 26 mM $NaHCO_3$, 0.5 mM $CaCl_2$, 5 $MgCl_2$, 212 mM sucrose, and 10 mM dextrose. 300 μm coronal sections were made using a vibratome (VT 1200S; Leica, Nussloch, Germany). Only slices containing the hippocampus were used. Slices were recovered for 1 hr at 30°C in a reservoir chamber filled with ACSF containing: 124 mM NaCl, 3.25 mM KCl, 1.25 mM NaH_2PO_4, 26 mM $NaHCO_3$, 2 mM $CaCl_2$, 1 mM $MgCl_2$, and 11 mM dextrose. ACSF and dissection buffer were equilibrated with 95% O_2-5% CO_2. Slices were then placed in a 12 well culture plate with 500 μm mesh inserts in 1.8 ml of ACSF +/− Picrotoxin. The culture plate was covered loosely and maintained in a pre-equilibrated static treatment chamber (aerated with 95% O_2-5% CO_2) for ~10 hr at 30°C.

Electrophysiology

Electrophysiology procedures were carried out as previously described (Park, Park et al.). Field recording of excitatory postsynaptic potential (fEPSP) of hippocampal CA1 neurons of postnatal day (P)21-30 male mice as described with

minor modifications (Huber, Kayser et al.). mGluR-LTD was induced by an mGluR1/5 agonist, (R,S)-3,5-DHPG, for 5 min (50 or 100 μM), or by paired-pulse low-frequency stimulation (PP-LFS: 50 ms interstimulus interval, 1 Hz, for 15 min) in the presence of D-APV (50 μM). NMDAR-dependent LTD was induced by using 900 single pulses delivered at 1 Hz (Huber, Kayser et al.).

LTP was measured in Schaffer collateral-CA1 synapses in hippocampal slices derived from 8- to 10-weeks old male mice. Late-phase LTP (L-LTP) was induced by four trains of high-frequency stimulation (HFS) (100 Hz, 1 s) with 3 s of intertrain interval.

For recording, coronal brain hemislices were transferred to an interface type chamber, maintained at 32 ºC for 1hr, and perfused continuously with nominally magnesium free-ACSF at a rate of 4-5 ml/min to reliably activate the N-methyl-D-aspartate receptor (NMDAR) (Calabresi, Pisani et al.). The recording electrodes filled with 0.9 % NaCl were located in the dorsomedial striatum, as previously described (Citri and Malenka). Extracellular field recordings were evoked by stimulation of the white matters between the cortex and the striatum with a parallel bipolar electrode (FHC, Bowdoin, ME). The test stimulus intensity was adjusted to elicit 30 % of the maximal population spike (PS). Test stimuli were delivered every 30 sec with 0.1 msec pulse duration.

A high frequency stimulation protocol (HFS, three 3sec duration, 100 Hz frequency, 20 sec interval) was used to induce long-term potentiation (LTP) in the dorsomedial striatum (Calabresi, Pisani et al.). The stimulus pulse duration of HFS was 0.2 msec, which was two times stronger than the test stimulus. A low frequency

stimulation (LFS, 2Hz, 10min) protocol was used to depotentiate LTP caused by prior HFS (Calabresi, Pisani et al.). The stimulus pulse duration of LFS was 0.1msec. The amplitudes of the PS were normalized to baseline values (-5 min to 0 min) before HFS. The n reported in figures is the number of slices. In all cases except Figure 7E, slices were obtained from >3 mice. Recordings of WT mice in 8E that examined the effect of SKF38393 used slices from 2 mice.

Tissue Processing, Immunohistochemistry and Electron Microscopy

For immunohistochemistry, mouse brains were prepared by cardiac perfusion with cold PBS and 4% PFA followed by one-night post fixation in the same solution at 4°C. Fixed brains were dehydrated in 30% sucrose before proceeding to embedding for frozen section. Brain sections were blocked in 1% BSA/10% goat serum/0.3% Triton/PBS solution for 1 hour at RT, and stained with first antibodies diluted in 1% BSA/1% goat serum/0.3% Triton/PBS solution for overnight at 4°C. Secondary antibodies were diluted in PBS with 1% goat serum and incubated for 1 hour at RT.

For LFB staining, brain sections were stained in 0.1% Luxol Fast Blue solution as standard procedure and counter-stained with 0.5% eosin and 0.1% cresyl violet. Black Gold staining was performed as Manufacturer's instructions (Millipore).

For electron microscopy, mice were perfused with 2% glutaraldehyde/2% paraformaldehyde in 0.1 M cacodylate buffer. Corpus callosum and optic nerves were dissected and post-fixed overnight in the same fixative buffer. Tissues were then processed as standard procedure before photograph.

Surface biotinylation assays

Surface biotinylation assay was carried out as described (Park, Park et al.). Briefly, drug-treated cortical neurons were cooled on ice, washed twice with ice cold PBS++ (1X PBS, 1 mM CaCl2, 0.5 mM MgCl2) and then incubated with PBS++ containing 1 mg/ml Sulfo-NHS-SS-Biotin (Pierce) for 30 min at 4 °C. Unreacted biotin was quenched by washing cells three times with PBS++ containing 100 mM Glycine (pH 7.4) (briefly once and for 5 min twice). Cultures were harvested in RIPA buffer and sonicated. Homogenates were centrifuged at 132,000 rpm for 20 min at 4 °C. Fifteen % of supernatant was saved as the total protein. The remaining 85% of the homogenate was rotated with Streptavidin beads (Pierce) for 2 hr. Precipitates were washed with RIPA buffer three times (5 min each time). All procedures were done at 4 °C.

CHAPTER 3:

Persistent mTORC1 down regulates G protein signaling

Introduction

mTOR signaling resides at a node that coordinates cellular responses to hypoxia, energy, DNA integrity, stress, amino acids and extracellular signals. As any of these input changes in an aberrant manner, the mTOR integration pathway becomes mis-regulated, and diseases may arise. Examples of neurological diseases that are suggested to be associated with alteration in mTOR signaling pathway include Neurofibromatosis type 1, Hamartomas, Alzheimer's Disease, Huntington's Disease (Hoeffer and Klann). Most of the diseases associated with mTOR signaling are due to a "gain of function" of the pathway wherein negative regulators of the pathway are disrupted due to mutations.

Type 2 diabetes is a well-characterized disease arising from persistent mTOR signaling. Following the canonical extracellular signaling pathway; insulin binding to the insulin receptor leads to the activation of the receptor, which in turn activates Phosphoinositol 3-Kinase (PI3K). PI3K phosphorylates Phosphatidylinositol 4,5-bisphosphate (PIP2) and yields Phosphatidylinositol 3,4,5-triphosphate (PIP3) thus activating Phosphoinisitol dependent kinase 1 (PDK1). This step is regulated by a phosphatase, Pten, a gene often mutated in diseases such as cancer. PDK1 activates Akt, which is a regulator of cell survival, metabolism and proliferation. Akt also

inhibits the tuberous sclerosis complex (TSC1/2). TSC1/2 possesses GTP Activating Protein (GAP) function that inhibits a small GTPase Rheb1. Rheb1 in turn activates mTOR complex 1 (mTORC1), identified by association with the Regulatory-associated-protein-of-mtor (Raptor). mTORC1 regulates ribosome biogenesis, autophagy and translation among other cellular processes (Figure 1A). Through evolution, cells have evolved a mechanism where activation of mTORC1 reduces insulin receptor signaling via Insulin Receptor Substrate (IRS) feedback inhibition. However, in type 2 Diabetes, persistent mTORC1 activity leads to chronic inhibition of IRS and prevents transmission of extracellular signals and activation of proper kinase cascade resulting in insulin resistance (Figure 1B). Mechanistic and functional studies of the mTOR pathway have utilized Rapamycin, which inhibits mTORC1 kinase activity with acute treatment thus revealing its regulations (Sabatini, Erdjument-Bromage et al.).

In my studies, we examined disruptions of the mTOR pathway in the brain and determined that mTORC1 signaling is dependent on Rheb1 and that persistent activation of mTORC1 leads to down-regulation of D1 dopamine receptor signaling in a manner analogous to down-regulation of insulin-receptor signaling in type 2 diabetes. These observations have implications for understanding the impact of persistent mTORC1 signaling in neurocognitive disorders. .

Results

The lab has generated genetically modified Rheb1 mice to enable studies on its contribution and function to mTOR signaling output (Zou, Zhou et al.) (Figure 4A). For our studies we utilized a conditional knockout mouse, where exon 3 was floxed (Figure 4B). In order to obtain a brain specific knockout mouse (KO), we crossed the Rheb1 floxed mouse (F/F) to a Nestin-Cre mouse Rheb1 mouse containing one lox P site (F/+ Nestin-Cre). We compared lysates made from the forebrain of KOs to control littermates by Western blot analysis. Rheb1 was efficiently excised in the KO. Moreover, Rheb1 is absolutely required for mTORC1 function as demonstrated by the reduction in p-s6 and p-4EBP. Interestingly, p-Akt (S473), which is upstream of mTORC1, showed an enhanced phosphorylation signal (Figure 4C). Published studies using heterologous systems suggested a feed back regulation from mTORC1 via s6 Kinase to mTORC2, which phosphorylates Akt at S473 (Sarbassov, Guertin et al.). This feedback inhibition is important in tuning down mTORC1 activity during a chronic stimulation or maintaining mTORC1 activity during lack of input signals. Our study was the first *in vivo* demonstration of this feedback loop (Zou, Zhou et al.). It is worth noting that brain structures were not altered through development with size being the only observable difference (Zou, Zhou et al.).

Another mouse line that we employed for our study was a myc-tagged Rheb1 (S16H) transgene knocked into the Rosa locus (Figure 4D) (Zou, Zhou et al.). The S16H mutation yields a constitutively active Rheb1 by reducing its sensitivity to the GAP activity of TSC complex (Yan, Findlay et al.). We also crossed this mouse to a Nestin-Cre expressing mouse to generate a brain specific myc-Rheb1 (S16H) over-

expresser. Western blotting analysis of forebrain lysate from littermate control and over-expresser show that the myc-Rheb1 (S16H) is expressed (Figure 4E). Rheb1 specific antibody detected endogenous Rheb1 in both lysates and was also able to detect myc-Rheb1 (S16H), which showed an increase in molecular weight due to the addition of the myc epitope tag. In the over-expresser mice, mTORC1 activity is increased with concomitant decrease in p-Akt (S473) (Figure 4E). This finding shows that the feedback inhibition through mTORC2 is preserved in this animal. The brain structures developed normally with the over-expresser animal showing an increase in brain size (data not shown) (Zou, Zhou et al.).

Established studies have provided convincing genetic mutations of mTOR pathway components contributing to ASD (Hoeffer and Klann). In collaboration Dr. Alena Sovenenko in the Department of Pathobiology at Johns Hopkins School of Medicine, we subjected the Nestin-Cre myc-Rheb1 (S16H) mice to a battery of behavioral tests. We examined the 5-month-old male mutant mice and littermate control mice in a social investigation paradigm (Figure 5A). The assay presented a 1-month-old juvenile male mouse three consecutive times to the test mouse. In control and mutant mice, robust habituation is observed, as the time of investigation reduces significantly for each subsequent trial the same juvenile mouse is presented. However, when a new 1-month-old juvenile mouse is presented in trial 4, the test mouse spent significantly more time investigating the new juvenile, most likely due to novelty recognition (Figure 5B). It is worth noting that the quality of investigation interaction of the mutant mice were not in an aggressive manner and were comparable to control mice. We also employed the classic sociability test to

examine the behaviors our cohorts. The behavior paradigm utilizes a three chamber setup where the test mouse is placed in the middle chamber and has the choice to explore a mouse held under a cup in another chamber (social chamber) or just a cup by itself in the third chamber. Typically a mouse will spend more time investigating the social chamber than the empty cup chamber. We found that mutant mice spend significant less time investigating the social chamber compared to control mice, while they both showed similar disinterest in the empty cup chamber (Figure 5C). Despite the social chamber preference trend being preserved in the mutant mice, they did spend significantly more time in the neutral chamber in comparison to their control littermates. Contacts made with the mouse under the cup were also significantly less by the mutant mice compared to the control mice (Figure 5C). Both the mutant and control mice had very minimal contact with the empty cup. Though dramatic differences in the social investigation behavior examinations were observed, mutant mice performed very similarly to control mice in motor activity, thigmotaxis, Y-Maze, and Plus Maze assays (Figure 5D). The comparable behavior tests performances suggest that the social behavioral deficit was fairly selective.

Intrigued by the impaired social investigation results of the mutant mice we examined striatum functions by employing assays that test motor activity induced by amphetamine. Amphetamine increases locomotor activity related to the dopamine and norepinephrine in the striatum by blocking dopamine transporters (DAT) thus increasing synaptic dopamine levels (Yates, Meij et al.). Intraperitoneal injection (i.p) of amphetamine induces motor activities that increases over a span of 30 minutes and allows for quantification studies. To examine the impact of mTOR

function in the striatum, we setup the following experimental paradigm (Figure 6A). 5-month-old male control mice were allowed to habituate in an open field box for 10 minutes and their motor activity were recorded. Subsequently, they were treated with vehicle or rapamycin (10 mg/kg i.p) and placed back into the open field box for an acute inhibition of mTORC1. After another 40 minutes of habituation and motor activity recording, they were treated with amphetamine (2 mg/kg i.p). Finally, they were placed back into the open field box with their motor activities recorded for the next 60 minutes. mTOR inhibition with rapamycin resulted in significantly less amphetamine induced motor activity, though no difference was observed during the habituation stage (Figure 6B; left panel). This result suggests that mTORC1 activity participates in the amphetamine induced motor response. We then examined the mutant mice under the same paradigm (Figure 6B; right panel). Interestingly, amphetamine induced motor activity was dramatically reduced in the mutant mice and acute rapamycin did not have an effect in these animals. The reduced effect of amphetamine suggests that myc-Rheb1 (S16H) over-expression blunted the dopaminergic pathway and acute rapamycin treatment was not able to alter the deficit. No distinguishable difference were observed when we expanded the habituation studies by exposing mutant and control mice to the same open field box over four sequential trials (Figure 6C). Lower doses of amphetamine (0.5 mg/kg, 1 mg/kg i.p) did not show any appreciable differences between the mutant mice and controls, thus substantiates the choice of 2 mg/kg treatment (Figure 6C). Mutant mice appear to have a lower response threshold to three consecutive injections of amphetamine in comparison to control mice suggestive that the amphetamine

induced motor deficit cannot be overcome with repeated stimulation (Figure 6C). These results suggest that mTORC1 signaling contributes to the normal locomotor response to amphetamine, and this component of the response is blocked as a consequence of persistent activation of mTORC1. To the extent that amphetamine responses are due to dopamine signaling, these results are consistent with the notion that persistent mTORC1 inhibits dopamine signaling.

Disruption in sensory gating is another characteristic behavior in ASD involving movement. Disruptions in sensory gating are correlated with disruption of prepulse inhibition (PPI) (Takahashi, Hashimoto et al.). The protocol we used was 120 dB pulse with or without an 8 dB above background noise level prepulse with recordings of startle reaction (Figure 7A). Typically prepulse is associated with a reduction in response amplitude in a normal behaving animal. We compared the mutant and control mice throughout a range of noise levels to which they behaved similarly (Figure 7B). However, the mutant mice displayed a significant decrease in PPI behavior as compared to control mice (Figure 7B). To explore this observation further, we tested NMDA receptor functions as previous studies have established linkage between NMDA receptors and PPI (Lyall, Swanson et al.). Furthermore, NMDA receptor functions are important component of synaptic plasticity and genetic mutations in the NMDA receptor functional pathway have also been linked to ASD (Tarabeux, Kebir et al.). Once again we employ the open field motor behavior assay paradigm by substituting amphetamine with a selective NMDA receptor inhibitor, dizocilpine or MK-801 (Figure 7C). MK-801 was shown to induce motor activity similar to that of amphetamine (Robbins and Murphy). Mice were treated

with rapamycin or vehicle for 40 minutes followed by MK-801 with their motor activity recorded throughout the study. Both the control and mutant mice responded similarly to MK-801 and acute pretreatment with rapamycin did not alter the responses (Figure 7C). This suggests that mTOR pathway does not participate in MK-801 induced motor activity in contrast to amphetamine-induced responses. Importantly, the maximal activity of the control and mutant mice was very similar indicating that mutant mice are capable of achieving similar levels of motor activity, thus further substantiating the differences in amphetamine response.

Dopamine released from presynaptic terminal bind postsynaptic dopamine receptors and mediates synaptic changes via signaling cascades. DAT clear dopamine from the synaptic cleft and diminishes dopamine signaling overtime. In collaboration with Dr. Karen Szumlinski in the Department of Psychological & Brain Sciences at University of California Santa Barbara we performed *in vivo* micro-dialysis experiments to examine presynaptic functions of control and mutant mice in response to amphetamine treatment. No significant differences were observed at basal level and post injection of amphetamine in the mutant and control animals within the time course of differential motor activation (Figure 8A). Dose dependent potassium depolarization triggering presynaptic vesicle fusion and neurotransmitter release also did not show any appreciable differences (Figure 8B). To study the expression of D1R, D2R and DAT, we isolated and dissected the striatum from brains of control and mutant mice. Subsequently, biochemical fractionations of total homogenate, nuclei/large debris and crude synaptosomal

membrane were made. SDS-PAGE followed by Western blot analysis of D1R, D2R and DAT showed similar expression patterns between control and mutant mice (Figure 8C). Together, these results suggest the preservation of presynaptic integrity and function as well as postsynaptic receptor expressions between the mutant and control animals.

In collaboration with Dr. David Linden and Dr. Joo Min Park in the Neuroscience Department at Johns Hopkins School of Medicine, we examined corticostriatal plasticity by electrophysiology studies in brain slice experiments. This experimental setup takes advantage of cortical stimulation with simultaneous recordings in the striatum to examine striatal plasticity (Dunnett). Recordings in control corticostriatal slices showed that long-term potentiation (LTP) can be induced with high frequency stimulation furthermore; depotentiation can be achieved with subsequent low-frequency stimulation (LFS) (Figure 9A). However, in slices treated with a D1R agonist, SKF 83959, depotentiation was attenuated while LTP remained intact (Figure 9A). The ability of SKF 83959 to selectively block depotentiation suggests a substantial influence of D1R function on the depotentiation plasticity in the corticostriatal network. Under the same experimental paradigm with vehicle treatment the mutant mice showed normal LTP induction and depotentiation response (Figure 9B.) However, application of SKF 83959 had minimal impact on depotentiation in contrast to the control slices. We also examined hippocampal plasticity to distinguish between global plasticity deficits versus specific regional alterations. We isolated hippocampal slices and tested (R,S)-Dihydroxyphenylglycine (DHPG)-induced mGluR long-term

depotentiation (mGluR-LTD). DHPG treatment induced indistinguishable mGluR-LTD in both control and mutant slices (Figure 9C). Furthermore, utilizing Theta Burst Stimulation (TBS), hippocampal slices derived from control and mutant mice showed similar LTP induction. Lastly, High Frequency Stimulation (HFS), which can induce long lasting LTP, was also preserved in the mutant hippocampal slices (Figure 9D, E). These data indicate that persistent up-regulation of mTORC1 results in diminished post-synaptic response to D1 dopamine receptor activation.

To determine if dopamine receptor functions in the mutant animals remain intact, we examined the dynamics of the signaling cascades in the striatum. We utilized the robust amphetamine induced motor behavioral protocol followed by immediate dissection to isolate the striatum for our examinations. Striatum lysates were made followed by SDS-PAGE and Western blot analysis. In striatum from control animals we saw a robust D1R response to amphetamine treatment as indicated by the increase of phosphorylation signals in MEK and ERK (Figure 10A). Interestingly, this response was inhibited with acute pretreatment with rapamycin. Strikingly, in the mutant animals, p-Mek was dramatically reduced at the basal level and p-Erk was not induced with amphetamine in contrast to the response in control animals. Furthermore, acute treatment with Rapamycin had no effects in the mutant animals. The drastic reduction in phospho- Mek and Erk, led us to examine phosphorylation of Dopamine- and cyclic AMP-regulated phosphoprotein 32 (DARPP-32), a key regulator of signaling in striatal neurons (Bateup, Svenningsson et al.). In striatum from control animals treated with Amphetamine, we saw a reduction of phosphorylation in p-DARPP-32 (T75) consistent with previous

published results (Figure 10B) (Bateup, Svenningsson et al.). The reduction in p-DARPP-32 (T75) has been demonstrated to be due to an increase inhibition of protein phosphatase 2A (PP2A) as a result of protein kinase A (PKA) activation indicating activation of D1R (Nishi, Snyder et al.). Immunoblot utilizing specific antibody against phospho-PP2A in striatum treated with Amphetamine showed a decrease in phosphorylation indicative of an activated PP2A (Figure 10B). Next we examined the protein phosphatase 1 (PP1), a target of DARRP-32 (Bateup, Svenningsson et al.). In striatum from control mice treated with amphetamine, we saw a reduction in p-PP1; suggestive that PP-1 phosphatase activity is increased (Figure 10B). Interestingly, acute pretreatment with rapamycin before amphetamine was able to reverse the changes in phosphorylation in Darpp-32, PP2A, and PP1 (Figure 10B). In the myc-Rheb1 (S16H) mutant mice, neither Amphetamine nor the acute pretreatment with rapamycin induced changes in the phosphorylation status of Darpp-32, PP2A and PP1 (Figure 10B). Furthermore, PP2A was hyper-phosphorylated and PP1 was hypo-phosphorylated in basal and treated conditions. This is suggestive that the phosphatase activities of PP2A are reduced while PP1 is increased.

Examination of the mTOR pathway in response to amphetamine injections revealed reduction in mTORC1 activity with a concomitant increase in mTORC2 activity as indicated by p-s6 and p-Akt (S473) respectively (Figure 11). Since GSK α/ß are targets of Akt, we examined their phosphorylation status (Roberts, Woods et al.). An increase in phospho-GSK α/ß was observed, thus substantiating the increase in mTORC2 kinase activity (Figure 11). Acute rapamycin pretreatments led

to a dramatic reduction in p-Akt (S473) and p-GSK α/ß. Curiously, acute rapamycin pretreatment also led to a restoration of mTORC1 activity as demonstrated by p-s6 immunoblot (Figure 11). In myc-Rheb1 (S16H) mutant mice, mTORC1 activity was consistently elevated throughout different treatment conditions (Figure 11). Moreover, mTORC2 activity was consistent inhibited in line with previous studies that persistent mTORC1 activation leads to a feedback inhibition of mTORC2. These disruptions were also observed in Nestin-Cre mediated TSC2 heterozygous knockout animals (data not shown).

We sought to recapitulate the blunted PKA Map kinase signaling observed in the myc-Rheb1 (S16H) mice in an *in vitro* system. We made neuronal cultures from control and mutant mice and treated them with Brain Derived Neurotropic Factor (BDNF). To eliminate mitogen, serum and amino acid input into the signaling pathway, we adapted the cultures to artificial cerebrospinal fluid (ACSF). Treatment with BDNF in control cultures activated Map kinase and mTORC1 pathway in a robust manner (Figure 12A). However, BDNF treatment in mutant cultures did not increase p-Erk to the same extent as in the control cultures. This reduction in Map kinase signaling was consistent with what our observations in the striatum of the mutant mice. We over-expressed Rheb1 in HEK293 cells with or without co-expression of Darpp-32 in attempt to recapitulate the PKA, Darpp-32, PP1 deregulation that we previously observed in the *in vivo* experiments. Rheb1 over expression increased mTORC1 activity as demonstrated by p-s6 (Figure 12B). Treatment with Epidermal Growth Factor (EGF) increased mTORC1 activity in cells without Rheb1 over-expression but did not further increase mTORC1 activity in

Rheb1 over-expressing cells. Rheb1 over-expression also prevented EGF induced p-Erk. Basal p-Darpp-32 was not altered with over-expression of Rheb1 (S16H) or wild type Rheb1, however addition of EGF led to the reduction Darpp-32 phosphorylation. Interestingly p–Darpp-32 reduction by addition of EGF was prevented in Rheb1 over-expressing cells, similar to the *in vivo* experiments. Furthermore, with Darpp-32 expression alone led to the phosphorylation of PP1 but not in cells co-expressing Rheb1 and addition of EGF (Figure 12B). These results indicate that chronic mTORC1 activation by over-expression of Rheb1 inhibits phosphorylation of Erk in response to stimuli, such as EGF. Chronic mTORC1 activation by over-expression of Rheb1 also prevents the phosphorylation and inhibition of PP1 in basal state and in response to stimuli. Thus persistent mTORC1 activation alters basal signaling dynamics and disrupts the induced cellular responses.

Discussion

Persistent elevation in mTOR signaling leads to detrimental diseases and disruption of homeostasis due to the involvement of mTOR in multiple fundamental cellular processes (Hoeffer and Klann). One well-characterized study of the pathological result in chronic elevation of mTOR signaling pathway is in diabetes, where a feedback inhibition of insulin receptor signaling pathway occurs as a consequence of persistent elevation of mTOR (Zoncu, Bar-Peled et al.). In this study, with the generation of the mutant mice lacking Rheb1 in the brain, we demonstrated

Rheb1 is essential for mTORC1 activity but not mTORC2. Furthermore, mTORC2 activity is elevated due to the relief of feedback inhibition from mTORC1 activity. This is the first in vivo demonstration of the regulation and is consistent with previous research results (Sarbassov, Guertin et al.).

We found that mice with brain specific over-expression of myc-Rheb1 (S16H) revealed ASD-like behaviors through social investigation behavioral experiments and PPI examination. The ASD-like behaviors were relatively specific as no appreciable differences were observed in other general behavioral tasks in comparison to control mice. These ASD- like behaviors have also been observed in mouse models of TSC and Pten (Tsai, Hull et al.) (Kwon, Luikart et al.). These mouse models all share persistent increase in mTORC1 activity suggesting that sustained mTORC1 activity as a strong casual link to ASD-like behaviors. Furthermore, disruption of the ability of mTORC1 to integrate changes experienced by the neurons leads to devastating outcomes for the neural circuitry and animal.

To find the causality of the social motivation deficits, we examined the striatum since it is involved in social motivation and reward integration. First, we established that mTOR pathway contributes to amphetamine induced motor activation behavior with rapamycin injection in the control mice. Mutant mice over-expressing myc-Rheb1 (S16H) showed a drastic reduction in amphetamine induced motor activation and in contrast to control mice, acute pretreatment with rapamycin had no effect. These results suggested two potential deficits in the mutants; D1R activation (striatonigral pathway) is disrupted or D2R (striatopallidal pathway) is persistently. Micro-dialysis experiments measuring synaptic dopamine

levels and dopamine vesicle release showed no significant changes between the mutant and control mice. Moreover, we did not detect any significant changes in D1R, D2R and DAT expression. Thus, led us to focus on examining the functions of D1R and D2R. Electrophysiology studies suggested that striatum plasticity disruptions were rather selective since depotentiation experiments in corticostriatal slices with D1R agonist showed that the mutant mice were not sensitive to D1R activation. Meanwhile, hippocampal plasticity remained intact. Moreover, biochemical analyses from the brains of mutant mice treated with different combinations of rapamycin and amphetamine revealed that PKA, p-Mek and mTOR pathways were not sensitive to stimulation and modulation. Furthermore, Darpp32 phosphorylation was uncoupled amphetamine induced regulations. Since we have established that expression of D1R was comparable between mutant and control animals, this result was intriguing, as it suggested that D1R function might be disrupted. D1R engages PKA pathway, which in turn contribute to the trafficking of AMPAR and NMDAR, which underlie synaptic plasticity responses. Moreover, PKA can also modulate voltage dependent ion channels that contribute to NMDAR function (Skeberdis, Chevaleyre et al.). Thus, disruption of the D1R signaling pathway would alter depotentiation plasticity in the corticostriatal network.

Autism Spectrum Disorders (ASDs) are a group of clinically and genetically heterogeneous neurodevelopment disorders characterized by impaired social interaction, repetitive behaviors, and restricted interests (Baird, Dewar et al.) (Zoghbi and Bear). Recent genetic studies have demonstrated that Pten and Tsc mutations result in persistent increase of mTOR signaling and contribute to ASDs

(Zoghbi and Bear). It is estimated that TSC1 mutations account for 30% familial cases and 15% sporadic causes while TSC2 accounts for 50% sporadic causes of ASD or Tuberous sclerosis (Zoghbi and Bear). In consideration of the social behavior deficits and repetitive behaviors, investigators have examined the basal ganglia, specifically striatum. Studies utilizing PET and MRI have shown deficits in striatum functions in patients with ASD (Duchesnay, Cachia et al.) (Gaetz, Bloy et al.). Striatum acts as an information integrator in the brain receiving sensory modalities; context, planning and memory inputs from different parts of the brain and outputs control motor activity, executive function and reinforce reward learning. Striatum is mostly composed of Gabaergic medium spiny neurons that receive glutamatergic inputs from the cortex, amygdala, hippocampus and thalamus (Shepherd) (Figure 2A). The striatum projects in two output pathways. The striatonigral pathway, also known as the direct pathway, is distinguished by coupling to Dopamine receptor 1 (D1R), while the Striatopallidal or indirect pathway is identified by the coupling to Dopamine receptor 2 (D2R). In a simplified representation, D1 pathway is also known as “go” pathway, whereas D2 pathway is the “no-go” pathway in terms of motor activity. (Figure 2B). D1R and D2R pathways have opposing actions on complex signal transduction cascade networks composed of multiple inputs and outputs (Beaulieu, Gainetdinov et al.) (Figure 3).

We characterized mTORC1 and mTORC2 signaling activities in the striatum and found that mice with brain specific over-expression of myc-Rheb1 (S16H) displayed persistent elevation of mTORC1 activity supportive of the notion that Rheb1 is critical for mTORC1 function. Furthermore, mTORC2 activity is decreased

in the brains of these animal, substantiating the feedback inhibition regulation is increased as a result of increased mTORC1 activity. The feedback inhibition also impacted the dynamics of D1R and D2R mediated signaling in the striatum from mutant mice. In the mutant mice the ability for mTOR signaling pathway to integrate changes due to intra- and extra- cellular environment was disrupted.

In conclusion, our results suggest that persistent mTORC1 activity down regulates G-protein signaling and reward pathway in the striatum. The loss of integration function by mTOR pathway in the striatum, which serves as an integrator for the central nervous system, can lead to devastating disorders such as ASD. Furthermore, myc-Rheb1 (S16H) over-expression in the brain is both necessary and sufficient to create an ASD-behavior like phenotypes and model of autism.

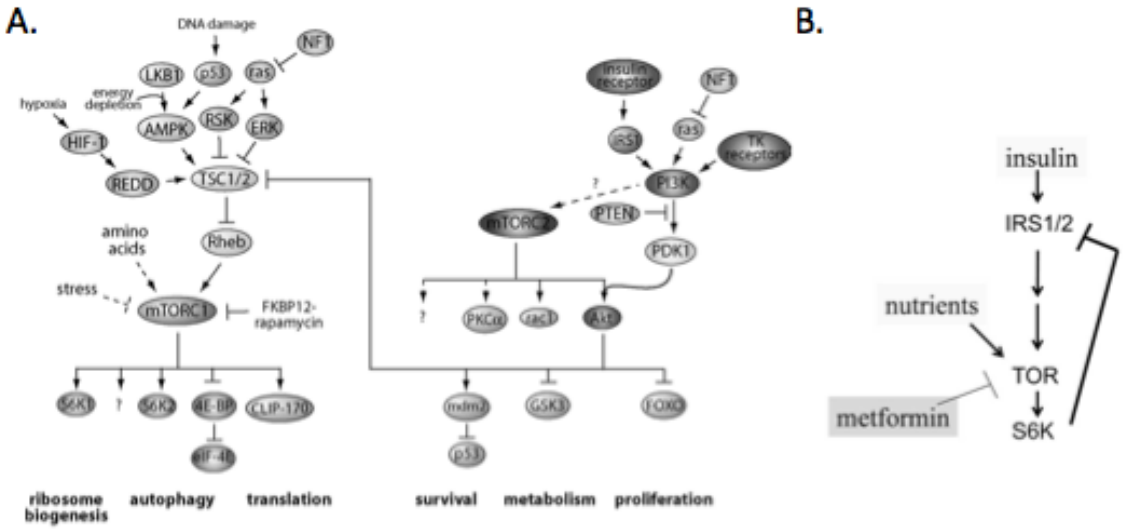

Figure 1. Diagram of mTORC1 Signaling Pathway. (A) mTORC1 signaling pathway and regulations (Laplante et al.) **(B)** Feedback inhibition of Insulin Receptor Substrate by mTORC1 (Blagosklonny et al.).

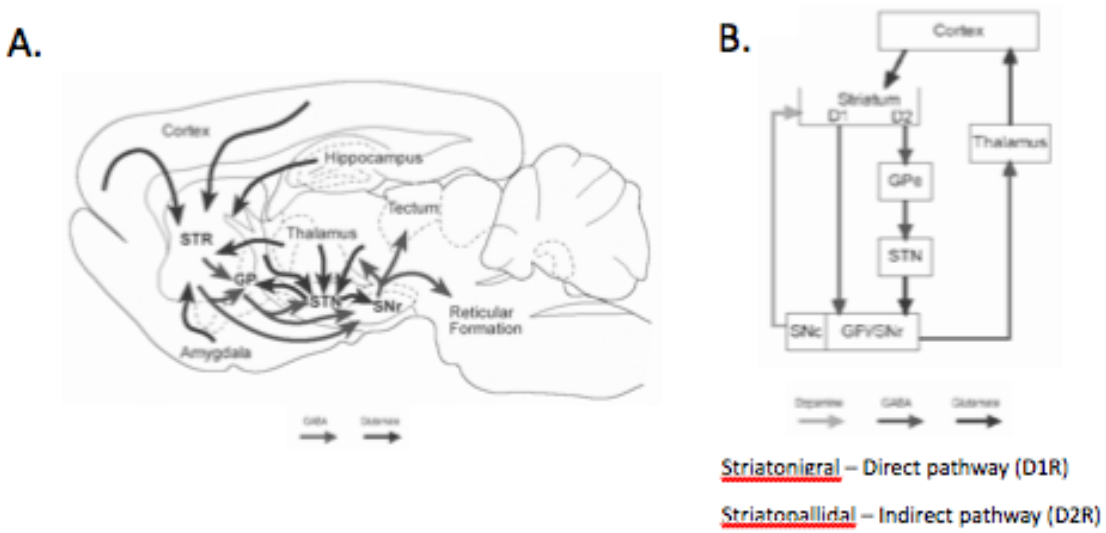

Figure 2. Principal Components and Organization of the Basal Ganglia. (A) Principal components of the mammalian basal ganglia (Scholarpedia). **(B)** Organization of intrinsic connections within the basal ganglia (Scholarpedia).

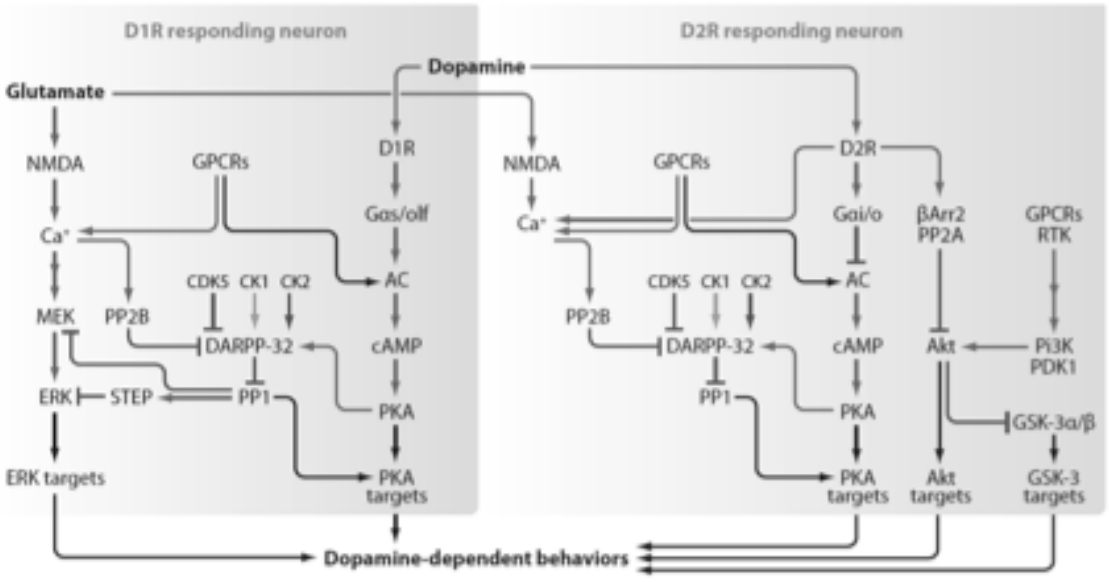

Figure 3. Complexity of Signaling Responses in vivo, Signaling Networks Regulated by Dopamine in D1 Receptors (D1R) and D2 Receptors (D2R) Containing Neurons in the Mouse Striatum (Beaulieu et al).

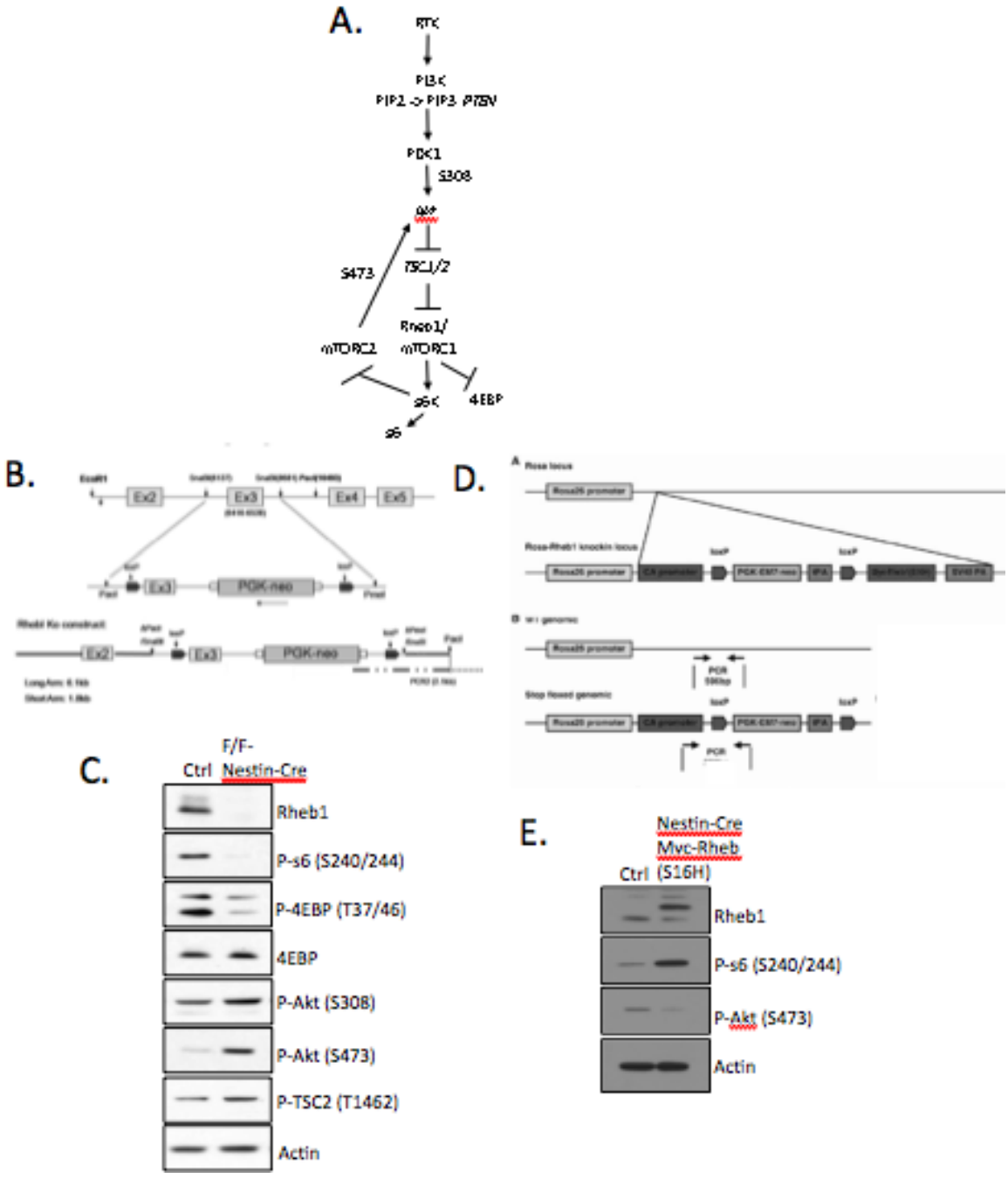
A.
RTK
PI3K
PIP2 -> PIP3 PTEN
PDK1
S308
Akt
S473
TSC1/2
Rheb1/
mTORC2
mTORC1
S6K
4EBP
S6
B.
Ex2
Ex3
Ex4
Ex5
PGK-neo
D.
C.
F/F-
Ctrl
Nestin-Cre
Rheb1
P-s6 (S240/244)
P-4EBP (T37/46)
4EBP
P-Akt (S308)
P-Akt (S473)
P-TSC2 (T1462)
Actin
E.
Nestin-Cre
Myc-Rheb
Ctrl
(S16H)
Rheb1
P-s6 (S240/244)
P-Akt (S473)
Actin

Figure 4. Biochemical Characterization of Conditional Rheb1 Knockout and Conditional Myc-Rheb1 (S16H) Over-expresser Mice. (A) Simplified PI3K-mTOR signaling pathway. **(B)** Schematic representation of the Rheb1 gene targeting strategy. Exon 3 of Rheb1 was inserted in the LoxP/PGK-neo cassette to make a conditional knockout (Zou et al.). **(C)** Forebrain lysates from P21 Nestin-Cre mediated Rheb1 knockouts (KOs) and control littermates were monitored by Western blot for changes in mTOR signaling pathway. Phosphorylation levels of mTORC1 pathway indicated by s6 and 4EBP are significantly reduced while phosphorylation levels of mTORC2 pathway indicted by Akt and TSC2 are increased in the KOs versus the controls. **(D)** Schematic representation of the Rosa26-Myc-Rheb1 (S16H) targeting strategy (Zou et al.). **(E)** Western Blot showed an increase in mTORC1 activity indicated by p-s6 and a concomitant decrease in mTORC2 activity indicated by p-Akt.

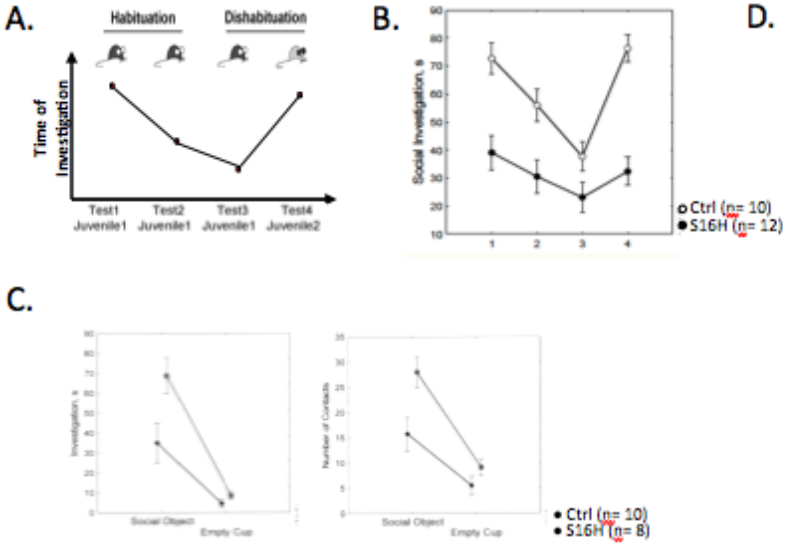

D.

Behavior	Experiment	Result
Motor	Motor activity	Normal
Novelty induced motor activity	Thigmotaxis	Normal
Willingness to explore new environment	Y maze	Normal
Anxiety levels	Plus maze	normal

Figure 5. Nestin-Cre Myc-Rheb1 (S16H) Mice Display Deficits in Social Investigation. (A) Illustration of a free-roaming stimulus mouse in consecutive trails of the habitation-dishabituation social Investigation experimental paradigm. **(B)** S16H mutant mice (n = 12) showed habituation through the procession of trials however had spent significantly reduced amount of investigation time compared with control mice (n = 10). **(C)** S16H mutant mice (n = 8) spent significantly less time and had less number of contacts investigating a caged intruder than control mice (n =10), but both showed similar amount of time investigating and number of contacts with an empty cup in the social novelty 3-chamber test. **(D)** No detectable difference were observed in motor activity assay, thigmotaxis assay, Y-maze and plus maze tests between control (n = 10) and S16H mutant mice (n = 12).

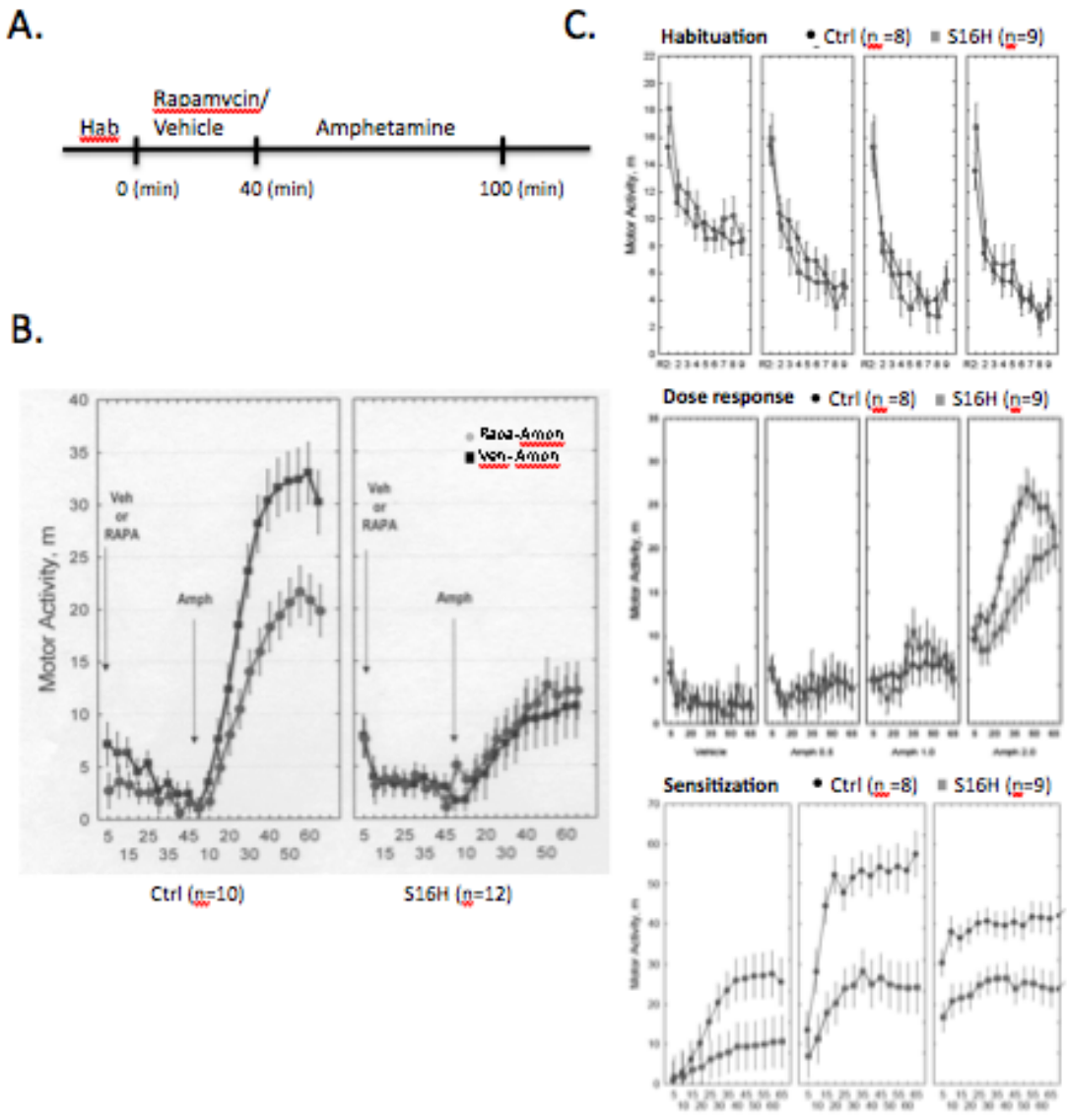
A.
Hab
Rapamycin/
Vehicle
Amphetamine
0 (min)
40 (min)
100 (min)
B.
Motor Activity, m
Veh
or
RAPA
Amph
Rapa-Amph
Veh-Amph
Ctrl (n=10)
S16H (n=12)
C.
Habituation
Ctrl (n =8)
S16H (n=9)
Dose response
Ctrl (n =8)
S16H (n=9)
Sensitization
Ctrl (n =8)
S16H (n=9)

Figure 6. Modulation of mTORC1 Activity Alters Amphetamine Induced Locomotor Activity. (A) Illustration of Amphetamine induced locomotor activity – open field experimental paradigm. **(B)** Left panel shows control mice (n =10) displayed similar habituation ± Rapamycin treatment (i.p 10mg/kg) 40 mins post injection. Rapamycin treated mice showed reduced locomotor activity after Amphetamine treatment (i.p 2mg/kg) compared to vehicle treatment. Right panel shows S16H mutant mice (n = 12) displayed similar habituation ± Rapamycin treatment and to control mice (left panel) (i.p 10mg/kg) 40 mins post injection. S16H mice showed similar locomotor activity after Amphetamine treatment ± Rapamycin and a significant reduction compared to controls (left panel). **(C)** S16H mutant (n = 9) and control (n = 8) mice showed similar habituation behaviors through four trials. Amphetamine dose dependent response showed differences at 2mg/kg between control and S16H mutant mice. Amphetamine injection (2mg/kg) repeated three times shows consistent lower locomotor activity response in the S16H mutant mice.

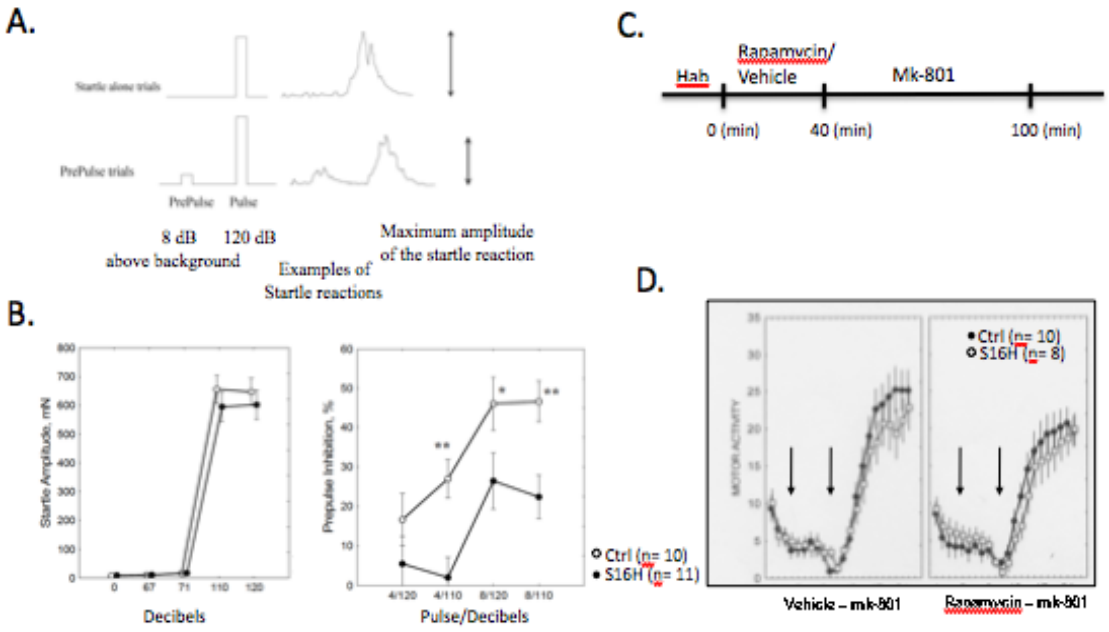

Figure 7. Nestin-Cre myc-Rheb1 (S16H) Mice Displayed Disruption in Prepulse Inhibition but Retains Normal MK-801 Locomotor Activity Response. (A) Illustration of Prepulse Inhibition (PPI) protocol. **(B)** Left panel; S16 mutant (n = 12) and control (n =10) mice showed similar acoustic startle reaction in increasing amplitude tests. Right Panel; Reactions to startle stimuli (110 dB or 120 dB) were significantly lower in S16H mutant mice than in control mice. **(C)** Illustration of MK-801 induced locomotor activity – open field experimental paradigm. **(D)** Control (n = 10) and S16H mutant (n =8) mice showed similar habituation and locomotor activity in response to MK-801 (i.p 0.2mg/kg). Treatment with Rapamycin (i.p 10mg/kg) had no effect on habituation or MK-801 (i.p 0.2mg/kg) induced locomotor activity in control or S16H mutant mice.

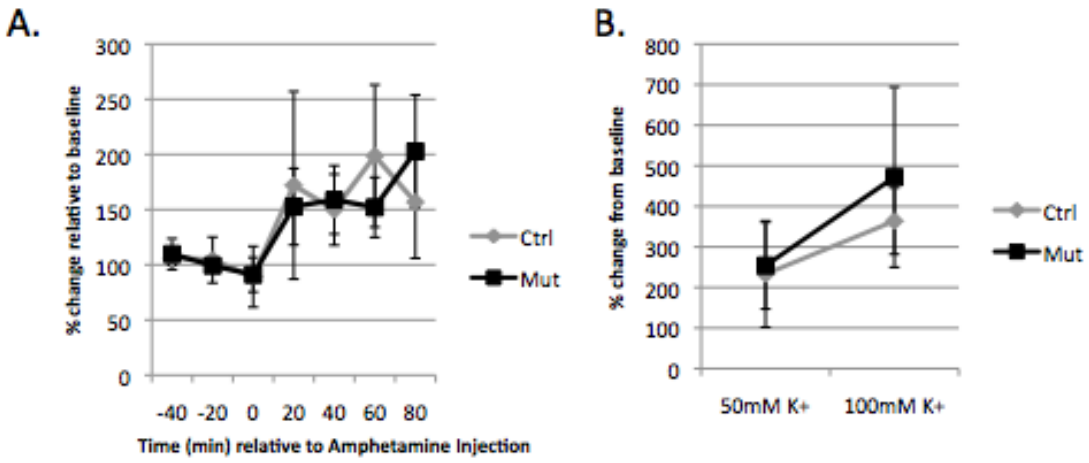

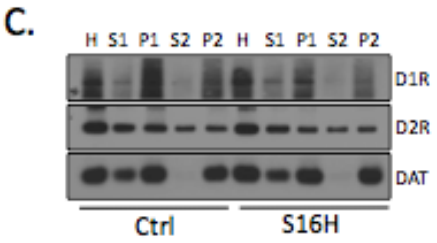

Figure 8. Dopamine Levels and Expression of Dopamine Receptors are Normal in Nestin-Cre myc-Rheb1 (S16H) Mice. (A) No differences in dopamine levels were observed in S16H mutant (n = 6) and control (n = 5) mice pre or post Amphetamine injection (i.n 2mg/kg). **(B)** S16H mutant (n = 6) and control (n =5) mice showed similar response to depolarization induction with 50mM K+ or 100 mM K+. Data were normalized to percent change from the average baseline value. **(C)** No significant changes were detected by Western blot analysis of Dopamine receptor -1, -2 and Dopamine transporter from biochemical sub-cellular fractionation of striatums derived control and S16H mutant mice. H: Total homogenate; P1: Nuclei/large debris; P2: Crude synaptosomal membrane.

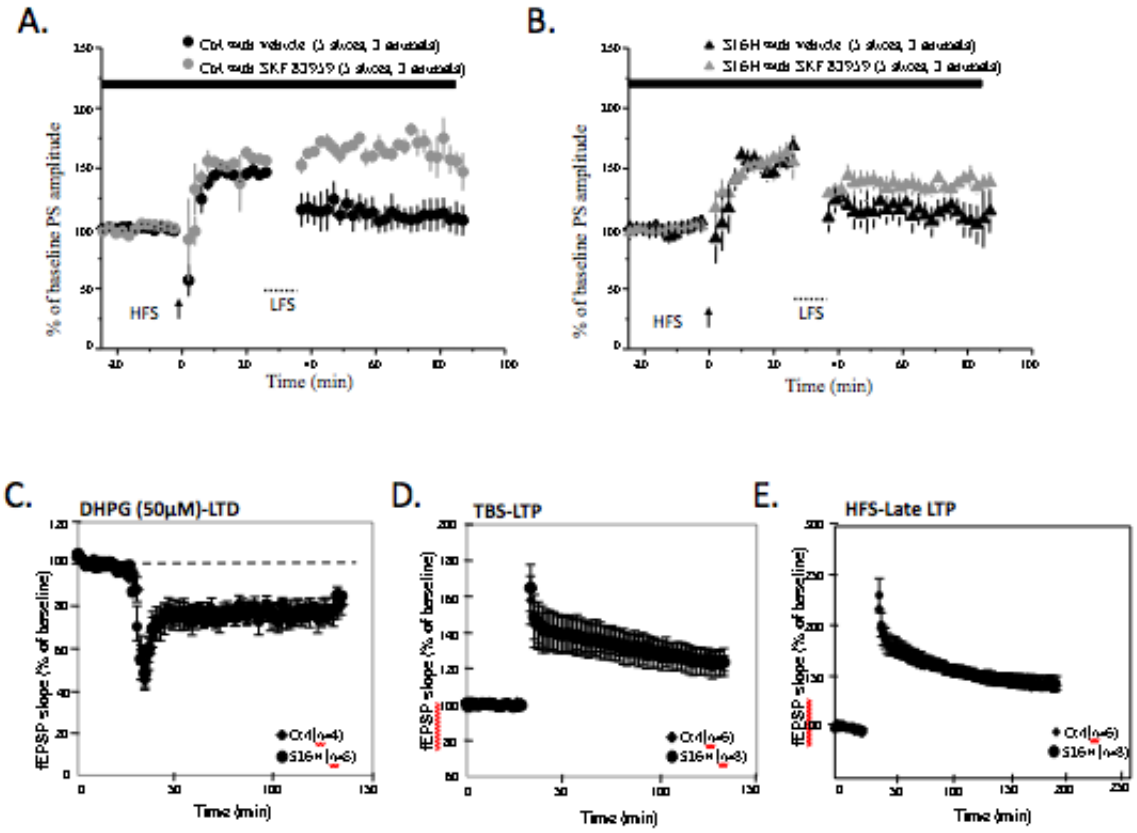
A.
B.
% of baseline PS amplitude
Time (min)
HFS
LFS
C.
DHPG (50μM)-LTD
D.
TBS-LTP
E.
HFS-Late LTP
fEPSP slope (% of baseline)
Time (min)

Figure 9. Nestin-Cre myc-Rheb1 (S16H) Mice Show Impaired Corticostriatal Plasticity in Response to D1 Receptor Agonist. (A) Average time course of the change in fEPSP slope induced by High Frequency Stimulation (HFS) induced LTP and Low Frequency Stimulation (LFS) induced depotentiation were recorded in control corticostriatal slices ± SKF 83959, selective D1R agonist. HFS-LTP was comparable at 146% ± 2.0% of base line (5 slices, 3 mice) with vehicle treatment and 155% ± 2.0% of base line at t = 20 min (5 slices, 3 mice) with SKF 83959. LFS-depotentiation yielded recordings at 118% ± 8.0% of base line at t = 70 min but was blocked in presence of SKF 83959 with recordings at 174% ± 2.0% of base line at t = 70 min. Error bars indicate the standard error of the mean. Measurements correspond to the time points indicated on the time course graph in this and all subsequent figures. **(B)** In corticostriatal slices from S16H mutant mice (5 slices, 3 mice) HFS-LTP recordings were similar comparable to controls at 148% ± 2.2% of base line with vehicle treatment and 158%± 2.8% of base line at t = 20 min. SKF83959 treatment reduced the LFS-depotentiation from 123%± 5.2% of base line to 148% ± 2.0% of base line at t = 70 min. **(C)** No significant difference in average time course of the change in fEPSP slope induced by the group I mGluR agonist (R,S)-DHPG (50 µM, for 5 min) was observed from hippocampal slices derived from control and S16H mutant mice. LTD of control mice (n=4) was 76.8% ± 2.3% of base line and S16H mutant mice (n = 5) was 78 ± 3.0% of base line at t = 70 min. **(D)** Average time course of the change in fEPSP slope induced by Theta Burst Stimulation (TBS) (10 trains, each consisting of ten 100 Hz burst (four pulse) given at 5 Hz, with intertrain intervals of 20 s). TBS-LTP of control mice was 134.8% ± 1.0% of base line (n = 6), in S16H mutant mice, fEPSP was 134% ± 6.5% of the baseline at t = 100 mins (n = 8).
(E) Time course of the change in fEPSP slope produced by High Frequency Stimulation (HFS) (3 stimulus trains (100 Hz each) with an intertrain interval of 20 s). HFS-LTD of control mice was 158% ± 2.5% of baseline (n = 6) and in S16H mutant mice fEPSPs were 163% ± 3.3% of the baseline at t = 100 mins (n = 8). Scale bars, 1 mV/ 10 ms.

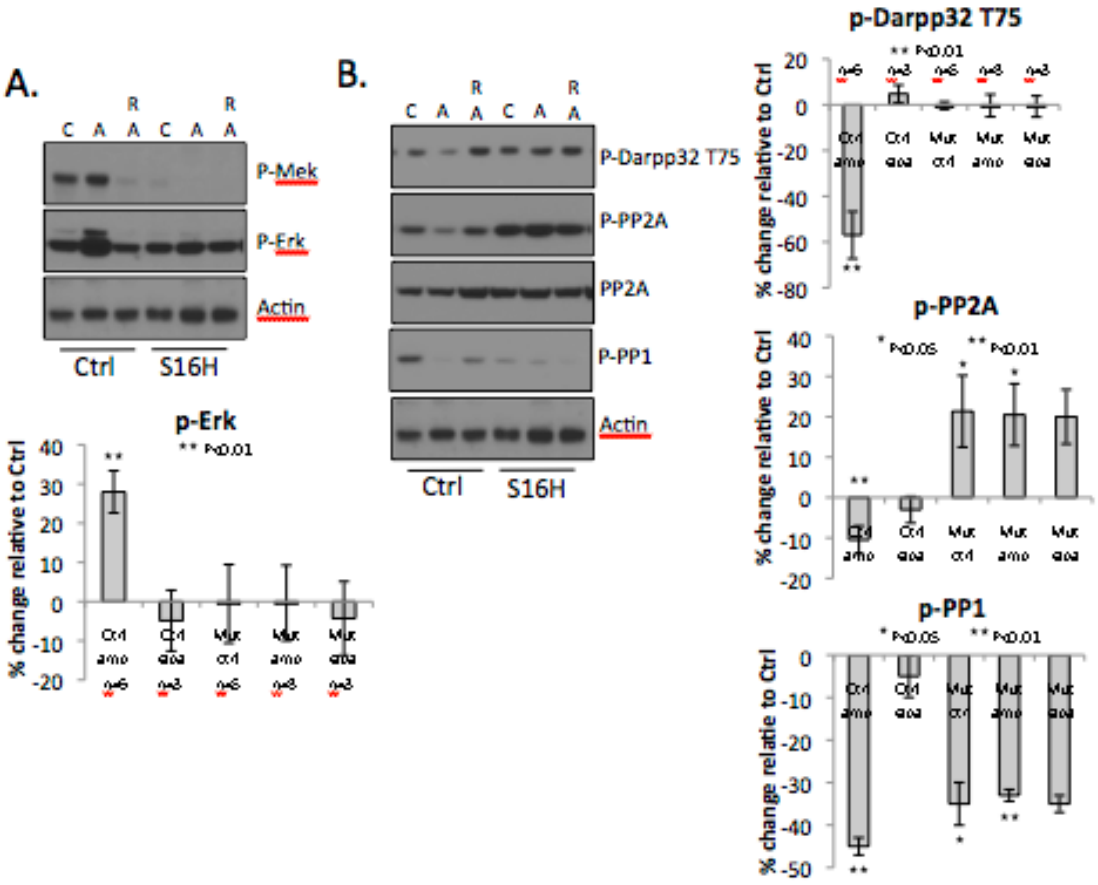
A.
C A A C A A
R R
P-Mek
P-Erk
Actin
Ctrl
S16H
p-Erk
** P<0.01
% change relative to Ctrl
B.
C A A C A A
R R
P-Darpp32 T75
P-PP2A
PP2A
P-PP1
Actin
Ctrl
S16H
p-Darpp32 T75
** P<0.01
p-PP2A
* P<0.05
** P<0.01
p-PP1
* P<0.05
** P<0.01
% change relative to Ctrl

Figure 10. Disrupted PKA, Map Kinase, and Darpp32 Signaling Pathways in Striatum of Nestin-Cre myc-Rheb1 (S16H). (A) Representative Western blot analysis of Map Kinase pathway in striatum lysates from control and S16H mutant mice under control (C), treatment with amphetamine (A) or pretreatment with rapamycin (RA) conditions. **(B)** Representative Western blot analysis of p--Darpp32, p-PP2A, total PP2A, p-PP1 and Actin in striatum lysates from control and S16H mutant mice under control (C), treatment with amphetamine (A) or pretreatment with rapamycin (RA) conditions. Statistical analysis of % change normalized to control condition and Actin, control/amphetamine (n = 6); control/ rapamycin/amphetamine (n = 3); S16H mutant/control (n =5); S16H mutant/amphetamine (n = 8); S16H mutant/rapamycin/amphetamine (n =3). Data represented are mean values ± SEM. p-values were calculated with Student's T-Test.

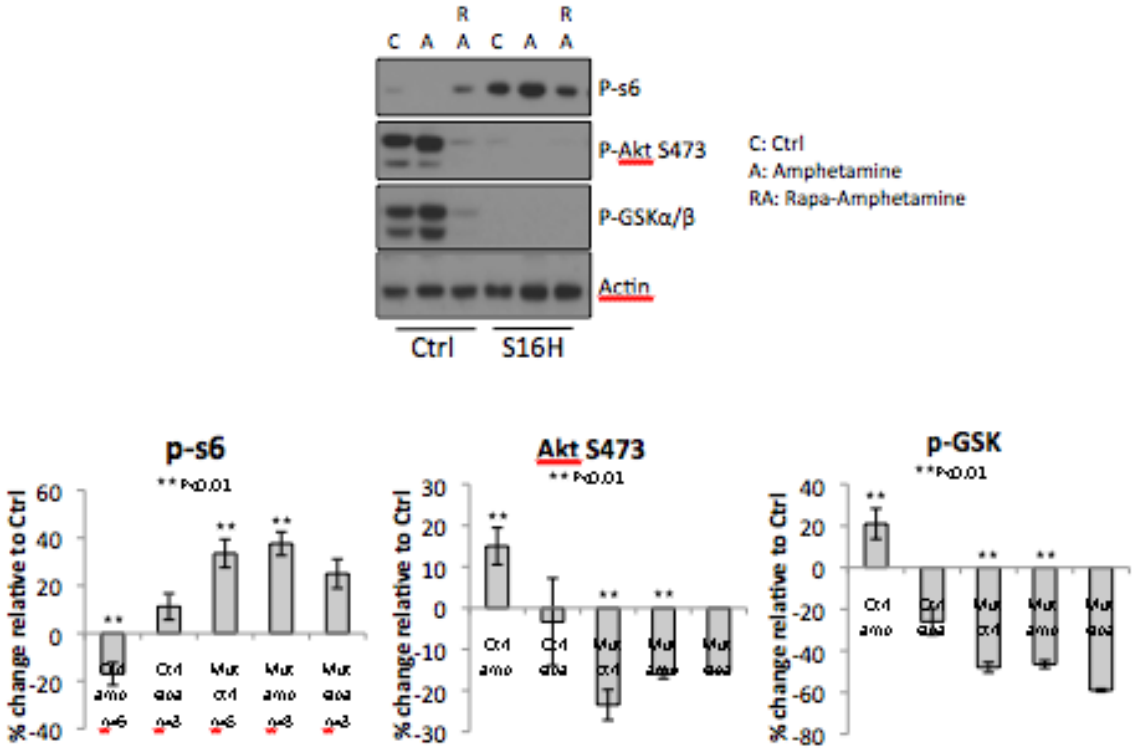

Figure 11. Elevated mTORC1 and Repressed mTORC2 Signaling Pathways in Striatum of Nestin-Cre myc-Rheb1 (S16H). (A) Representative Western blot analysis of mTORC1 and mTORC2 signaling pathway in striatum lysates from control and S16H mutant mice under control (C), treatment with amphetamine (A) or pretreatment with rapamycin (RA) conditions. Statistical analysis of % change normalized to control condition and Actin, control/amphetamine (n = 6); control/rapamycin/ amphetamine (n = 3); S16H mutant/control (n =5); S16H mutant/amphetamine (n = 8); S16H mutant/ rapamycin/amphetamine (n =3). Data represented are mean values ± SEM. p-values were calculated with Student's T-Test.

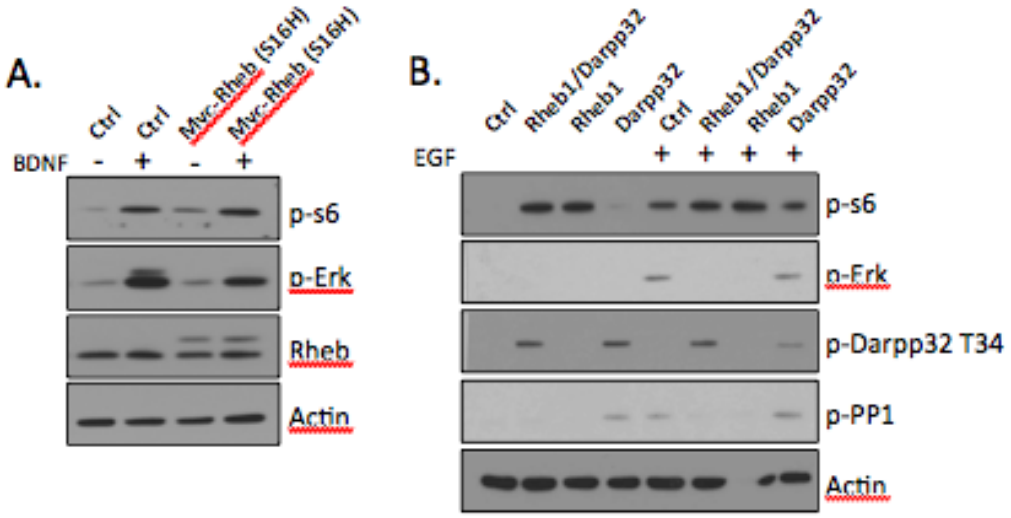

Figure 12. in vitro Over-expression of Rheb1 Recapitulate Feedback Inhibition of Signaling Pathways. (A) Western blot analysis of DIV-21 dissociated cortical neuron cultures from control and Nestin-Cre myc-Rheb1 (S16) mice that were adapted to artificial cerebrospinal fluid (ACSF) for 2 h then treated with with vehicle or 75ng/ml of BDNF for 15 min. **(B)** Western blot analysis of HEK293 cells over-expressing Rheb1 and/or Darpp32 with vehicle or 20ng/ml of EGF treatment for 20 min.

A.

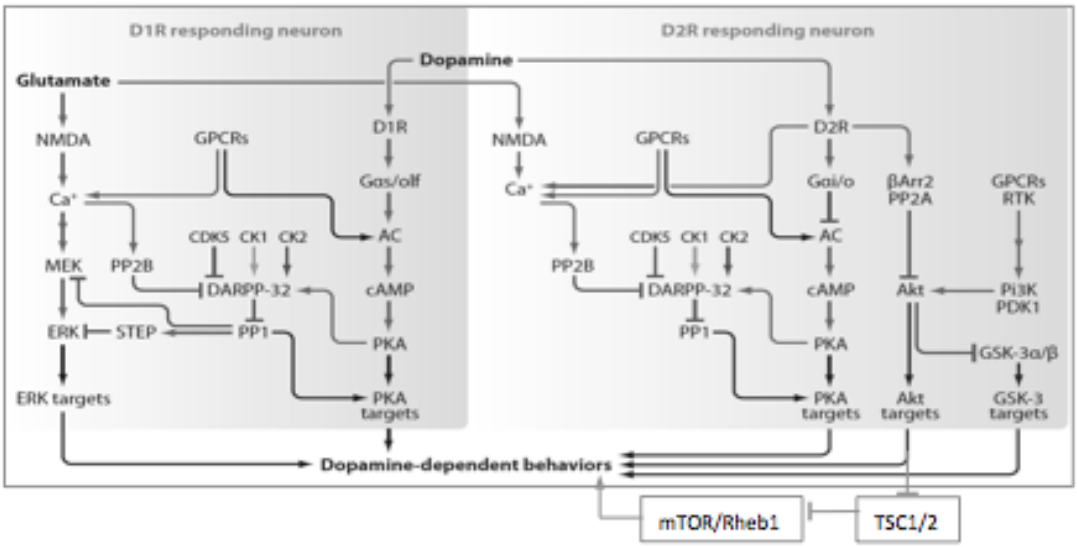

B.

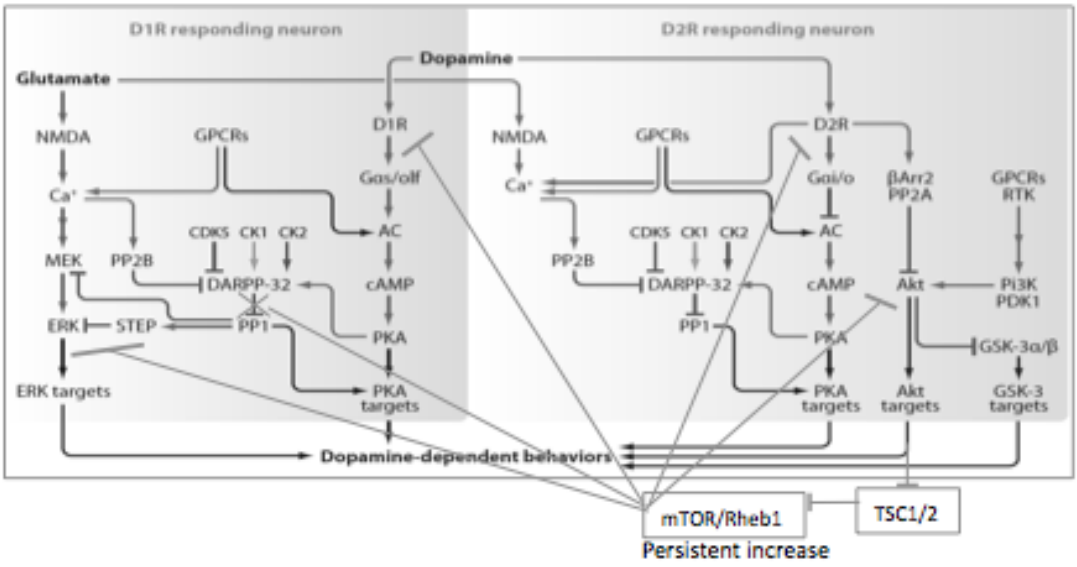

Figure 13. mTOR Signaling in Dopamine in D1 Receptors (D1R) and D2 Receptors (D2R) Containing Neurons in the Mouse Striatum. (A) Incorporation of mTORC1 signaling pathway in D1R and D2R containing neurons in the mouse striatum (Beaulieu et al.). **(B)** Persistent mTORC1 signaling produces feedback inhibition and disruption of D1R and D2R signaling

CHAPTER 4:

Rheb1 and activation of mTORC1

Introduction

Cellular signaling pathways have evolved to facilitate cells' ability to adapt to constant changes of intracellular and extracellular environments. The complex post-translational protein-modification signaling cascades underlie the output function by cells to ensure survival and proper function. Cellular signaling relies on many components of the trafficking machinery. Endosomes are membrane inclusion vehicles that transport proteins and macromolecules inside cells. Maturation and trafficking of endosomes have been under intensive study, which yielded identification of protein markers that can be utilized to track their status and function (Palfy, Remenyi et al.). In neurons, endosomes are the membrane vehicles that aid receptor recycling or initiate protein degradation pathways. Biomarkers such as the members of the small GTPase family, Rabs, are often used to identify maturation stages of endosomes. Endosomes are categorized into three compartments, which suggest their maturation status. Rab4 identifies early endosomes, Rab7 identifies late endosomes and Rab11 have been identified to associate with recycling endosomes (Huotari and Helenius). Since endosomes are lipid membrane entities that contain phosphatidylinositol (PtdIns) moieties, protein kinases that modify PtdIns are often found to regulate and associate with endosomes. One major class of protein kinases that modify PtdIns is the

Phosphatidylinositidies 3- kinase family (PI3Ks). PI3Ks are a family of enzymes that phosphorylates the 3 position hydroxyl group of the inositol ring of PdtIns and thus act as signaling transducers (Murphy, Padilla et al.).

PI 3-kinases have been demonstrated to participate in mechanisms facilitating learning and memory and specifically glutamate receptor trafficking (Kim, Lee et al.). PI3K and mammalian Target of Rapamycin (mTOR) belong to the PI 3-kinase superfamily. PI3K-mTOR signaling pathway mediates cellular functions to ensure proper proliferation and survival (Laplante and Sabatini). Aberrant PI3K-mTOR signaling leads to detrimental outcome for the cell and organism (Laplante and Sabatini). In response to extra- and intra- cellular environmental changes, mTOR signaling pathway regulates protein translation, protein turnover, cellular skeletal remodeling, lipid biosynthesis and transcriptional changes (Sarbassov, Ali et al.). Recent immunocytochemistry studies by investigators demonstrated that active mTOR associates with late endosomes/lysosomes and is dependent on amino acid availability (Sancak, Peterson et al.). Furthermore, mTOR kinase activity was found to be dependent on functional V-ATPase ion pump that acidifies the lumen of the endosomes as it matures from early to late endosomes. Further characterization studies revealed that Rag GTPases were the mediators of mTOR activity and V-ATPase function by conjugating mTOR to the lysosome (Zoncu, Bar-Peled et al.). However, the contribution of Rheb1 to mTOR activation remains elusive. Previous studies have demonstrated that Rheb1 is essential for mTOR complex 1 (mTORC1) activation (Zou, Zhou et al.). We sought to identify the molecular and cellular basis of Rheb1-dependent activation of mTORC1 in neurons.

Results

To study the localization of the protein components of the mTOR pathway we made biochemical sub-cellular fractions from forebrains of Wild Type (WT) mouse at the age of postnatal 30 days (Figure 1A, 1B). Treatment with different density of sucrose and sequences of centrifugation allows sub-cellular compartments to be isolated, including total homogenate (H), nuclei/large debris (P1), crude synaptosomal membrane (P2), light membrane (P3), synaptosomal membrane (LP1) and synaptic vesicle enriched fraction (LP2) (Hallett, Collins et al.). Western blot analysis shows that Rheb1 is significantly enriched in the LP2 fraction coinciding with the most significant p-mTOR signal (Figure 1B). This finding is consistent with previous finding that Rheb1 is necessary for mTOR activation (Zou, Zhou et al.). Furthermore, we observed other components of the mTORC1 pathway way such as TSC2 and s6 in the LP2 fraction. Early and late endosomes demonstrated by Rab4 and Rab7 immunoblots, indicate that we were able to isolate synaptic trafficking vehicles in the LP2 fraction. Utilizing specific antibodies against Shank3, we show that the biochemical fractions are specific as Shank3 is only enriched in the LP1 and P3 fractions. GluR1, GluR2, NR1 and NR2A immunoblots also demonstrate specific enrichment of the glutamate receptors at the LP1 fraction. Consistent with previous reports, only GluR2 and NR1 but not GluR1 or NR2A are observed in the LP2 fractions (Hallett, Collins et al.). We also employed continuous sucrose density gradient centrifugation technique and identify the association of Rheb1 with vesicle-enriched fractions. Isolated fractions were subjected to SDS-PAGE and Rheb1 was visualized by Western blot analysis utilizing specific Rheb1

antibody (Figure 1C). Rheb1 signals were observed in fractions 10, 11, and 12 containing large protein complexes and vesicles such as endosomes, lysosomes, and multi-vesicular bodies. Observations of Rheb1 in fraction 1-6 may be due to the disruptive nature of centrifugation force or the existence of Rheb1 in smaller protein complexes.

In order to gain insight on how Rheb1 might contribute to mTOR activity we sought to identify proteins that associate with Rheb1. We employed the Nestin-Cre mediated expression of Myc-Rheb1 (S16H) mouse model (Mutant) for our biochemical assays. Myc epitope allows for specific immunoprecipitation (IP) of myc-Rheb1 since no specific antibodies against endogenous Rheb1 are available at the present time. Substitution of Rheb1 at Serine 16 with Histidine (S16H) makes it resistant to the inhibition of Tuberous Sclerosis Complex (TSC) thus yielding a more competent Rheb1 to activate mTORC1 (Yan, Findlay et al.).

Taking advantage of the knowledge that farnesylation of Rheb1 is required for its membrane association and function, we made forebrain lysates with ice cold 1% Triton-X 100 buffer from Postnatal (P)30 control and mutant mice (Yamagata, Sanders et al.). Ice cold 1% Triton-X 100 buffer lysis treatment is relatively non-denaturing thus preserves selective membrane association and integrity. SDS-PAGE followed by silver staining visualization procedures showed that anti-myc IP from mutants had a dramatic enrichment of proteins associated with Myc-Rheb1 compared to the anti-Myc IP in control brains (Figure 2A). More efficient elution of associated proteins were achieved with the addition Beta-MercaptoEthanol in the presence of 4% SDS in anti-myc IP from the mutant brains while no significant

difference was observed in the control IPs. “Lysates after IP” lane shows similar protein band pattern as “lysate input” lane demonstrates that protein integrity was preserved during the IP procedure. Next, we compared the same IP procedure in control and mutant forebrains prepared in RIPA with 0.1% SDS buffer. RIPA with 1% SDS buffer is a relatively stringent condition to examine protein associations (Figure 2B). SDS-PAGE followed by silver staining showed significant less association of proteins in the anti-myc IP compared with anti-myc IP in 1% Trition-X 100 buffer condition. Furthermore, only a few protein band signals were observed in the anti-myc IP sample from mutant brains while no significant protein band signals were detected in the anti-myc IP sample from control brains. We then examined anti-myc IPs from mutant and control brains for association with membranes by confocal microscopy. We treated the magnetic beads with a different myc antibody conjugated with Alexa-555 fluorophore to allow for visualization (Figure 2C). With 1% Triton-X 100 lysis condition, anti-myc IP from mutant brains showed large clusters of fluorescence where as anti-myc IP from control brains were void fluorescent signal. The fluorescent signal difference was consistent with the biochemical results found with SDS-PAGE and silver staining suggesting that 1% Triton-X 100 lysis treatment preserves association of myc-Rheb1 (S16H) with membranes and proteins. To identify proteins that associate with myc-Rheb1 (S16H) we provided elutions from anti-myc IPs to the Taplin Mass Spectrometry Facility at Harvard University for Liquid Chromatography-tandem mass spectrometry method (LC/MS/MS) analysis. We compared anti-myc IP samples from 1% Triton-X 100 with anti-myc IP samples from RIPA with 0.1% SDS (Figure

3A). Interestingly, proteins identified in 1% Triton-X 100 are enriched with receptors, ion channels, synaptic proteins, ubiquitinylating proteins and vesicle associated proteins. Moreover, subunits of lysosomal H+ ATPase were identified by LC/MS/MS analysis. This finding is consistent with previously published results that demonstrated Rheb1 associates with lysosomes to facilitate mTOR kinase activation (Zoncu, Bar-Peled et al.). Furthermore, the transmembrane proteins including GluR2 and other ion channels suggest that myc-Rheb1 (S16H) associates with trafficking endosomes possibly throughout endosome maturation process. It is also worth to note that kinases and phosphatases involved in signaling cascade such as protein phosphatase -1, -2 and calcium/calmodulin-dependent kinase II were also found to associate with myc-Rheb1 (S16H). LC/MS/MS analysis of elution samples from myc-Rheb1 (S16H) IP in RIPA with 0.1% SDS buffer yielded much less proteins (Figure 3B). This is likely due to the stringent and denaturing conditions of RIPA buffer with the addition of SDS. Proteins identified with this method are likely to be more stably associated or interact directly with Myc-Rheb1 (S16H). Interestingly, the list of proteins from two different anti-myc IP conditions did not overlap. It is worth to note that Rheb1 was the identified by LC/MS/MS in both IP methods and that the lists of proteins identified are not comprehensive. Encouraged by the LC/MS/MS data, we sought to identify other potential proteins associated with myc-Rheb1 with 1% Trition-X 100 lysis by Western blot analysis (Figure 4). Rheb1 immunoblot shows endogenous Rheb1 in both control and myc-Rheb1 (S16H) inputs. Myc-Rheb1 (S16H) showed an increase in molecular weight due to the myc epitope tag and was only identified in the myc-Rheb1 (S16H) lane as indicated. Furthermore, we

confirmed that myc-Rheb1 (S16H) was successfully enriched in our anti-myc IP (Figure 4A). Utilizing specific antibodies in multiple Western blot analysis we found that association of myc-Rheb1 (S16H) with GluR2, GluR4, Grip, NR1, mGluR5, Homer, Arc, Shank3 and various forms of APP (Figure 4B). Most of these proteins are localize to the synapse and participates in synaptic plasticity. However, these interactions are rather specific since not all synaptic proteins or membrane-associated proteins were found to interact with myc-Rheb1 (S16H) (Figure 4C). Moreover, we did not find components of the mTOR pathway to associate with the myc-Rheb1 (S16H). No significant signals were detected in immunoblots using specific antibodies for Rag GTPases, mTOR (Figure 4C) or TSC2 (data not shown). We did not find GluR1 to associate with the myc-Rheb1 (S16H) which parallels the findings in the sub-cellular fractionation experiment that GluR1 was not significantly enriched in the LP2 fraction (Figure 1B). Intrigued by the LC/MS/MS finding that myc-Rheb1 (S16H) associated with ubiquitin modification proteins and components of the degradation machinery such as lysosome and ubiquitin, we examined the anti-myc IP for enrichment of ubiquitinylated proteins. Ponceau staining of input lysate to anti-myc IP showed anti-myc IP yielded significantly less proteins as demonstrated by the reduced staining compared with input (Figure 4D). However, using a specific polyubiquitin antibody, Fk1, we observed that anti-myc IP enriched for polyubiquitinylated proteins in comparison to input. This result suggested that proteins associated with myc-Rheb1 (S16H) enriched for proteins destined for degradation via proteosome as well as lysosome pathways.

Previous studies have demonstrated that growth factors in serum and amino acids can stimulate mTORC1 kinase activity (Nobukuni, Joaquin et al.). We employed Human Embryonic Kidney 293 (HEK293) cells for mTORC1 functional studies. We depleted serum and amino acids by adapting HEK293 cells in Hank's Balanced Salt Solution (HBSS) for 2 h, which reduced mTORC1 activity to baseline demonstrated by p-s6 immunoblotting. With the addition of serum or amino acid for 20 minutes we were able to increased mTORC1 activity significantly. Following our observation that myc-Rheb1 (S16H) associated with ubiquitinylated proteins destined for proteosome processing, we tested whether inhibition of proteosome would reduce mTORC1 activity. Treatment with proteosome inhibitor, MG132 for 2 h in DIV-17 dissociated cortical neuron cultures derived from control or myc-Rheb1 (S16H) mice reduced mTORC1 activity (Figure 5B). Treatment with vehicle or MG132 did not alter MAP-kinase signaling shown by p-Erk immunoblot. It is worth to note that despite of the elevated mTORC1 activity in the myc-Rheb1 (S16H) over-expressing neurons cultures, MG132 was still able to reduce mTORC1 activity. Combining the results that amino acid stimulates mTORC1 activity and proteosome inhibition reduces mTORC1 activity, our finding suggest that amino acids generated from proteosome processing of proteins facilitate mTORC1 function. Next we tested whether inhibition of group 1 metabotropic receptors would alter mTORC1 signaling due to the observation that myc-Rheb1 (S16H) associates with mGluR5. Addition of Bay 36-7620 (an inverse agonist of mGluR1) and MPEP (a mGluR5 antagonist) for 2 h in DIV-17 dissociated cortical neuron cultures dramatically reduced mTORC1 activity (Figure 5B). Map-Kinase signaling pathway reductions

were observed in contrast to MG132 treatment demonstrated by p-Erk immunoblot. Consistent with dissociated cortical neuron culture experiments, intraperitoneal injection of AIDA, an mGluR1 antagonist and MPEP in P40 control mice also reduced both mTORC1 and MAP-kinase activity (Figure 5C). The reduction of mTORC1 activity was further substantiated by the observation that p-TSC2 was increased upon treatment with AIDA and MPEP, most likely due to the feedback regulation of mTORC1 to mTORC2.

Discussion

Our results suggest a model where Rheb1 is enriched in endosomal-like trafficking vesicles and associates proteins that are destined for degradation processes. The turn over of proteins generates amino acids thus activate mTORC1 activity (Figure 6). Rheb1 function and association with membrane is most likely through the CAAX domain, which allows for farnesylation modifications. Myc-Rheb1 (S16H) associates with membranes and a large yet specific set of proteins by immunofluroescence, immunoblotting and LC/MS/MS analysis. The specificity of the protein associations are demonstrated by the fact that many proteins are found in the same LP2 sub-cellular fractions as Rheb1, however only very specific interactors were identified. We found myc-Rheb1 (S16H) associates with and transport receptors such as GluR2 most likely after receptor endocytosis driven by synaptic activity, but not GluR1. We also found myc-Rheb1 (S16H) associate with ubiquitinylated proteins such as Shank3 and ubiquitinylation regulating proteins. These associations suggest myc-Rheb1 (S16H) may traffic proteins to either

lysosomes or proteosomes for degradation. Subsequent to the protein degradation process by the lysosome and or proteosomes, amino acids are generated which promotes mTORC1 translation to the lysosomal surfaces for activation via Rag protein complex (Bar-Peled and Sabatini). It is noteworthy that we found myc-Rheb1 (S16H) to specifically associate with a set of proteins from the LP2 fraction but not all of the proteins that were found in the LP2 fraction. This indicates that the associations are rather selective and not due to enrichment of the overall proteins in the LP2 fraction. Our finding that Rheb1 and mTOR are enriched in synaptic vesicle-enriched fractions by biochemical experiments supports this notion. Moreover, p-mTOR signal by Western blot analysis showed enrichment in the LP2 fraction indicating active mTOR is localized in the same fraction as Rheb1. In support that mTOR activity is dependent on amino acids availability, we found that inhibition of proteosomes with MG132 or amino acids withdraw reduces mTORC1 activity significantly. Addition of amino acids alone was able to rescue the mTORC1 activity in cells adapted to nutrient and amino acids free media.

Amyloid Precursor Protein (APP) is a synaptic transmembrane protein that is subjected proteo-cleavage events by Bace1 through endocytosis (Cole, Stock et al.). Previous studies showed that APP processing is activity dependent and regulated by Arc through the endosomal pathway (Wu, Petralia et al.). We found myc-Rheb1 (S16H) association with Arc, Amyloid Precursor Protein (APP) and fragments of processed APP by Western blot analysis in co-IP experiments. These association are intriguing as it suggest that myc-Rheb1 associates with endosomes that are involved in APP processing that is dependent on Arc. Base on previous studies that in

Alzheimer's Disease (AD) mTOR signaling is elevated, it would suggest that increase in APP processing due to mutations may drive endosome trafficking and elevate mTOR signaling through Rheb1 (Ma, Hoeffer et al.). Our findings provide addition protein and mechanistic therapeutic targets in AD treatment.

Curiously, we found interaction of Rheb1 with mGluR5 in a membrane dependent fashion as the association was preserved only with 1% Triton-X 100 treatment. We demonstrated that inhibition of group 1 metabotropic receptors results in reduction of mTORC1 activity. These results suggest a tight linkage between group 1 metabotropic receptors and mTOR activity. However, it is not understood as to the signal transduction mechanism of mGluRs to mTOR. Previous investigations have shown that stimulation of mGluR5 have positive impact on mTORC1 activity (Ronesi and Huber 2008). It will be important to determine whether mGluR signaling is couple on the plasma membrane or requires endocytic mechanisms. Investigations that demonstrate elegant TRKB and MAP-kinase signaling mechanism is dependent on endocytic machineries have previously been demonstrated (Harrington, St Hillaire et al.). Examinations to decipher if agonist induced activation of mGluR5 causes endocytosis of the receptor and association with Rheb1 to form a signalosome-like entity is warranted as the implications for underlying mGluR and mTOR signaling mechanisms are tremendous in learning and memory (Osterweil, Krueger et al.).

Together these findings suggest that basal synaptic activity driven protein turnover provides a baseline for mTORC1 activity level in the distal dendrite or at the synapse of neurons via turnover of synaptic proteins. Thus mTOR activity

responds in a synaptic activity-dependent manner. Subsequent intra- or extra-cellular may changes alter the mTOR pathway and impact mTORC1 integration function and outputs. Aberrant drives of the endocytic pathway due to enhanced protein turnover by ubiquitinylation or APP processing due to mutations would lead to a persistent mTORC1 activity and devastating outcomes.

A.

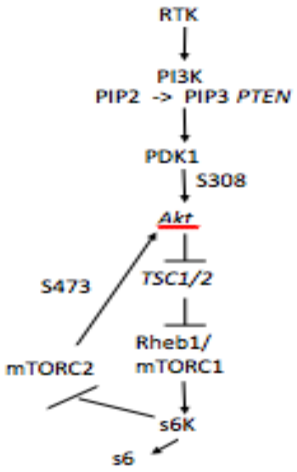
RTK
PI3K
PIP2 -> PIP3 PTEN
PDK1
S308
Akt
S473
TSC1/2
Rheb1/
mTORC2
mTORC1
s6K
s6

B.

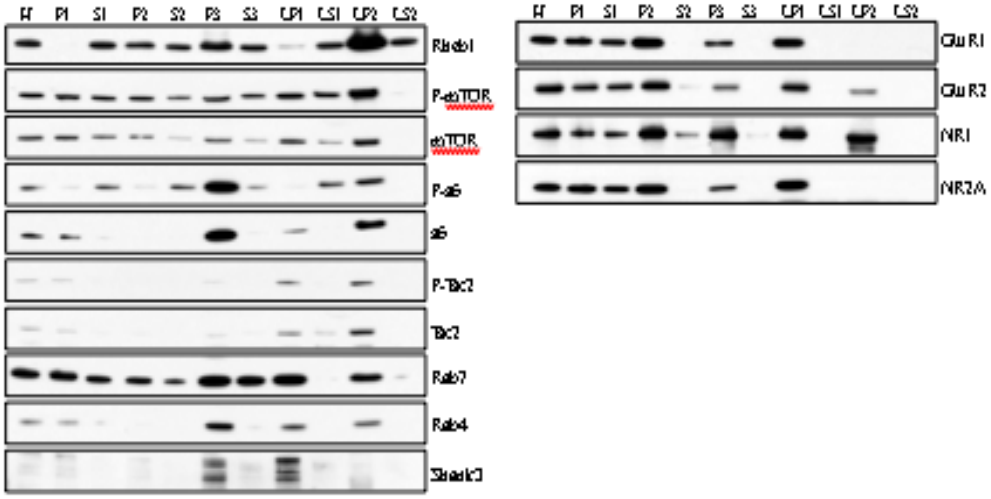
H P1 S1 P2 S2 P3 S3 UP1 LS1 UP2 LS2
Rheb1
P-mTOR
mTOR
P-s6
s6
P-Tsc2
Tsc2
Rab7
Rab4
Stard3
GluR1
GluR2
NR1
NR2A

C.

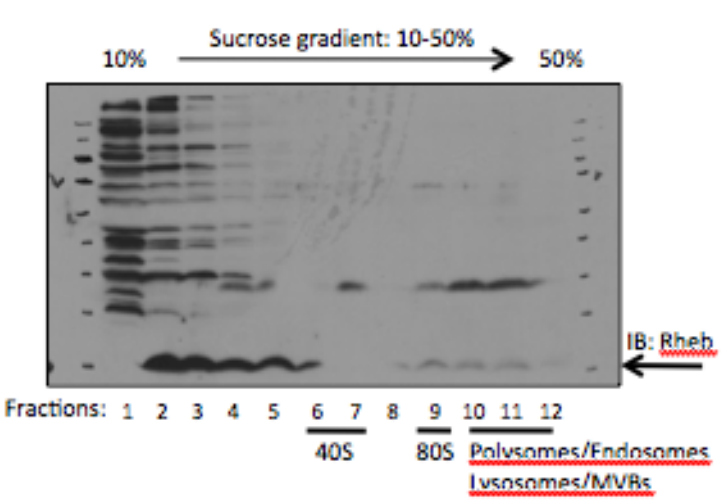
10%
Sucrose gradient: 10-50%
50%
IB: Rheb
Fractions: 1 2 3 4 5 6 7 8 9 10 11 12
40S
80S
Polysomes/Endosomes
Lysosomes/MVBs

Figure 1. Rheb1 is Enriched in Synaptic Vesicles. (A) Diagram of mTOR signaling pathway. **(B)** Subcellular localization of Rheb1, components of mTOR signaling pathway and glutamate receptor subunits. The isolated subcellular compartments from sucrose density centrifugation (without detergent), from P30 wild type mouse forebrain were examined by Western blot analysis. H, total homogenate; P1, nuclei and large debris; P2, crude synaptosomal membrane fraction; P3 light membrane fraction; LP1, synaptosomal membrane fraction: LP2, synaptic vesicle-enriched fraction. S1, S2, LS1, LS2 are supernatants from P1, P2, LP1 and LP2 respectively. **(C)** Rheb1 associates with trafficking machinery. Fractionation of subcellular compartments by continuous sucrose gradient (10-50%) and centrifugation followed by Western blot analysis of Rheb1.

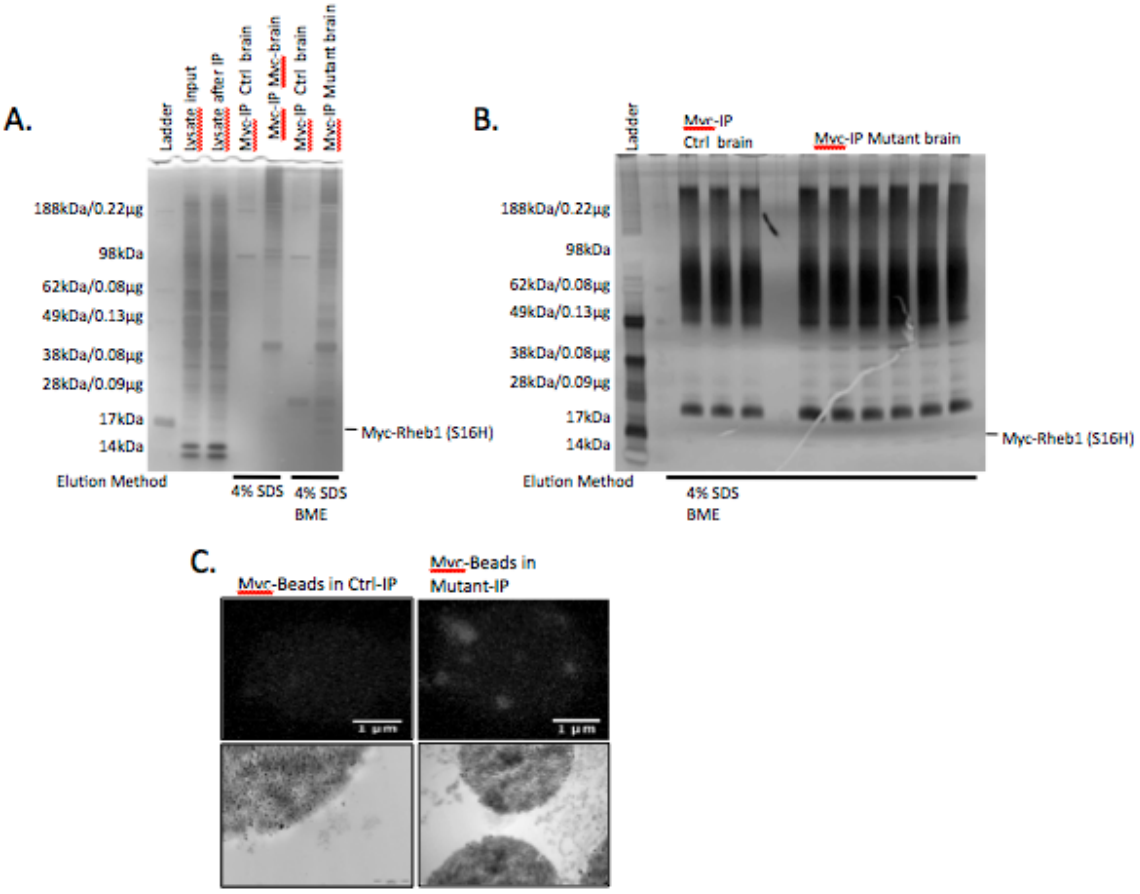
A.
Ladder
lysate input
lysate after IP
Myc-IP Ctrl brain
Myc-IP Myc-brain
Myc-IP Ctrl brain
Myc-IP Mutant brain
188kDa/0.22µg
98kDa
62kDa/0.08µg
49kDa/0.13µg
38kDa/0.08µg
28kDa/0.09µg
17kDa
14kDa
Myc-Rheb1 (S16H)
Elution Method
4% SDS
4% SDS BME
B.
Ladder
Myc-IP Ctrl brain
Myc-IP Mutant brain
188kDa/0.22µg
98kDa
62kDa/0.08µg
49kDa/0.13µg
38kDa/0.08µg
28kDa/0.09µg
17kDa
14kDa
Myc-Rheb1 (S16H)
Elution Method
4% SDS BME
C.
Myc-Beads in Ctrl-IP
Myc-Beads in Mutant-IP
1 µm
1 µm

Figure 2. Myc-Rheb1 (S16H) Associates with Membrane and Numerous Proteins. (A) SDS-PAGE followed by silver staining of cell extracts and anti-myc immunoprecipitations (IPs) prepared with 1% Triton-X 100 from P30 control and Nestin-Cre myc-Rheb1 (S16H) forebrains. **(B)** SDS-PAGE followed by silver staining of cell extracts and IPs prepared with RIPA buffer with 0.1% SDS from P30 control and Nestin-Cre myc-Rheb1 (S16H) forebrains. **(C)** Anti-myc antibody coupled magnetic beads incubated with forebrain lysates prepared as in (A) shows immunoisolated membrane associated complexes by electron microscopy (500 nm).

A.

Symbol	Entrez Gene Name
UBA1	ubiquitin-like modifier activating enzyme 1
UBE2N	ubiquitin-conjugating enzyme E2N (UBC13 homolog, yeast)
CACNA2D1	calcium channel, voltage-dependent, alpha 2/delta subunit 1
GRIA2	glutamate receptor, ionotropic, AMPA 2
STX1B	syntaxin 1B
EPHA4	EPH receptor A4
CAMK2A	calcium/calmodulin-dependent protein kinase II alpha
CNRIP1	cannabinoid receptor interacting protein 1
ANXA2	annexin A2
EFNB1	ephrin-B1
PRNP	prion protein
RTN4RL2	reticulon 4 receptor-like 2
SCARB2	scavenger receptor class B, member 2
AKAP4	A kinase (PRKA) anchor protein 4
GDI1	GDP dissociation inhibitor 1
MAPT	microtubule-associated protein tau
SSR4	signal sequence receptor, delta (translocon-associated protein delta)
SYTL3	synaptotagmin-like 3
ADAM22	ADAM metallopeptidase domain 22
DPP6	dipeptidyl-peptidase 6
BLMH	bleomycin hydrolase
NLN	neurolysin (metallopeptidase M3 family)
PSMA6	proteasome (prosome, macropain) subunit, alpha type, 6
SEC11A	SEC11 homolog A (S. cerevisiae)
THOP1	thimet oligopeptidase 1
PPP3CB	protein phosphatase 3 (formerly 2B), catalytic subunit, beta isoform
PTPRD	protein tyrosine phosphatase, receptor type, D
IMPA1	inositol(myo)-1(or 4)-monophosphatase 1
PPP1CA	protein phosphatase 1, catalytic subunit, alpha isoform
PPP2R1A	protein phosphatase 2 (formerly 2A), regulatory subunit A, alpha isoform
PPP3CA	protein phosphatase 3 (formerly 2B), catalytic subunit, alpha isoform
UBA52	ubiquitin A-52 residue ribosomal protein fusion product 1
ABCA1	ATP-binding cassette, sub-family A (ABC1), member 1
ATP1A1	ATPase, Na+/K+ transporting, alpha 1 polypeptide
SLC1A1	solute carrier family 1 high affinity glutamate transporter member 1
SYNGR1	synaptogyrin 1
TFRC	transferrin receptor (p90, CD71)
ATP6V0D1	ATPase, H+ transporting, lysosomal 38kDa, V0 subunit d1
ATP6V1A	ATPase, H+ transporting, lysosomal 70kDa, V1 subunit A
ATP6V1B2	ATPase, H+ transporting, lysosomal 56/58kDa, V1 subunit B2
ATP6V1E1	ATPase, H+ transporting, lysosomal 31kDa, V1 subunit E1
NSF	N-ethylmaleimide-sensitive factor
SV2A	synaptic vesicle glycoprotein 2A
SYT1	synaptotagmin I
TMED10	transmembrane emp24-like trafficking protein 10 (yeast)

B.

Symbol	Entrez Gene Name
LAMC1	laminin subunit C1
LAMB2	laminin subunit B2
LAMA5	laminin subunit A5
Actin	Actin beta
TBA1A	Tubulin Alpha
C1QB	Complement C1 subunit QB
ELAV4	Elavl like protein
GAP	Glyceraldehyde
H2A1F	Histone H2A
H4	Histone 4
H2B1A	Histone H2B
MYL6B	Myosin
H12	Histone 1
MBP	Myelin basic protein

Figure 3. LC/MS/MS Identifies Synaptic Trafficking Proteins and Receptors from Anti-mvc Immunoprecipitation of Myc-Rheb1 (S16H). (A) Sample proteins found by LC/MS/MS from Anti-mvc Immunoprecipitation (IP) from P30 forebrains extracts of myc-Rheb1 (S16H) mice in 1% Triton-X 100. **(B)** Sample proteins found by LC/MS/MS from anti-mvc IP from P30 forebrain extracts of myc-Rheb1 (S16H0 mice in RIPA + 0.1% SDS buffer.

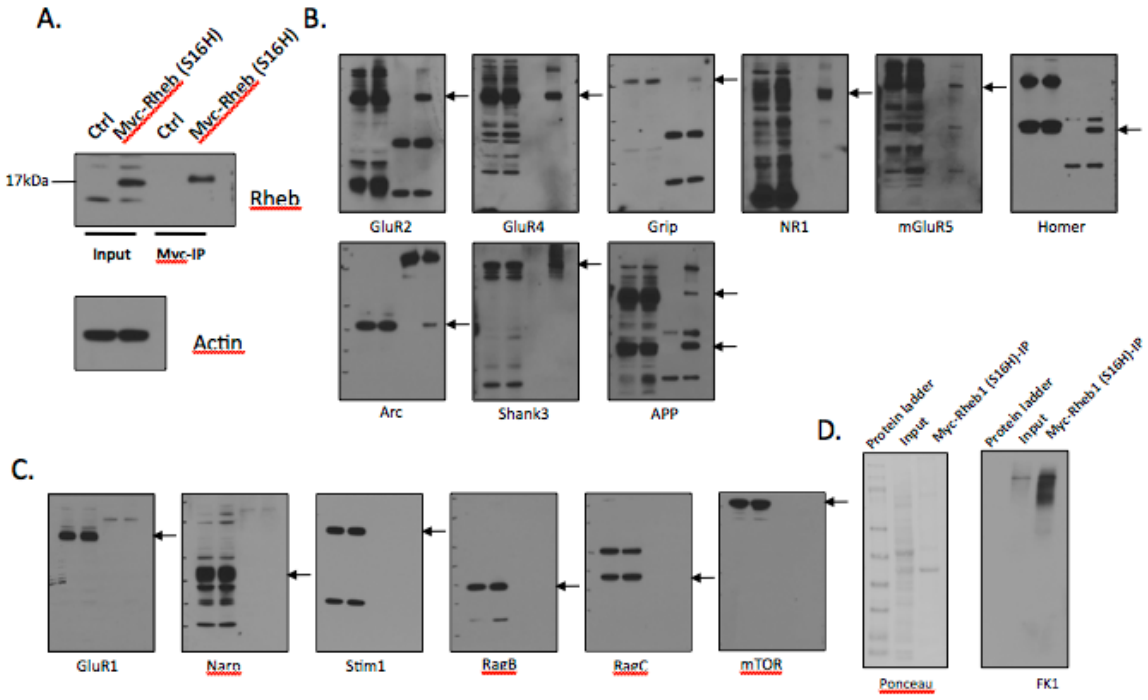

Figure 4. Myc-Rheb1 (S16H) Associates with Specific Set of Synaptic Proteins and Degradation Signal. (A) Western blot analysis of myc-Rheb1 (S16H) immunoprecipitation (IP) with Rheb1 antibody. **(B)** myc-Rheb1 (S16H) co-immunoprecipitated (co-IP) with GluR2, GluR4, Grip, NR1, mGluR5, Homer, Arc, Shank3 and APP by Western blot analysis. **(C)** myc-Rheb1 (S16H) did no co-IP GluR1, Narp, Stim1, RagB, RagC or mTOR by Western blot analysis. **(D)** Ponceau S staining shows proteins from forebrain lsvate prepared from myc-Rheb1 (S16H) and proteins associated after IP. Ubiquinated proteins were visualized with anti-FK1 antibody by Western blot analysis.

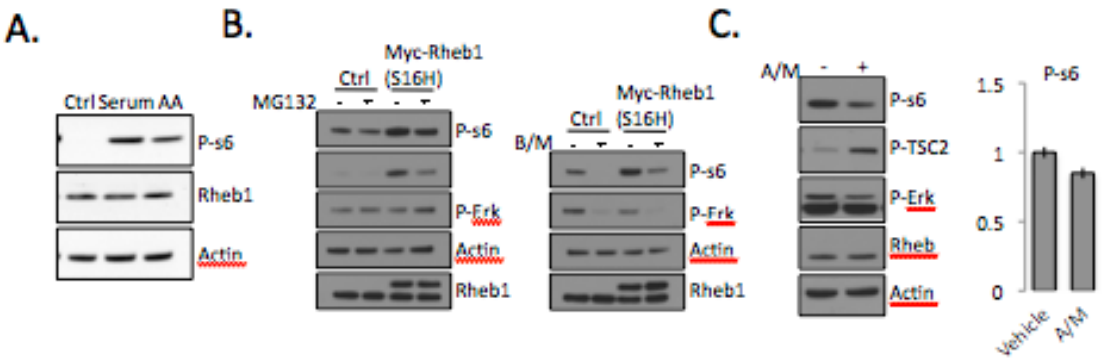

Figure 5. mTORC1 Activity is Dependent on Amino Acid, Proteosome and mGluR1/5. (A) HEK 293 cells were adapted to HBSS for 2h followed with treatment with 2% serum or amino acids for 20 mins. **(B)** DIV-21 dissociated cortical neuron cultures from control and Nestin-Cre myc-Rheb1 (S16H) mice were a proteosomal inhibitor MG132 (25µM) or mGluR1/5 inhibitors Bay (10µM)/MPEP (5µM) for 2. **(C)** Forebrain lysates from P40 wild type mice that were injected with mGluR1/5 inhibitors AIDA (5mg/kg)/MPEP (30mg/kg) or vehicle (i.p) for 1 h. (A-C) Cell or forebrain lysates were analyzed by Western blot analysis with the indicated antibodies.

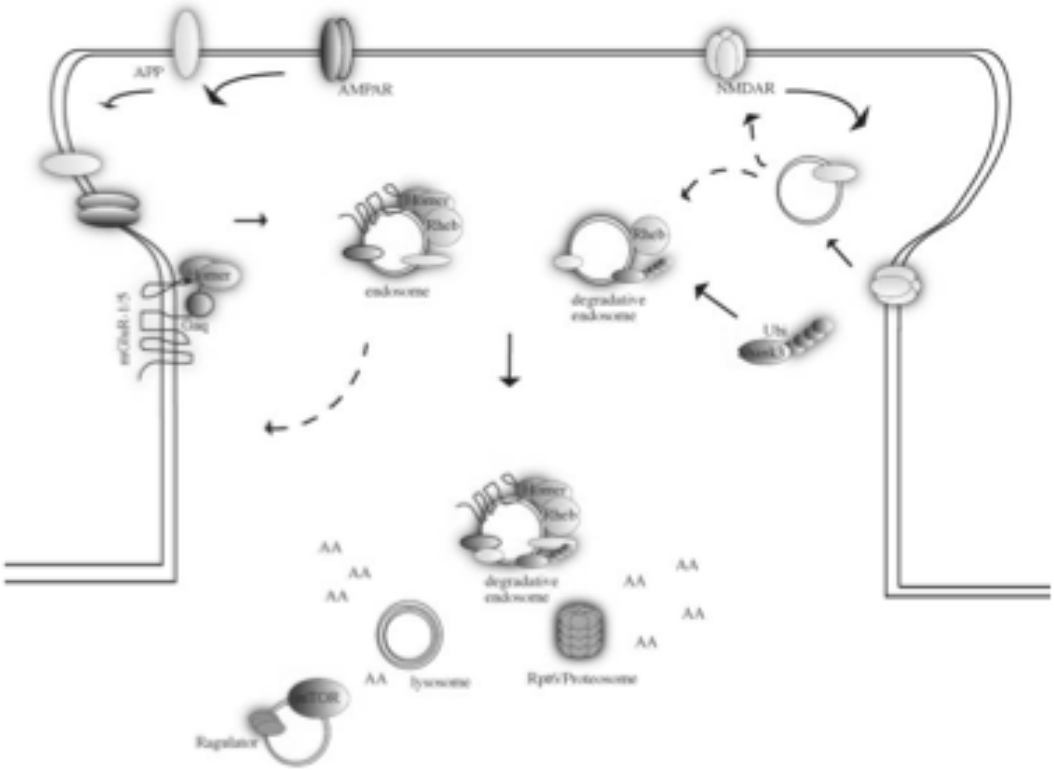

Figure 6. Model of Activity-Dependent Synaptic Protein Turnover Controls mTORC1 Signaling Via Trafficking of Rheb1.

CHAPTER 5:

Calcium dependent regulation of mTORC1 signaling.

Introduction

Calcium signals are fundamental to numerous types of synaptic plasticity events including LTP and LTD (Yasuda). In pilot studies described here, we found that elevation of intracellular Ca2+ can activate mTORC1. Biochemical studies that assay phosphorylation of Akt and TSC suggest that Ca2+ activates mTORC1 by a mechanism that is distinct from canonical growth factor or receptor-activated mTORC1. This "non-canonical" mechanism may be important in diseases such as Alzheimer's disease, as a mechanism for persistent activation of mTORC1. My studies further suggest a role Ca2+ influx through Orai channels gated by STIM1 as a mechanism for Ca2+ influx-dependent activation of mTORC1, and provide one of the rationales for detailed studies in STIM1 KO mice (Chapter 6).

Results

We crossed CamKII-Cre with floxed Rheb1 mice to generate CamKII-Cre mediated Rheb1 knockout mice (Rheb1-KO). Rheb1-KOs also did not display any gross anatomical or phenotypical abnormalities. The excision of Rheb1 and alterations of the mTOR signaling pathway were examined by Western blot analysis of forebrain lysates derived from Rheb1-KOs and littermate controls (Figure 2). Rheb1-KOs showed a selective deficit for mTORC1 signaling as demonstrated by reduced phosphorylation of s6. The reduction of S6 kinase activity reduces the negative feed back loop on mTORC2, thus leading to an increase in phosphorylation of Akt S473 and TSC2. In order to dissect the pathways that affect mTOR signaling we utilized the cortical neuron culture system derived from homozygous, heterozygous Rheb1-KOs and control mice. Cultured neurons derived from Rheb1-KOs showed a loss of mTOR-mediated phosphorylation of s6 (Figure 3). VDCC activation has been demonstrated to play crucial role in various forms of LTP (Kato, Kassai et al.). Treatment with a VDCC agonist, BayK S-, led to an increase in intracellular calcium concentration and enhanced mTORC1 activity in the floxed (F/F) and heterozygous KO (Het) in the neurons but not in the Rheb1-KO neurons. Furthermore, treatment with Rapamycin in combination with BayK S- diminished the phosphorylation of s6 demonstrating that the phosphorylation of s6 is dependent on mTOR signaling. mTORC1 activation in this set of experiments showed that basal and stimulated mTORC1 activity responds in a Rheb1 dose dependent manner.

We examined further the observation that VDCC stimulation can activate mTORC1 signaling (Figure 4). In WT neuronal cultures, application of BayK S- did not lead to any significant changes in the kinase cascade of the known upstream activators of mTORC1 such as Akt and TSC2. As expected, addition of 10-DEBC, a specific pharmacological inhibitor of Akt, resulted in a reduction of s6 phosphorylation. However, this reduction was reverted upon application of BayK S-. Immunoblotting of known upstream activators of mTORC1 demonstrated that inhibition of Akt lead to a subsequent disruption of phosphorylation in Akt, TSC2, and mTOR suggesting that calcium activation of mTORC1 is not through the canonical pathway. The decrease in mTORC1 activity by 10-DEBC applications in the cultures also resulted in an increase in eEF2 phosphorylation (T56). P-eEF2 is dependent on eEF2 kinase, which is inhibited by mTOR to facilitate elongation in the protein translation step. The combination treatment of 10-DEBC and BayK S- led to a slight increase in the phosphorylation of mTOR (S2448) suggesting that mTOR is activated. Concurrent with the rescue of P-s6, eEF2 phosphorylation was also slightly reduced, suggesting a rescue of mTORC1 function. Rheb1 levels were examined to confirm that the change in mTORC1 activity was due to signal transduction cascade rather than variation in Rheb-1 protein levels.

Next, we examined whether mTORC1 signaling would be affected by the inhibition of Ca^{2+} influx. SKF 96365 was utilized to inhibit wide range of Ca^{2+} channels including TRPC family and Orai channels (Figure 5). P-s6 was drastically reduced upon treatment with SKF 96365, at the same time that P-eEF2 increased. There were no apparent changes in the canonical mTOR signaling pathway

suggested by the preserved level of P-Akt. Other Ca^{2+} channel inhibitors such as a stereoisomer of BayK S- also blocked signaling mediated by mTORC1 (data not shown).

In combination with pharmacological manipulations, we utilized biochemical and molecular approaches to examine Ca2+ and activation of mTORC1. Previous investigations have characterized the mechanisms of calcium store activation and refilling (Soboloff, Rothberg et al.). Orai activating fragment of STIM1, termed Stim-Orai-Activation-Region (SOAR), can trigger calcium influx from extracellular space through the plasma membrane (Yuan, Zeng et al.). Orai mRNA is expressed in brain. Expression via Sinbis virus encoding GFP-tagged SOAR in dissociated neuron cultures resulted in robust increase in mTORC1 activity (Figure 6). At the time I did these experiments, SOAR was thought to be entirely specific for Orai channels. However, recent studies suggest SOAR may also activate VSCC. Accordingly, these studies will need to be extended by additional approaches to directly implicate Orai. For example, we could check that this effect is not blocked by VSCC antagonists, or that effects of SOAR are absent in Orai1/2/3 KO neurons.

The lack of a calcium responsive participant in the well-studied canonical mTORC1 activating pathway lead me to a pharmacological screen of calcium sensitive proteins that may modulate mTORC1 activity. Cortical neurons were treated with 10-DEBC, W7, a relatively selective Ca^{2+}/Calmodulin inhibitor, or the combination of both (Figure 7). W7 treatment of neuron culture eliminated pS6. Inhibition of Akt with 10-DEBC also reduced pS6. BayK S- in the presence of W7 did not rescue the loss of mTORC1. This contrasts with the previous experiment where

BayK S- was able to rescue the inhibitory effect of 10-DEBC, and suggests that Ca^{2+}/Calmodulin may be a calcium responsive modulator of mTORC1 that is not dependent on Akt. Published studies have shown that activation of Mitogen Activated Protein Kinase (MapK) pathway may lead to phosphorylation of s6 via the activation of TSC2 or s6 kinase (Ronesi and Huber). I used U1026, a specific MapK inhibitor, to exclude this possible mechanism as a mediator of the Ca^{2+} activation of mTORC1. In the presence of U1026, phosphorylation of Erk was abolished, however, Ca^{2+} flux by the addition of BayK S- compound was still able to activate mTORC1 (Data not shown).

Having implicated a non-canonical pathway that can bypass the canonical pathway to activate mTORC1, we examined if the vice versa regulation would be possible. In cortical neurons treated with insulin, and BayK S- was able to increase mTORC1 activity. Inhibition of Ca^{2+}/Calmodulin with W7 abolished mTORC1 activity and BayK S- was not able to rescue mTORC1 activity in the presence of W7 (Figure 8). However, the addition of insulin rescued mTORC1 activity in the presence of W7. This suggests that W7 does not block canonical signaling to activate mTORC1.

Based on the preceding findings, I hypothesized that non-canonical activation of mTORC1 might occur when pS6 increases in the absence of increases of AKT308 phosphorylation. I then examined mice that were engaged in a learning protocol that could invoke LTP-like plasticity in hippocampus. 4 weeks old mice were individually caged and desensitized for 7 days. On day 7, brains from Control and Rheb1-KO mice were isolated from either cage controls or after being subjected to

activity chamber for 10 min. The brain was dissected sagittally into halves. Immunostaining showed increase p-s6 levels in the Dentate Gyrus, CA3 and CA1 region in the animals that engaged in exploration compared to caged controls. Immunoblotting confirmed an increase in pS6. However, with phospho specific antibodies against the canonical pathway did not show increased phosphorylation of PDK1, Akt, or TSC2 (Figure 9). Western blot analysis also indicated that the signaling by MapK pathway in the explored group was not significantly more than the control caged group (data not shown). This preliminary result suggests that the activation of mTORC1 in the in-vivo exploration paradigm is due to the activation of a non-canonical pathway.

Ca2+ signaling is reportedly disrupted in neurons that express APPswe/PS1Δe9 transgene. We examined dissociated cortical neuron cultures derived from WT and APP_{Swe}/PS1 on DIV-14 for basal mTORC1 activity and insulin response. Western analysis showed an increase of p-s6 in neurons derived from APP_{Swe}/PS1 at the basal level upon comparison with control neurons (Figure 10). In contrast to control neurons, APP_{Swe}/PS1 neurons were no longer sensitive to Insulin stimulation. Immunoblotting of p-IRS showed a slight increase of signal in APP_{Swe}/PS1 neurons, suggesting that elevated mTORC1 activity feeds to IRS to inhibit insulin stimulations. To examine the feedback inhibition in more detail, we looked at Phosphoinositol dependent kinase 1 (PDK1), a kinase responsive to PI3K activation. Insulin receptor activation causes dimerization of its subunits clustering insulin receptor substrate leading to phosphorylation and activation of PI3K. Subsequently, PI3K phosphorylates PIP2 and produces PIP3 that triggers the

activation of PDK1. PDK1 in APP_{Swe}/PS1 neurons was not activated with the treatment of insulin in contrast to the control neurons.

Discussion

The presented studies suggest the existence of a non-canonical mTOR activation pathway via calcium signals, which is also Ca^{2+}/Camodulin dependent. These observations offer an interesting alternative to the canonical mTOR activation cascade, which does not include any calcium responsive participants. The non-canonical mTOR activation pathway via calcium signals are particularly intriguing in cell types that harbor extensive numbers of calcium channels and are extremely sensitive to varying calcium concentrations such as lymphocytes, cardio-myocytes and neurons. Dynamic calcium fluxes in these cell types mediate cellular functions such as contractions, differentiations, and modifications of synaptic efficiency (Efe, Hilcove et al.) (Oh-Hora, Yamashita et al.) (Zamponi and Currie). In neuron culture preparations we used pharmacological modulators of calcium channels and molecular expression constructs modulating CRAC and STIM1 to demonstrate a direct correlation of mTOR activity with calcium availability. Increasing calcium influx with stimulation of VDCC or expression of SOAR increased mTORC1 activity while inhibition of VDCC, TRPC or expression of dominant negative SOAR and ORAI reduced mTORC1 activity in our studies. Moreover, through a pharmacological screen, we identified Ca^{2+}/Calmodulin has a candidate mediator of the non-canonical mTORC1 signaling using W7 compound. Characterization of the molecular pathway mediating the calcium response in the mTOR pathway revealed that the

canonical pathway was not involved. Using 10-DEBC, we demonstrated that calcium activation of mTORC1 pathway did not require the canonical activation of Akt. In addition, we were able to activate mTORC1 signaling by stimulation with Insulin in the presence of W7. These results suggest the existence of separately regulated canonical and non-canonical mTORC1 signaling pathway (Figure 11). Furthermore, using *in vivo* exploration activity experiments that activate L-type VDCC in hippocampus, findings suggest that a non-canonical mTORC1 signaling pathway mediates the increase in mTORC1 signaling.

Alzheimer's Disease (AD) has been highly associated with impairment of cognitive function, which reduces to interrupted function at the neuronal synapses (Selkoe). As compelling mouse models, which over-express the APP_{Swe} human transgene in the background with a Presenilin-1 ∇e9 mutation have been well established, it provides a platform for careful dissection of the contributing factors to the disease. Correlation between disruptions in Ca^{2+} homeostasis and AD has been well established after the initial presentation of the "Calcium hypothesis for Alzheimer's Disease and brain aging" by Zaven Khachaturian in 1989 (LaFerla). Evidences of human and mice models demonstrating alterations in calcium signaling during the initial phase of the disease before development of symptoms have been provided. Furthermore, careful studies have demonstrated that APP/Swe/PS1 transgenic mice with cortical plaques have disrupted spine-dendritic calcium compartmentalization and regulations, which are highly regulated *in-vivo* (Kuchibhotla, Goldman et al.). The increase in intracellular Ca^{2+} levels, $[Ca^{2+}]_I$, has been correlated with Aβ generated from APP by the γ-Secretace, Bace1, by forming

Ca^{2+} permeable pores at the plasma membrane. Another possible contributing factor to the rise in $[Ca^{2+}]_i$ is the PS1 ∇e9 mutation, which enhances IP3R induced Ca^{2+} release from the ER (LaFerla). Recent studies have linked hyper mTORC1 activity with AD by the observation that mTOR and its target eIF4-EBP were highly phosphorylated (Li, Alafuzoff et al.). In a separate study, the over-active mTORC1 signaling can be further correlated with the observation that APP transgenic mice have an increase in cortical neuron size implicative of the establish role of mTORC1 function in cell size growth (Ohne, Takahara et al.). Furthermore, mTORC1 has been shown to facilitate the translation of Tau, a protein when hyper-phosphorylated is a hallmark AD pathology. (Liu, Zhou et al.). The facilitated translation is through the signature 5'TOP sequence motif found in 5' UTR region of the mRNA, which highly regulated and specific to the function of mTORC1. Interestingly, insulin resistance as well as increased phosphorylation of the Insulin Receptor Substrate-1 (IRS-1) indicative of inactivation by mTORC1 has been observed (Moloney, Griffin et al.). Insulin induced signaling of Akt/mTORC1 can also be described as the canonical mTORC1 signaling pathway. The paradoxical observation that mTORC1 signaling is elevated while IRS-1 is inactive presents an interesting platform for studying the relative contributions of the canonical and non-canonical pathway in mTORC1 signaling. Combining the loss of homeostasis regulation of Ca^{2+} and rise of $[Ca^{2+}]_i$ with the observation that mTORC1 is overactive, the working model is such that the non-canonical pathway is over represented in AD thus feeding back to IRS-1 and inhibiting the canonical pathway.

Utilizing cultured neurons derived from mouse models of AD we found increased mTORC1 activity in comparison with control neurons. Moreover, cultured neurons from AD mouse models were not sensitive to Insulin stimulation. These findings suggest that the increase in basal mTORC1 activity due to the activation of non-canonical pathway is capable of eliciting the well-characterized feedback inhibition to the insulin receptor, thus blunting normal response to extracellular stimuli. The lack of response to insulin stimulation in AD brains have been studied, discussed and often termed as "Type III diabetes" by other researchers (de la Monte). Future experiments to dissect the non-canonical pathway will be necessary to gain further understanding of the role that it plays in AD pathology.

A published study suggests that amino acids activate mTORC1 via Ca^{2+}/Calmodulin signaling to a PI3K class III member, VPS-34 (Gulati, Gaspers et al.). Upon the characterization of VPS-34 in the non-canonical pathway, it may present as a valuable target to specifically disrupt the non-canonical pathway in the AD model. shRNA mediated knock down of VPS-34 would be utilized to inhibit the non-canonical pathway in attempt to restore the sensitivity of the canonical pathway.

The presented data suggest that Transient Receptor Potential Cat-ion Channel (TRPC), VDCC, and stores from the endoplasmic reticulum (ER) can provide a source of calcium to modulate mTORC1. It would be an objective to resolve the course that calcium takes from these channels and stores. One possibility is that the calcium enters through the calcium channels and raises intracellular calcium concentrations directly. Another potential mechanism would be that calcium enters through channels and fills the calcium store in the ER then subsequently raises the

intracellular levels. The two contrasting paths of Ca^{2+} flux may be differentiated with the recent identification of Ca^{2+} release-activating Ca^{2+} channel (CRAC) Orai, and Stromal Interaction molecule (STIM). STIM is the transmembrane Ca^{2+} sensor located on the ER that activates Orai upon store depletion for refilling store calcium. Such an investigation allows for the understanding of the role that calcium, as a second messenger, dynamically regulate protein translation to facilitate plasticity events (Soboloff, Rothberg et al.).

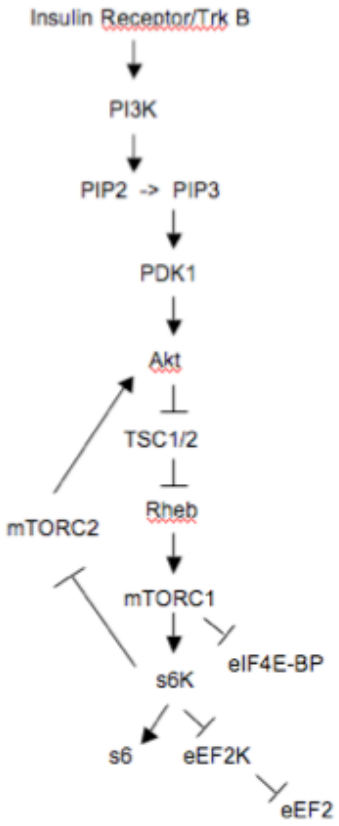

Figure 1. Diagram of mTOR Signaling Pathway.

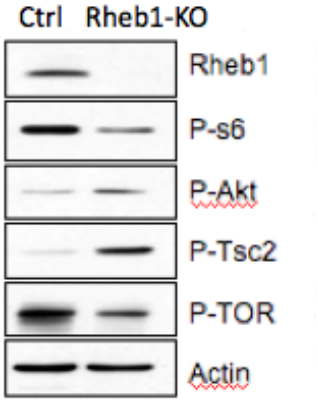

Figure 2. CamKII-Cre Mediated Rheb1 Knockout Shows mTORC1 Pathway Disruption. Western blot analysis of mTOR1 signaling pathway from forebrain lysates of P25 conditional knockout (Rheb1-KO) and littermate control (Ctrl) mice.

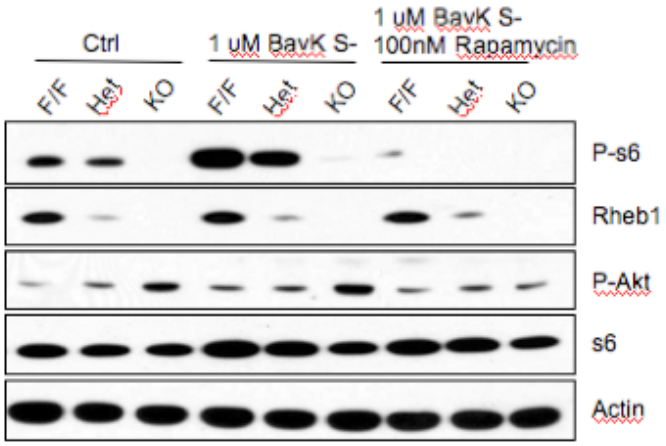

Figure 3. Rheb1 is Essential for Calcium Mediated mTORC1 Activation. Western blot analysis of cell lysates from DIV-14 dissociated cortical neuron cultures derived from floxed (F/F), Heterozygous knockout (Het) or Nestin-Cre Rheb1 knockouts (KO) that were treated with vehicle or Rapamycin (100 nM), a selective mTOR inhibitor, for 3 h followed by BavK S- (1 µM) , a selective VDCC agonist, for 1 h.

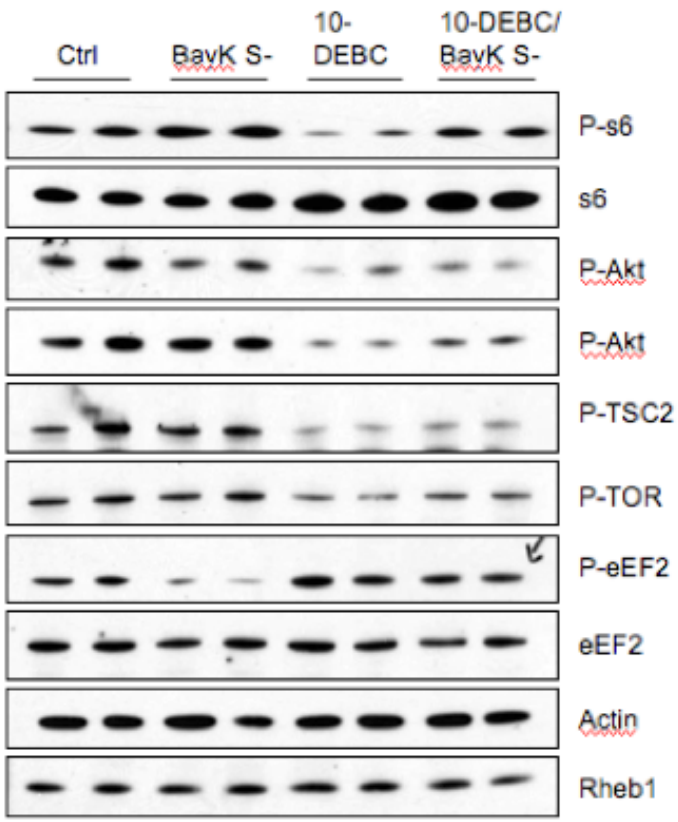

Figure 4. Calcium Activates mTORC1 Through a Non-canonical Pathway. Western blot analysis of cell lysates from DIV-14 wild type dissociated cortical neuron cultures treated with vehicle or a selective Akt inhibitor, 10-DEBC (10 µM), BayK S- (1 µM) for 1 h or a combination treatment of 10-DEBC (10 µM) 1 h followed by BayK S- (1 µM) for 1 h.

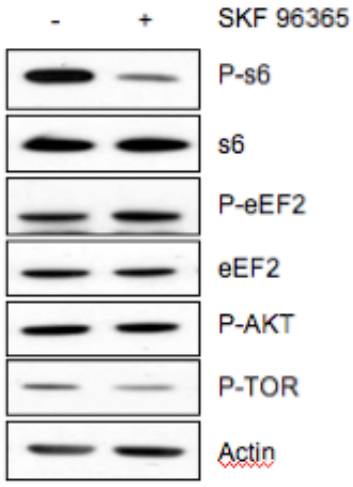

Figure 5. Inhibition of TRPC Channels Reduces mTORC1 Activity. Western blot analysis of cell lysates from DIV-14 wild type dissociated cortical neuron cultures treated with vehicle or TRPC channel inhibitor, SKF 96365 (10 µM) for 30 min.

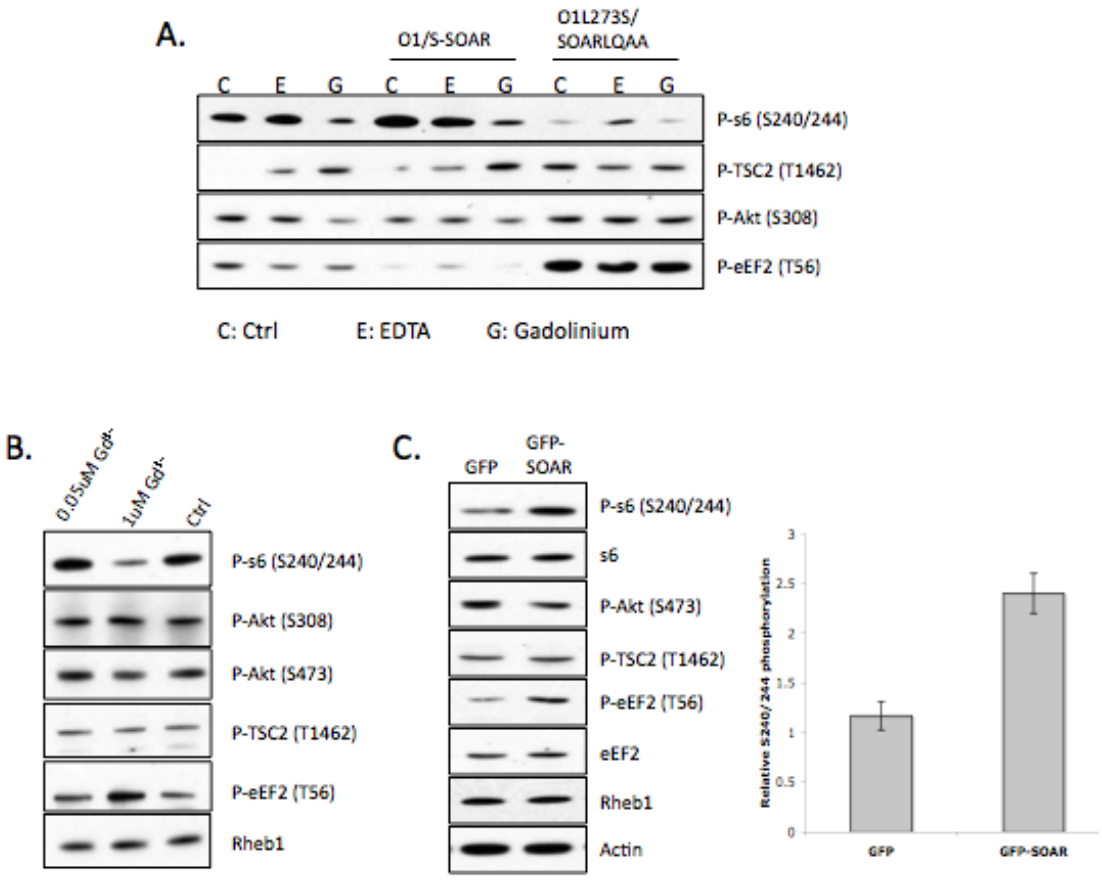

Figure 6. mTORC1 Activity is Coupled to Store-operated Calcium Entry. (A) HEK293 cells over-expressing constutively active store-operated calcium molecules, Orai1/S-SOAR or dominant negative versions O1L273S/ SOARLQAA were treated with calcium chelator EDTA (2 mM), or Orai channel inhibitor Gd^{3+} (1 µM) for 30 min. **(B)** DIV-17 wild type dissociated cortical neuron cultures were treated with vehicle or Gd^{3+} (50 nM or 1 µM) for 1 h. **(C)** Western blot analysis of cell lysates from DIV-17 dissociated cortical neuron cultures infected with Sinbis virus encoding GFP as control or GFP-SOAR for 10 h. Statistical analysis of p-s6 normalized to Actin (n =3). Mean value presented ± SEM. **(A-C)** Cell lysates were examined by Western blot analysis utilizing indicated antibodies.

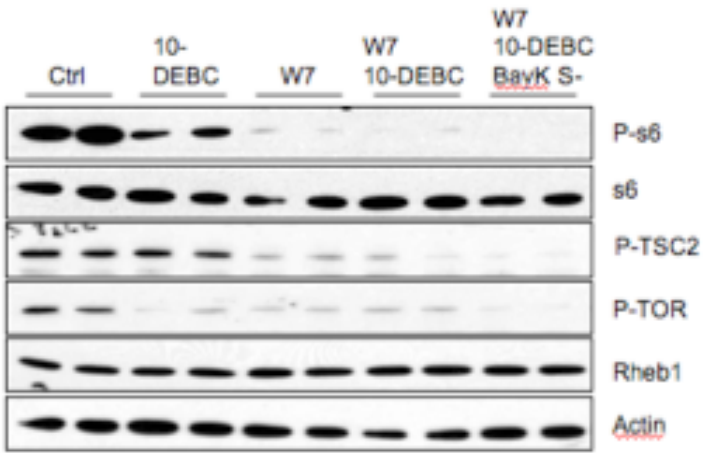

Figure 7. Ca^{2+}/Calmodulin Mediates Non-canonical mTORC1 Activation. Western blot analysis of cell lysates from DIV-14 wild type dissociated cortical neuron cultures that were treated with vehicle or 10-DEBC (10 µM), a selective Ca^{2+}/Calmodulin inhibitor W7 (50 µM) or a combination of 10-DEBC and W7 for 1 h followed by BayK S- (1 µM) for 1 h.

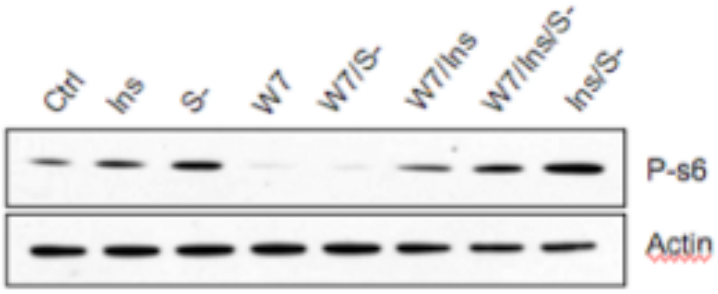

Figure 8. Canonical and Non-Canonical mTORC1 Signaling Pathway are Not Interdependent. Western blot analysis of cell lysates from DIV-14 wild type dissociated cortical neuron cultures that were treated with vehicle, Insulin (Ins) (150 nM), BayK S- (1 µM), W7 (50 µM), Insulin and BayK S- for 1 h or a combination of W7 for 1 h followed by Insuin and/or BayK S- for 1 h.

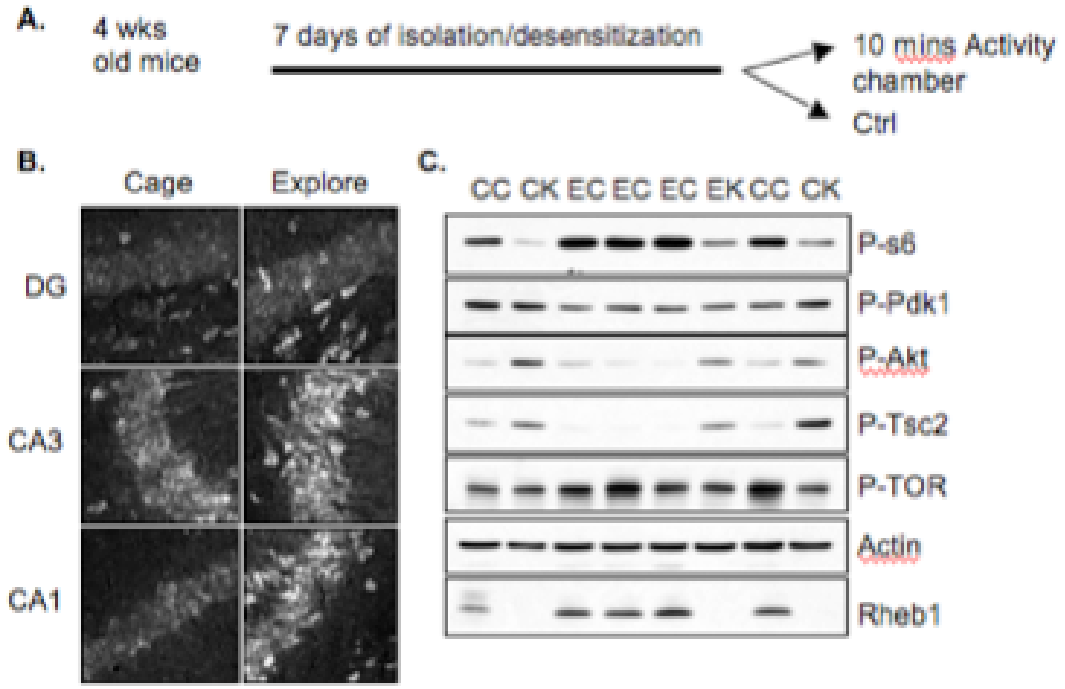

Figure 9. Novel Exploration Activates mTORC1 via Non-canonical Signaling Pathway. (A) Illustration of novel exploration experimental paradigm tested with P40 control and CamKII Cre Rheb1 knockout male mice (KO). **(B)** Immunohistochemistry studies of Dentate Gyrus (DG), Cornus Ammonis area 1 (CA1), and Cornus Ammonis region 3 (CA3) in hippocampus of wild type mice after control or exploration experiments using p-s6 antibody. **(C)** Western blot analysis of hippocampal lysates from experimental conditions described in (A). Caged control (CC); Caged KO (CK); Explored control (EC); Explored KO (EK).

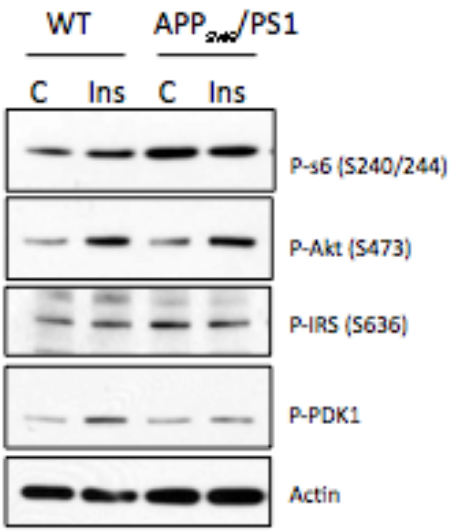

Figure 10. APP_{swe}/ΔPS1 Expressing Neurons Show Inhibition of Canonical mTORC1 Signaling. Western blot analysis of lysates from DIV-1 wild type or APP_{swe}/ΔPS1 derived dissociated cortical neuron cultures that were treated with vehicle or Insulin (Ins) (150 nM) for 20 min.

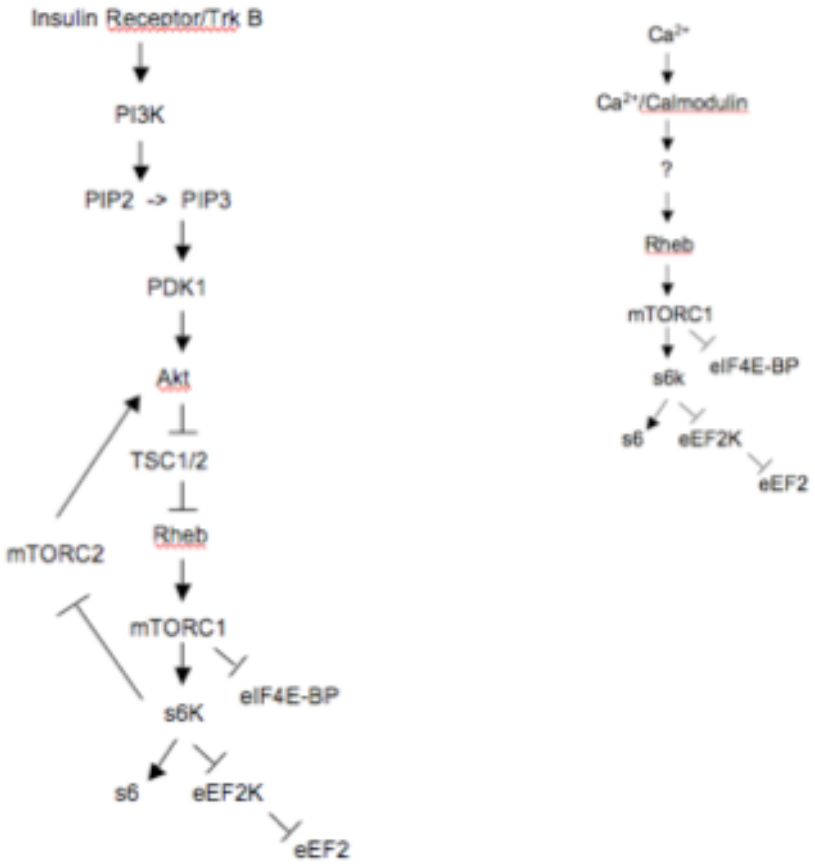

Figure 11. Diagram of canonical and non-canonical mTORC1 Signaling Pathway.

CHAPTER 6:

STIM1 regulates hippocampal NMDA-LTD through Calcinuerin

Introduction

My preliminary studies in Chapter 5 suggested that Ca2+ entry through Orai or other store-dependent ion channels may be important in activation of mTORC1, and other aspects of synaptic physiology. Recent advances in understanding the molecular basis of Ca2+ entry into cells via non-voltage sensitive channels lead me to focus on these pathways and their role in synaptic plasticity.

Calcium mobilization underlies essential processes to achieve different forms of plasticity in a neuron. In addition to calcium import from extra-cellular space, ER store calcium releases into the cytosol also have a significant role in many forms of synaptic plasticity (Woods and Padmanabhan) (Bogeski, Kilch et al.). Recent research has demonstrated that the induction of LTP and LTD can be blocked by prior depletion of ER calcium with compounds such as thapsigargin (Wang, Rowan et al.). Furthermore, studies have shown that mice that lack Ryanodine receptor (RyR3) have impaired LTD, while mice that lack type 1 Inositol Phosphate (IP_3) receptors have enhanced LTP. It has also been suggested that the dynamic function and modulation of store Ca^{2+} may be the underlying mechanism differentiating homo- vs. heterosynaptic plasticity (Fitzjohn and Collingridge). The long sought after molecules that contribute mediate the Ca^{2+} during Store-Operated Ca^{2+} Entry (SOCE) was identified through an RNAi screen reported in 2006. Stromal Interacting

Molecule 1 and 2 (STIM1, STIM2) are type-I membrane protein and detects store calcium by its EF-Hand domain located in the lumen of the ER. The EF hand domain of STIM1 has a $K_{1/2}$ of approximately 200-600μM for Ca^{2+} while STIM2 has a higher sensitivity to Ca^{2+} changes with a $K_{1/2}$ of approximately 400μM. The difference in the binding kinetics is suggestive that STIM2 controls the basal cytoplasmic and ER Ca^{2+} levels. Store depletion of Ca^{2+} causes rapid oligomerization of STIM1 and migration of the cluster associated with the ER membrane to the plasma membrane where STIM1 binds and activates the Store-Operated Ca^{2+} Entry (SOCE) channel component, Orai (Model) (Clapham). Studies have shown that the active pore is composed of four Orai molecules while during the resting state, Orai proteins are found as dimers. Three Orai proteins have been identified, namely Orai1, Orai2, and Orai3, with their ability to elicit Calcium-Release Activated Calcium Current (CRAC) respectively (Varnai, Hunyady et al.). Despite the important regulation of store Ca^{2+} of STIM and Orai, their contribution to cellular function has only been described in immunological cells. Functional characterizations of the role that STIM1 and Orais contribute in synaptic plasticity will further the understanding of the involvement of store Ca^{2+} in plasticity events.

Results

In order to investigate the specific functions of STIM1, Exon 6 was targeted. "Floxed" STIM1 (F/F) mouse lines were generated by ES cell-mediated gene targeting and subsequently crossed to Nestin promoter-driven Cre line or CamKII promoter-driven Cre lines (Figure 1A). STIM1 knock out mice (F/F Nestin-Cre) did

not display any gross anatomical or phenotypical abnormalities. Western blot analysis of forebrain lysates derived from P25 day old STIM1-KO mice showed efficient excision and depletion of STIM1 (Figure 1B). STIM1 protein is detectable starting at P4 and maintains peak expression from P17 to adulthood (Figure 1C). Next, we examined expression and localization of STIM1 in the brain with biochemical sub-cellular fractionation experiments utilizing sucrose and differential centrifugation followed by SDS-PAGE and Western blot analysis (Figure 1D). STIM1 was found in membrane fractions including endoplasmic reticulum, crude synaptosomal membrane, synaptosomal membrane and synaptic vesicle-enriched fractions. This finding is consistent with previous reports of STIM1 expression in heterologous cell system (Onodera, Pouokam et al.). Furthermore, we examined the expressions of proteins that mediate synaptic plasticity such as AMPA receptors, NMDA receptors and Calcineurin in the STIM1-KO forebrains (Figure 1D). No appreciable difference in expression and localization of GluR1, GluR2, NR1, NR2A and Calcineurin was detected with our fractionation assay.

Dr. David Linden and Dr. Joo Min Park from the Neuroscience Department at Johns Hopkins School of Medicine employed a series of electrophysiology recordings focusing on the Schaffer collateral-CA1 synapses in hippocampal slices and surveyed STIM1-KO for alterations in synaptic plasticity. STIM1-KOs mediated by Nestin-Cre showed a selective deficit in NMDA-LTD induced by low frequency stimulations (Figure 2A). We were also able to recapitulate the NMDA-LTD deficit in STIM-1 KOs mediated by CamKII- Cre, which suggests that loss of STIM1 in excitatory neurons only was enough to disrupt NMDA-LTD (Data not shown). To further understand the

NMDA-LTD deficit seen in the electrophysiology experiment, we employ biochemical studies in the hippocampal slices. With the same hippocampal slice preparation procedure, we induced NMDA-LTD by incubating slices with 20μM of NMDA for 3 minutes followed by 30 minutes of recovery time (Figure 2B). In hippocampal control slices, the treatment with NMDA induced a significant reduction of p-GluR1 (S845) indicative of GluR1 endocytosis and NMDA-LTD occurrence. However, pretreatment with APV, a selective NMDA inhibitor abolished the dephosphorylation of p-GluR1 (S845). In hippocampal slices derived from STIM1-KO mice, NMDA treatment did not lead to the reduction of p-GluR1 (S845) suggesting that GluR1 was retained on the surface and NMDA-LTD, consistent with the finding in electrophysiology studies (Figure 2B). Moreover, pretreatment with APV did not have any effect on p-GluR1. To examine surface expression of GluR1 directly, we used DIV-21 dissociated hippocampal neuron cultures in combination with surface biotinylation technique. Control neurons showed a reduction of surface GluR1 levels upon treatment with 100μM of NMDA for 5 minutes followed by 40 minutes of recovery (Figure 2C). The reduction of surface GluR1 by treatment with NMDA was blocked by pretreatment with APV. However, in STIM-KO neurons neither the treatment with NMDA nor with additional pretreatment with APV altered the surface expression of GluR1 (Figure 2C). Thus, biochemical examination of GluR1 surface expression in hippocampal slices and neuron cultures in STIM1-KO showed a deficit in NMDA-LTD.

With the finding that STIM1-KOs have a deficit in NMDA-LTD, we surveyed other forms of synaptic plasticity by electrophysiology studies. DHPG mediated mGluR-LTD studies showed comparable results in hippocampal slices from STIM1-KOs and controls (Figure 3A). Moreover, mGluR-LTD elicited by pair pulse-low frequency stimulations (PP-LFS) in the presence of NMDA receptor inhibitor APV, was also preserved in STIM1-KOs (Figure 3B). Paired-pulse ratio studies and fiber volley amplitude studies showed presynaptic release and synaptic transmission are not altered in the STIM1-KOs (Figures 3C-D). Two different forms of LTP were also examined in hippocampal slices from STIM1-KOs and littermate controls. LTP induced by Theta Burst Stimulation (TBS) remained intact in STIM1-KOs (Figure 4A). LTP induced by High Frequency Stimulation (HFS) was also preserved in STIM1-KOs in comparison to control littermates (Figure 4B). While mGluR-LTD and different forms of LTP remained intact in STIM1-KOs, we next examined a phenomena described as mGluR priming of NMDA-LTP. It has previously been documented that ER Ca^{2+} store release can be triggered by mGluR activation followed by Diacylglycerol and IP3 generation to activate IP3 receptors (Abdul-Ghani, Valiante et al.). Furthermore, store Ca^{2+} also participates in LTP since depletion of Ca^{2+} store with application of thapsigargin inhibits LTP (Cong, Takeuchi et al.). We examined mGluR priming of NMDA-LTP and argue that any alterations would reveal that integrity and the requirement of functional Ca^{2+} store refilling mediated by STIM1 is essential in synaptic plasticity. DHPG pretreatment followed by HFS showed an increase in fEPSP In control hippocampal slices compared to conditions where only HFS was applied (Figure 5). This observation demonstrated

that prior mGluR activation followed by elicitation of LTP produced a more robust LTP. However, in the STIM1-KO hippocampal slices, DHPG stimulation prior to HFS did produce a normal LTP but not a more robust LTP upon comparison with HFS only (Figure 5). This deficit suggests that although mGluR-LTD and HFS-LTP remained intact in STIM1-KO, however, stringent requirement of STIM1 remains under specific and multi-faceted plasticity paradigm.

In collaboration with Dr. Alena Savonenko in the Department of Neuropathology at Johns Hopkins School of Medicine, we assess the impact of 5-month-old male STIM1-KOs and littermate controls in behavioral studies. STIM1-KOs showed normal levels of anxiety and motor activity in novel environments (Figure 6A-B). Furthermore, learning and memory test revealed that spatial working memory was intact (Figure 6C-E). To test for NMDA receptor function, we employed dizocilpine (MK-801), a noncompetitive NMDA receptor antagonist. STIM1-KOs showed significantly lower motor activation induced by MK-801 in comparison to littermate controls (Figure 7).

Discussion

Synaptic plasticity is the ability of synapse to be strengthened or weakened by activity dependent process and underlies learning and memory. Diseases of cognition impact the ability of individuals to acquire and store information that is mediated by the synapse (Paoletti, Bellone et al.). In neurons ER contributes to the regulation of calcium in a multi-faceted fashion. ER serves as a calcium buffer by up-taking calcium influx from surface calcium transporters at the dendrites locally and

at the cellular level globally. ER also contributes to the rise of calcium level in specific "hot spots" in response to synaptic activation via mGluR-triggered IP3 production. The stringent regulation of local calcium concentration is necessary to mediate plasticity phenomena and ensure cellular integrity. Thus examinations of molecular mechanisms of ER calcium regulations and contribution to mediate synaptic activities afford a better understanding of synaptic plasticity.

We identified synaptic plasticity deficits in NMDA-LTD and mGluR priming of LTP in the Nestin- and CamKII- Cre mediated STIM1 conditional knockouts in this study. These deficits are rather specific since mGluR mediated LTD and various forms of LTP are intact in the STIM1-KOs. The finding that NMDA-LTD is abolished was further substantiated by biochemical studies that indicate GluR1 dephosphorylation was blunted. Previous studies have demonstrated that Calcineurin is the key phosphatase regulating GluR1 (S845) (Snyder, Galdi et al.). Calcineurin activity is directly correlated with cytosolic Ca^{2+} levels (Baumgartel and Mansuy). Our study showed that the expression and localization of Calcineurin was not altered in the STIM1-KOs thus it suggests that the activation of Calcineurin in STIM1-KOs may be disrupted due to lower cytosolic Ca^{2+} levels. Future studies utilizing STIM1-KOs crossed with conditionally expressed genetically encoded Ca^{2+} indicator GCaMP3 would be valuable to examine store and cytosolic Ca^{2+} levels by imaging acute brain slices using 2-photon microscopy. Furthermore, expression of a FRET-based Calcineurin activity sensor that Dr. Jin Zhang in the Neuroscience Department at Johns Hopkins University has developed, in STIM1-KO dissociated neuronal cultures would be valuable to assess Calcineurin's activity.

NMDA receptor hypo-function have been associated with many psychiatric diseases (Paoletti, Bellone et al.). Furthermore, calcineurin deregulation has also been demonstrated to be involved in schizophrenia, Huntington's Disease and Alzheimer's Disease (Monti, Berteotti et al.) (Reese and Taglialatela) (Ermak, Hench et al.). Behavioral tests with STIM1-KOs showed that spatial working memory remained intact. Furthermore, anxiety levels in open field and plus maze assays remained normal. The reduced response to psychostimulant MK-801 in the STIM1-KOs is a curious one and would be interesting to compare to amphetamine induced motor activation. In comparison of MK-801 to amphetamine, differentiation of glutamatergic and dopaminergic networks could be made and further understanding of motor activation mechanisms could be gained. Conditional calcineurin knockout mice showed a selective NMDA-LTD deficit and delay in extinction of fear memory. Since our data strongly support the notion that Calcineurin activity are reduced in the STIM1-KOs, it would be interesting to examine facilitation of fear acquisition and fear extinction in STIM1-KOs. Ongoing studies in the Worley laboratory will examine the role of STIM1 in mTORC1 activation.

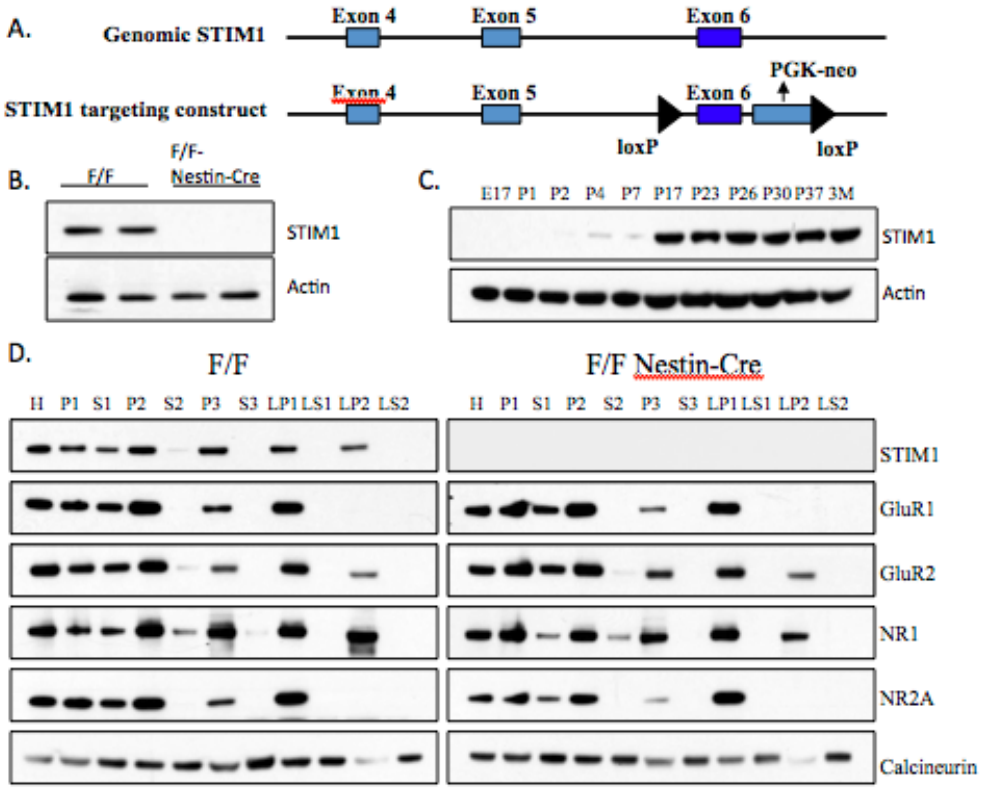
A.
Genomic STIM1
Exon 4
Exon 5
Exon 6
STIM1 targeting construct
Exon 4
Exon 5
Exon 6
PGK-neo
loxP
loxP
B.
F/F
F/F-
Nestin-Cre
STIM1
Actin
C.
E17 P1 P2 P4 P7 P17 P23 P26 P30 P37 3M
STIM1
Actin
D.
F/F
F/F Nestin-Cre
H P1 S1 P2 S2 P3 S3 LP1 LS1 LP2 LS2
STIM1
GluR1
GluR2
NR1
NR2A
Calcineurin

Figure 1. Generation of Forebrain-Specific STIM1 Knockout Mice (A) Targeting strategy. **(B)** Absence of STIM1 protein was confirmed by Western blot of forebrain brain lysates from P25 mice. **(C)** Developmental expression of STIM1. Western blot analysis of forebrain lysates. **(D)** Biochemical fractionation of forebrain lysates prepared from indicates that STIM1 is localized to membrane fractions. The absence of STIM1 does not alter the expression and localization of glutamate receptors and Calcineurin. Abbreviations : H, total homogentate; P1, Nuclei/large debris; S1, supernatant from P1; P2, Crude synaptosomal membrane; S2, supernatant from P2; P3, Light membrane (ER, golgi, mitochondria); S3, supernatant from P3; LP1, synaptosomal membrane (PSD); LS1, supernatant from LP1; LP2, synaptosomal vesicle-enriched; LS2, supernatant from LP2.

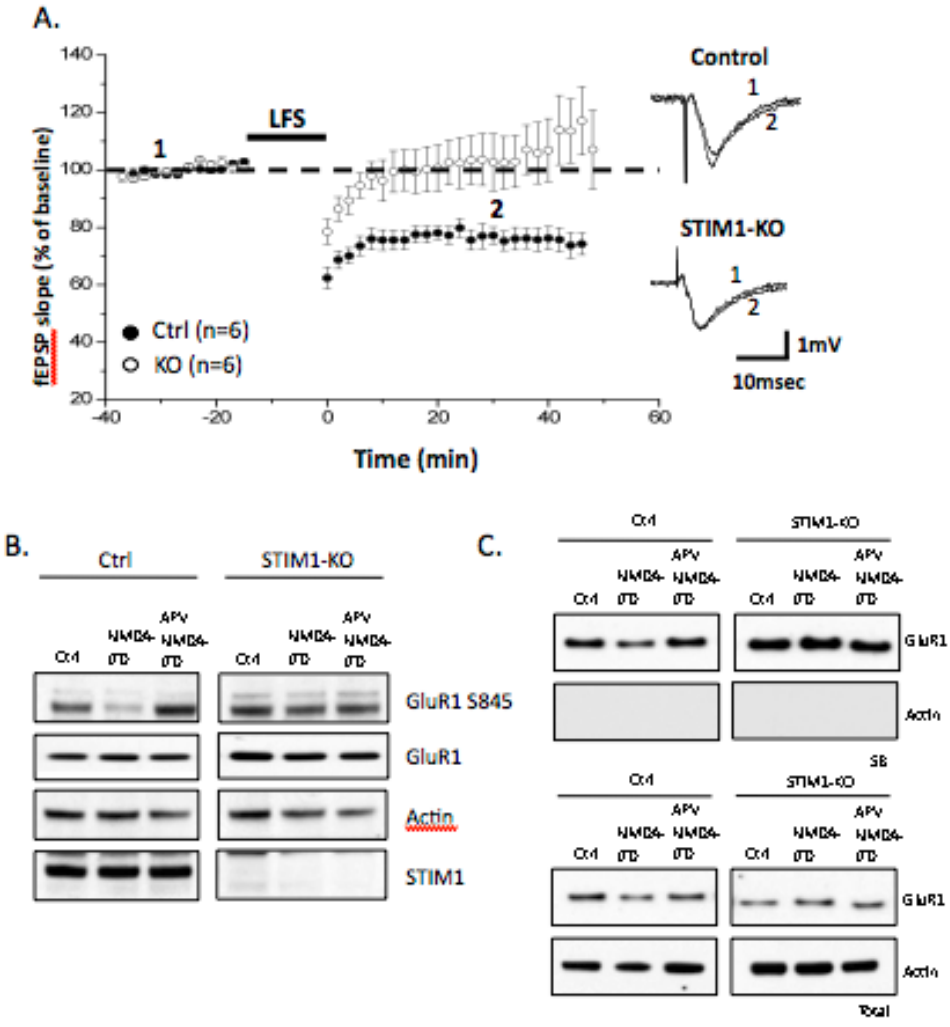
A.
Control
STIM1-KO
LFS
1
2
fEPSP slope (% of baseline)
Time (min)
Ctrl (n=6)
KO (n=6)
1mV
10msec
B.
Ctrl
STIM1-KO
Ctrl
NMDA-ER
APV NMDA-ER
GluR1 S845
GluR1
Actin
STIM1
C.
Ctrl
STIM1-KO
GluR1
Actin
SE
Total

Figure 2. NMDA Receptor Mediated LTD is Disrupted in Forebrain-Specific STIM1 Knockout Mice. (A) LFS stimulation (1 Hz) induced LTD in control slices but not in STIM1-KO slices. **(B)** Dephosphorylation of GluA1 on S845 during chemical-LTD is absent in STIM1-KO slices . Chemical-LTD was induced by application of 20μM NMDA for 3 min, and lysates were prepared from slices after 30 mins. In Control slices NMDA treatment induced dephosphorylation of GluR1 S845, which was blocked by incubation with 100μM AP5 prior and during NMDA treatment. In STIM1-KO slices dephosphorylation was disrupted. **(C)** NMDA-LTD induced GluA1 endocytosis is impaired in STIM1-KO cortical cultures. Surface biotinylation was performed after incubation with 100μM NMDA. Chemical-LTD that was blocked by incubation with 100μM AP5 prior and during NMDA treatment. Surface biotinylated proteins (top; SB) and total lysate (bottom; Total) proteins were subjected to Western blot analysis for GluA1 and Actin.

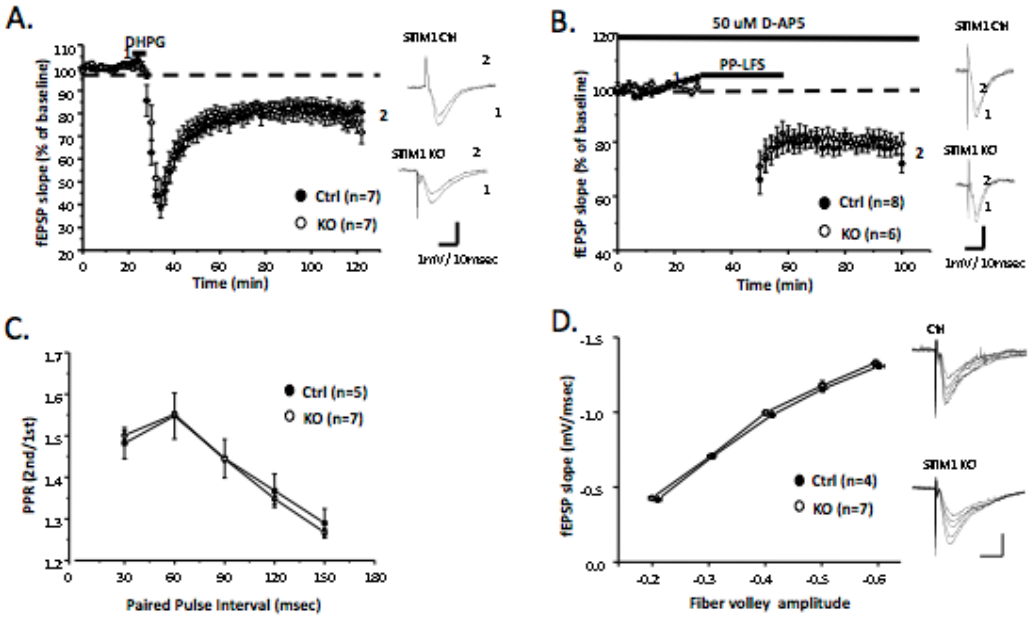
A.
DHPG
fEPSP slope (% of baseline)
Time (min)
Ctrl (n=7)
KO (n=7)
STIM1 CN
STIM1 KO
1mV/ 10msec
B.
50 uM D-APS
PP-LFS
fEPSP slope (% of baseline)
Time (min)
Ctrl (n=8)
KO (n=6)
STIM1 CN
STIM1 KO
1mV/ 10msec
C.
PPR (2nd/1st)
Paired Pulse Interval (msec)
Ctrl (n=5)
KO (n=7)
D.
fEPSP slope (mV/msec)
Fiber volley amplitude
Ctrl (n=4)
KO (n=7)
CN
STIM1 KO

Figure 3. mGluR Mediated LTD is Unaltered in STIM1-KO. (A) Average time course of the change in fEPSP slope induced by the group I mGluR agonist (R,S)-DHPG (100 µM, for 5 min). LTD of control mice was 80.8% ± 2.0% of base line at t = 70 min (n = 7). In STIM-1 KO, fEPSP was 81% ± 2.4% of the baseline at t = 70 mins (n = 7). Scale bars, 1 mV/ 10 ms. Error bars indicate the standard error of the mean. Measurements correspond to the time points indicated on the time course graph in this and all subsequent figures. **(B)** Time course of the change in fEPSP slope produced by paired-pulse low-frequency stimulation (PP-LFS: at 1Hz, 50 ms interstimulus interval, for 15 mins) in the presence of the NMDA receptor antagonist D-APV (50 µM). LTD of control mice was 78% ± 2.4% of baseline at t = 80 mins (n = 8). In STIM1-KO mice, fEPSPs were 78.5% ± 2.8% of the baseline at t = 80 mins (n = 6). Scale bars, 1 mV/ 10 ms. **(C)** Relationship between paired-pulse interval and paired pulse ratio (PPR) of the Schaffer collateral-CA1 synapse of control (n = 5) and STIM1-KO (n =7) mice. Exemplar traces are shown with 30 msec interval. **(D)** Relationship between fiber volley amplitude and fEPSP slope of the Schaffer collateral-CA1 synapse of control (n = 4) and STIM1-KO (n= 7) mice. Each point represents the mean for a narrow range of fiber volley amplitudes.

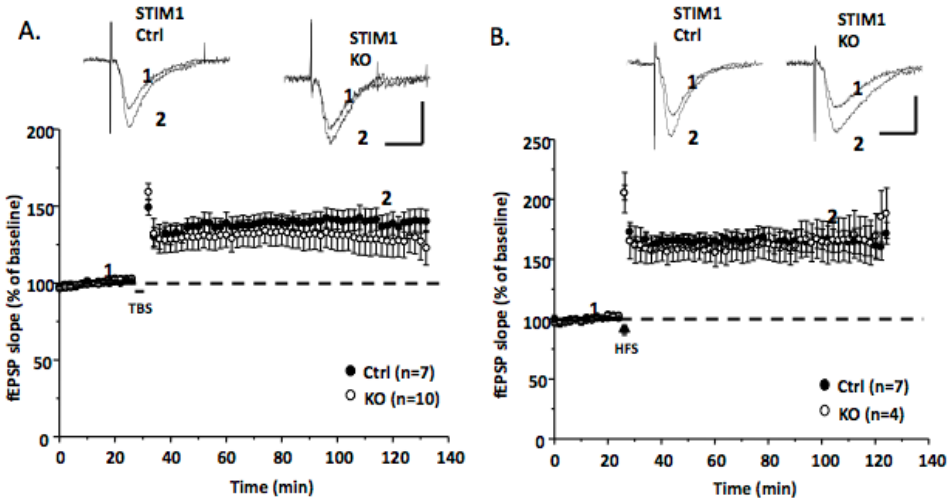

Figure 4. Normal Response to LTP Induction Stimulation in STIM1-KO. (A) Average time course of the change in fEPSP slope induced by Theta Burst Stimulation (TBS) (10 trains, each consisting of ten 100 Hz burst (four pulse) given at 5 Hz, with intertrain intervals of 20 s). TBS-LTP of control mice was 127.8% ± 6.0% of base line at t = 100 min (n = 7). In STIM-1 KO, fEPSP was 134% ± 6.5% of the baseline at t = 100 mins (n = 100). Scale bars, 1 mV/ 10 ms. Error bars indicate the standard error of the mean. Measurements correspond to the time points indicated on the time course graph in this and all subsequent figures. **(B)** Time course of the change in fEPSP slope produced by High Frequency Stimulation (HFS) (3 stimulus trains (100 Hz each) with an intertrain interval of 20 s). HFS-LTD of control mice was 168% ± 7.5% of baseline at t = 100 mins (n = 7). In STIM1-KO mice, fEPSPs were 171% ± 8.1% of the baseline at t = 100 mins (n = 4). Scale bars, 1 mV/ 10 ms.

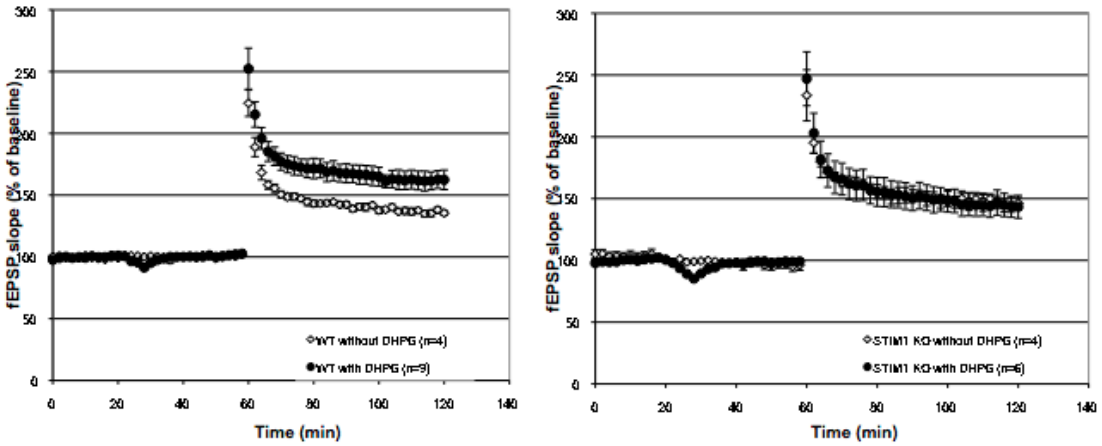

Figure 5. STIM1 Contributes to mGluR Priming of NMDA-LTP. (A) Average time course of the change in fEPSP slope induced by High Frequency Stimulation (HFS) with and without the pretreatment of group I mGluR agonist (R,S)-DHPG (10 µM, for 5 min). HFS-LTP of control mice without DHPG was 142% ± 1% of base line at t = 100 min (n = 4) compared to HFS-LTP of control mice with DHPG pretreatment was 169% ± 4.4% of base line at t = 100 min (n = 9). **(B)** In STIM-1 KO without DHPG, HFS-LTP was 148% ± 3.4% of the baseline at t = 100 mins (n = 4) compared with pretreatment with DHPG was 149% ± 2.8% of base line at t = 100 min (n = 6). Error bars indicate the standard error of the mean.

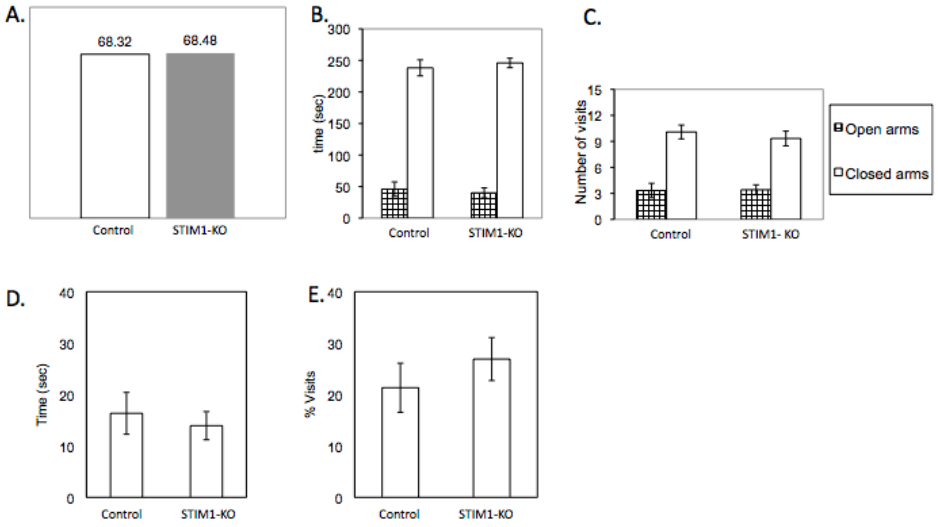

Figure 6. Spatial Working Memory and Anxiety levels are Normal in STIM1-KOs. (A) Control (n = 11) showed 68.32% of alternations and STIM-KO (n =10) showed 68.48% of alternations when they were individually placed into a symmetrical Y-maze. **(B-E)** are performed in elevated plus maze. **(B)** Control mice (n = 10) spent 50 s ± 8 s in the open arm and 242 s ± 10 s in the close arm. STIM1-KO mice (n = 10) spent 43 s ± 7 s in the open arm and 249 s ± 5 s in the close arm. **(C)** Control mice (n = 10) visited the open arm 3 times ± 1.5 and visited 10 times ± 2 to the close arm. STIM1-KO mice (n = 10) visited the open arm 3 times ± 1.5 s and visited 9 times ± 1.5 to the close arm. **(D)** Control mice spent 16.4% ± 5.2% of time and STIM1-KOs spent 14.8% ± 4.4% of time in the open arms. **(E)** Control mice spent 22% ± 5% of the time visiting the open arms and STIM1-KOs spent 27% ± 5% of the time visiting the open arms. Data are presented as mean ± SEM.

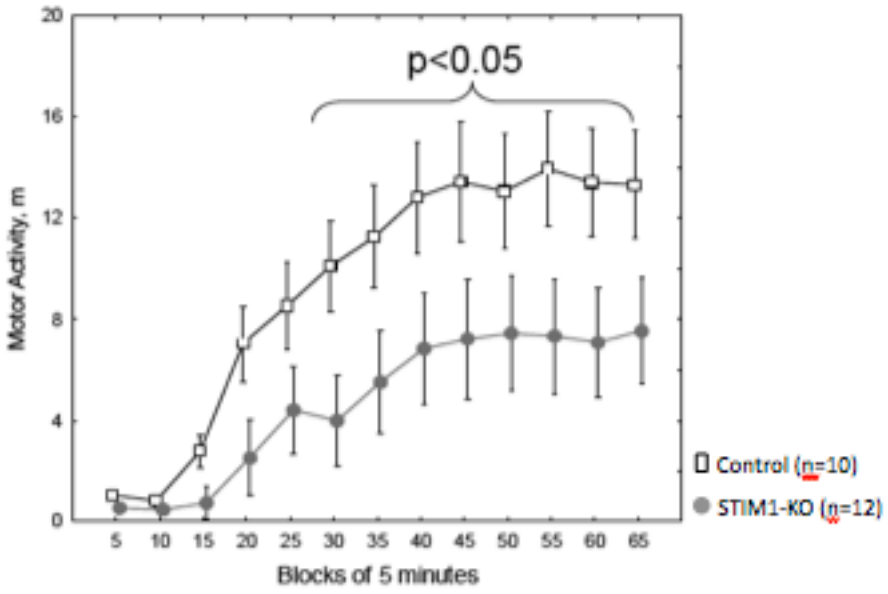

Figure 7. STIM1-KOs Show Rreduced MK-801 Induced Motor Activity. MK-801 induced motor activation (ip, 0.3 mg/kg) was tested after a 45-min habituation to an open field (n=10-13 per genotype per treatment). Data are presented as mean ± SEM. P-Values were calculated by Student's t-test and ANCOVA

CHAPTER 7:

Conclusions and Future Directions

Learning and memory relies on the ability of the synaptic connection network to alter their efficacy in response to activity termed synaptic plasticity. Proper cognitive function requires neurons to maintain homeostasis and elicit different modes of synaptic plasticity in an activity-dependent manner. mTOR is ubiquitously expressed in the central nervous system and its signaling pathway mediate cellular functions to maintain homeostasis. Aberrant activation or the blunting of stimuli induced activity of the mTOR signaling pathway disrupts the ability of the neurons to adapt and function. mTOR signaling pathway in neurons is coupled to plasma membrane receptors that influence synaptic plasticity. Dysregulation of the mTOR signaling pathway due to genetic mutations or cellular insults lead to devastating diseases such as cancer, diabetes, AD, ASD among others. The use of rapamycin to inhibit mTOR activity in experiments have proved valuable and revealed many cellular functions that are mTOR dependent. However, conditional Rheb1 knockout and over-expresser mice provide significant advantages in studying mTOR signaling in specific tissues and disease states. Moreover, conditional Rheb1 over-expresser mouse may be utilized to mimic disease states by specific expression in targeted tissues for *in vivo* studies. Importantly, conditional Rheb1 over-expresser mouse may serve as a novel mouse model platform for therapeutic discovery and treatment developments for diseases that are correlated with elevated mTORC1 activity.

Genetic and biochemical studies have provided a detailed mTOR signaling pathway cascade with the revelation of the regulatory functions of its components. Extra-cellular ligand binding to plasma surface receptors initiates the canonical mTOR signaling pathway. Subsequently, PI3K activation leads to the phosphorylation of PDK1, which in turn activates Akt. Akt inhibits Tsc relieving its inhibition on Rheb1 thus activating mTORC1. Through a broad panel of pharmacological drug screen, we uncovered a calcium dependent non-canonical mTORC1 signaling pathway that could modulate mTORC1 activity independently from the canonical signaling pathway. mTORC1 signaling directly correlates with stimulation or inhibition of TRP channels, L-type VDCC and Orai channels demonstrated by treatment with pharmacological reagents and molecular expression approaches. Further experiments showed that the non-canonical pathway is dependent on Ca^{2+}/Calmodulin and is activated in the hippocampus during exploration activities by mice. Neurons derived from AD mouse models displayed “type III diabetes”-like insensitivity to insulin stimulation of the canonical pathway while the basal activity of mTORC1 was elevated. The stimulatory input of mTORC1 in AD neurons may be attributed to the postulated disruptions in calcium homeostasis (LaFerla). Detail studies of the molecules mediating the non-canonical pathway will provide further understanding of the novel pathway. Studies aim to restore the canonical pathway in AD neurons and mice with pharmacological inhibition of the non-canonical pathway may provide insights to future therapeutic treatments in AD.

The utility of the conditional myc-Rheb1 (S16H) mouse model is exemplified through our biochemical, behavioral and electrophysiological experiments. Anti-Myc immunoprecipitations of myc-Rheb1 (S16H) under non-denaturing conditions revealed an intriguing and selective set of synaptic proteins, vesicle associated proteins and enrichment of ubiquitinylated proteins. The proteins associated with myc-Rheb1 (S16H) suggest a model where Rheb1 traffics proteins destined for degradation through lysosomal or proteosomal processing and generate amino acids to facilitate mTORC1 activation. Consistent with the proposed model, pharmacological inhibition of proteosome or disruption of lysosomal activities lead to reduction in mTORC1 signaling (Bar-Peled, Schweitzer et al.). Previous studies demonstrated mGluR1/5 activation induces mTORC1 signaling and mGluR-dependent LTD is dependent on down regulation of surface receptors such as GluR2 (Huber, Kayser et al.) (Anggono and Huganir). Interesting we found mGluR5 associates with myc-Rheb1 (S16H) in a membrane dependent manner. mGluR5 and Rheb1 may associate to form a signalosome-like entity and together with internalized GluR2 destined for degradation could lead to the activation of mTORC1. Future biochemical and immunocytochemistry experiments examining the activity-dependent modulation of mGluR5 and its association with Rheb1 is warranted.

Genetic mutations in TSC1/2, PTEN, FMR and EIF4E are highly correlated with ASD-like behaviors and elevated mTOR activity (Emamian). Researchers have suggested that elevated mTOR activity appears to be the central theme in studies of ASD (Emamian). Moreover, PET and MRI imaging studies have shown deficits in the

striatum of ASD patients (Duchesnay, Cachia et al.) (Gaetz, Bloy et al.). Consistent with the hypothesis, brain specific myc-Rheb1 (S16H) mice display ASD-like behavioral phenotypes with reduced social motivation, disruption in sensory-gating and reduced amphetamine-induced locomotor activity. Biochemical characterization of the striatum revealed feedback inhibition to dopamine receptor signaling, disruptions in PKA pathway, Darpp32 phosphorylation, and aberrant activities in phosphatases. Furthermore, electrophysiological experiments showed corticostriatal plasticity disruptions and insensitivity to D1R stimulation. The feedback inhibition of dopamine receptors offers another example consistent with diabetes, that persistent elevation of mTORC1 activity results in disruption in integration of signals as a response to extra-cellular stimulation. Acute rapamycin treatment revealed that mTOR activity participates in the amphetamine induced locomotor activity. However, it did not rescue biochemical or behavioral phenotypes in the myc-Rheb1 (S16h) over-expresser mice. Future experiments employing a chronic treatment of rapamycin or other pharmacological reagents to reduce mTOR activity in the over-expresser mice would provide insightful therapeutic treatment strategies in ASD.

Much remains to be understood of the interplay between canonical and non-canonical mTOR signaling pathway and how they contribute to neural plasticity and function. Persistent elevated mTORC1 activity is associated devastating cognitive diseases. The conditional myc-Rheb1 (S16H) mice allow for expression with temporal and cell specific control. Future studies utilizing different promoter driven Cre-recombines crossed with myc-Rheb1 (S16H) may help to reveal the

developmental and aging dependence of cognitive diseases and their mechanism of manifestation.

REFERENCES:

Abdul-Ghani, M. A., T. A. Valiante, et al. (1996). "Metabotropic glutamate receptors coupled to IP3 production mediate inhibition of IAHP in rat dentate granule neurons." J Neurophysiol **76**(4): 2691-2700.

Anggono, V. and R. L. Huganir (2012). "Regulation of AMPA receptor trafficking and synaptic plasticity." Curr Opin Neurobiol **22**(3): 461-469.

Baird, A., B. K. Dewar, et al. (2006). "Social and emotional functions in three patients with medial frontal lobe damage including the anterior cingulate cortex." Cogn Neuropsychiatry **11**(4): 369-388.

Banko, J. L., L. Hou, et al. (2006). "Regulation of eukaryotic initiation factor 4E by converging signaling pathways during metabotropic glutamate receptor-dependent long-term depression." J Neurosci **26**(8): 2167-2173.

Bar-Peled, L. and D. M. Sabatini (2012). "SnapShot: mTORC1 signaling at the lysosomal surface." Cell **151**(6): 1390-1390 e1391.

Bar-Peled, L., L. D. Schweitzer, et al. (2012). "Ragulator is a GEF for the rag GTPases that signal amino acid levels to mTORC1." Cell **150**(6): 1196-1208.

Bateup, H. S., P. Svenningsson, et al. (2008). "Cell type-specific regulation of DARPP-32 phosphorylation by psychostimulant and antipsychotic drugs." Nat Neurosci **11**(8): 932-939.

Baumgartel, K. and I. M. Mansuy (2012). "Neural functions of calcineurin in synaptic plasticity and memory." Learn Mem **19**(9): 375-384.

Beaulieu, J. M., R. R. Gainetdinov, et al. (2009). "Akt/GSK3 signaling in the action of psychotropic drugs." Annu Rev Pharmacol Toxicol **49**: 327-347.

Bogeski, I., T. Kilch, et al. (2012). "ROS and SOCE: recent advances and controversies in the regulation of STIM and Orai." J Physiol **590**(Pt 17): 4193-4200.

Cafferkey, R., P. R. Young, et al. (1993). "Dominant missense mutations in a novel yeast protein related to mammalian phosphatidylinositol 3-kinase and VPS34 abrogate rapamycin cytotoxicity." Mol Cell Biol **13**(10): 6012-6023.

Calabresi, P., A. Pisani, et al. (1992). "Long-term Potentiation in the Striatum is Unmasked by Removing the Voltage-dependent Magnesium Block of NMDA Receptor Channels." Eur J Neurosci **4**(10): 929-935.

Cammalleri, M., R. Lutjens, et al. (2003). "Time-restricted role for dendritic activation of the mTOR-p70S6K pathway in the induction of late-phase long-term potentiation in the CA1." Proc Natl Acad Sci U S A **100**(24): 14368-14373.

Carroll, M., O. Warren, et al. (2004). "5-HT stimulates eEF2 dephosphorylation in a rapamycin-sensitive manner in Aplysia neurites." J Neurochem **90**(6): 1464-1476.

Citri, A. and R. C. Malenka (2008). "Synaptic plasticity: multiple forms, functions, and mechanisms." Neuropsychopharmacology **33**(1): 18-41.

Clapham, D. E. (2009). "A STIMulus Package puts orai calcium channels to work." Cell **136**(5): 814-816.

Cole, D. C., J. R. Stock, et al. (2008). "Acylguanidine inhibitors of beta-secretase: optimization of the pyrrole ring substituents extending into the S1 and S3 substrate binding pockets." Bioorg Med Chem Lett **18**(3): 1063-1066.

Cong, Y. L., S. Takeuchi, et al. (2004). "Long-term potentiation of transmitter exocytosis expressed by Ca2+-induced Ca2+ release from thapsigargin-sensitive Ca2+ stores in preganglionic nerve terminals." Eur J Neurosci **20**(2): 419-426.

de la Monte, S. M. (2012). "Brain insulin resistance and deficiency as therapeutic targets in Alzheimer's disease." Curr Alzheimer Res **9**(1): 35-66.

Duchesnay, E., A. Cachia, et al. (2011). "Feature selection and classification of imbalanced datasets: application to PET images of children with autistic spectrum disorders." Neuroimage **57**(3): 1003-1014.

Dunnett, S. (2003). "L-DOPA, dyskinesia and striatal plasticity." Nat Neurosci **6**(5): 437-438.

Efe, J. A., S. Hilcove, et al. (2011). "Conversion of mouse fibroblasts into cardiomyocytes using a direct reprogramming strategy." Nat Cell Biol **13**(3): 215-222.

Emamian, E. S. (2012). "AKT/GSK3 signaling pathway and schizophrenia." Front Mol Neurosci **5**: 33.

Ermak, G., K. J. Hench, et al. (2009). "Regulator of calcineurin (RCAN1-1L) is deficient in Huntington disease and protective against mutant huntingtin toxicity in vitro." J Biol Chem **284**(18): 11845-11853.

Fitzjohn, S. M. and G. L. Collingridge (2002). "Calcium stores and synaptic plasticity." Cell Calcium **32**(5-6): 405-411.

Gaetz, W., L. Bloy, et al. (2013). "GABA estimation in the brains of children on the autism spectrum: Measurement precision and regional cortical variation." Neuroimage.

Griffin, R. J., A. Moloney, et al. (2005). "Activation of Akt/PKB, increased phosphorylation of Akt substrates and loss and altered distribution of Akt and PTEN are features of Alzheimer's disease pathology." J Neurochem **93**(1): 105-117.

Guertin, D. A., D. M. Stevens, et al. (2006). "Ablation in mice of the mTORC components raptor, rictor, or mLST8 reveals that mTORC2 is required for signaling to Akt-FOXO and PKCalpha, but not S6K1." Dev Cell **11**(6): 859-871.

Gulati, P., L. D. Gaspers, et al. (2008). "Amino acids activate mTOR complex 1 via Ca2+/CaM signaling to hVps34." Cell Metab **7**(5): 456-465.

Hallett, P. J., T. L. Collins, et al. (2008). "Biochemical fractionation of brain tissue for studies of receptor distribution and trafficking." Curr Protoc Neurosci **Chapter 1**: Unit 1 16.

Han, Y. L., J. Y. Chen, et al. (2011). "Real world clinical performance of the zotarolimus eluting coronary stent system in Chinese patients: a prospective, multicenter registry study." Chin Med J (Engl) **124**(20): 3255-3259.

Harrington, A. W., C. St Hillaire, et al. (2011). "Recruitment of actin modifiers to TrkA endosomes governs retrograde NGF signaling and survival." Cell **146**(3): 421-434.

Hoeffer, C. A. and E. Klann (2010). "mTOR signaling: at the crossroads of plasticity, memory and disease." Trends Neurosci **33**(2): 67-75.

Huber, K. M., M. S. Kayser, et al. (2000). "Role for rapid dendritic protein synthesis in hippocampal mGluR-dependent long-term depression." Science **288**(5469): 1254-1257.

Huotari, J. and A. Helenius (2011). "Endosome maturation." EMBO J **30**(17): 3481-3500.

Kato, H. K., H. Kassai, et al. (2012). "Functional coupling of the metabotropic glutamate receptor, InsP3 receptor and L-type Ca2+ channel in mouse CA1 pyramidal cells." J Physiol **590**(Pt 13): 3019-3034.

Kim, J. I., H. R. Lee, et al. (2011). "PI3Kgamma is required for NMDA receptor-dependent long-term depression and behavioral flexibility." Nat Neurosci **14**(11): 1447-1454.

Kuchibhotla, K. V., S. T. Goldman, et al. (2008). "Abeta plaques lead to aberrant regulation of calcium homeostasis in vivo resulting in structural and functional disruption of neuronal networks." Neuron **59**(2): 214-225.

Kwon, C. H., B. W. Luikart, et al. (2006). "Pten regulates neuronal arborization and social interaction in mice." Neuron **50**(3): 377-388.

LaFerla, F. M. (2002). "Calcium dyshomeostasis and intracellular signalling in Alzheimer's disease." Nat Rev Neurosci **3**(11): 862-872.

Laplante, M. and D. M. Sabatini (2012). "mTOR Signaling." Cold Spring Harb Perspect Biol **4**(2).

Laplante, M. and D. M. Sabatini (2012). "mTOR signaling in growth control and disease." Cell **149**(2): 274-293.

Li, X., I. Alafuzoff, et al. (2005). "Levels of mTOR and its downstream targets 4E-BP1, eEF2, and eEF2 kinase in relationships with tau in Alzheimer's disease brain." FEBS J **272**(16): 4211-4220.

Liu, R., X. W. Zhou, et al. (2008). "Phosphorylated PP2A (tyrosine 307) is associated with Alzheimer neurofibrillary pathology." J Cell Mol Med **12**(1): 241-257.

Lyall, A., J. Swanson, et al. (2009). "Neonatal exposure to MK801 promotes prepulse-induced delay in startle response time in adult rats." Exp Brain Res **197**(3): 215-222.

Ma, T., C. A. Hoeffer, et al. (2010). "Dysregulation of the mTOR pathway mediates impairment of synaptic plasticity in a mouse model of Alzheimer's disease." PLoS One **5**(9).

Maiese, K., Z. Z. Chong, et al. (2013). "mTOR: on target for novel therapeutic strategies in the nervous system." Trends Mol Med **19**(1): 51-60.

Malenka, R. C. and M. F. Bear (2004). "LTP and LTD: an embarrassment of riches." Neuron **44**(1): 5-21.

Moloney, A. M., R. J. Griffin, et al. (2010). "Defects in IGF-1 receptor, insulin receptor and IRS-1/2 in Alzheimer's disease indicate possible resistance to IGF-1 and insulin signalling." Neurobiol Aging **31**(2): 224-243.

Monti, B., C. Berteotti, et al. (2005). "Dysregulation of memory-related proteins in the hippocampus of aged rats and their relation with cognitive impairment." Hippocampus **15**(8): 1041-1049.

Murphy, J. E., B. E. Padilla, et al. (2009). "Endosomes: a legitimate platform for the signaling train." Proc Natl Acad Sci U S A **106**(42): 17615-17622.

Nishi, A., G. L. Snyder, et al. (1999). "Role of calcineurin and protein phosphatase-2A in the regulation of DARPP-32 dephosphorylation in neostriatal neurons." J Neurochem **72**(5): 2015-2021.

Nobukuni, T., M. Joaquin, et al. (2005). "Amino acids mediate mTOR/raptor signaling through activation of class 3 phosphatidylinositol 3OH-kinase." Proc Natl Acad Sci U S A **102**(40): 14238-14243.

Oh-Hora, M., M. Yamashita, et al. (2008). "Dual functions for the endoplasmic reticulum calcium sensors STIM1 and STIM2 in T cell activation and tolerance." Nat Immunol **9**(4): 432-443.

Ohne, Y., T. Takahara, et al. (2009). "Evaluation of mTOR function by a gain-of-function approach." Cell Cycle **8**(4): 573-579.

Onodera, K., E. Pouokam, et al. (2013). "STIM1-regulated Ca2+ influx across the apical and the basolateral membrane in colonic epithelium." J Membr Biol **246**(4): 271-285.

Osterweil, E. K., D. D. Krueger, et al. (2010). "Hypersensitivity to mGluR5 and ERK1/2 leads to excessive protein synthesis in the hippocampus of a mouse model of fragile X syndrome." J Neurosci **30**(46): 15616-15627.

Palfy, M., A. Remenyi, et al. (2012). "Endosomal crosstalk: meeting points for signaling pathways." Trends Cell Biol **22**(9): 447-456.

Paoletti, P., C. Bellone, et al. (2013). "NMDA receptor subunit diversity: impact on receptor properties, synaptic plasticity and disease." Nat Rev Neurosci **14**(6): 383-400.

Park, S., J. M. Park, et al. (2008). "Elongation factor 2 and fragile X mental retardation protein control the dynamic translation of Arc/Arg3.1 essential for mGluR-LTD." Neuron **59**(1): 70-83.

Reese, L. C. and G. Taglialatela (2011). "A role for calcineurin in Alzheimer's disease." Curr Neuropharmacol **9**(4): 685-692.

Robbins, T. W. and E. R. Murphy (2006). "Behavioural pharmacology: 40+ years of progress, with a focus on glutamate receptors and cognition." Trends Pharmacol Sci **27**(3): 141-148.

Roberts, M. S., A. J. Woods, et al. (2004). "Protein kinase B/Akt acts via glycogen synthase kinase 3 to regulate recycling of alpha v beta 3 and alpha 5 beta 1 integrins." Mol Cell Biol **24**(4): 1505-1515.

Ronesi, J. A. and K. M. Huber (2008). "Homer interactions are necessary for metabotropic glutamate receptor-induced long-term depression and translational activation." J Neurosci **28**(2): 543-547.

Rumbaugh, G., G. M. Sia, et al. (2003). "Synapse-associated protein-97 isoform-specific regulation of surface AMPA receptors and synaptic function in cultured neurons." J Neurosci **23**(11): 4567-4576.

Sabatini, D. M., H. Erdjument-Bromage, et al. (1994). "RAFT1: a mammalian protein that binds to FKBP12 in a rapamycin-dependent fashion and is homologous to yeast TORs." Cell **78**(1): 35-43.

Sancak, Y., T. R. Peterson, et al. (2008). "The Rag GTPases bind raptor and mediate amino acid signaling to mTORC1." Science **320**(5882): 1496-1501.

Sarbassov, D. D., S. M. Ali, et al. (2005). "Growing roles for the mTOR pathway." Curr Opin Cell Biol **17**(6): 596-603.

Sarbassov, D. D., D. A. Guertin, et al. (2005). "Phosphorylation and regulation of Akt/PKB by the rictor-mTOR complex." Science **307**(5712): 1098-1101.

Saucedo, L. J., X. Gao, et al. (2003). "Rheb promotes cell growth as a component of the insulin/TOR signalling network." Nat Cell Biol **5**(6): 566-571.

Sawicka, K. and R. S. Zukin (2012). "Dysregulation of mTOR signaling in neuropsychiatric disorders: therapeutic implications." Neuropsychopharmacology **37**(1): 305-306.

Schellenberg, G. D., G. Dawson, et al. (2006). "Evidence for multiple loci from a genome scan of autism kindreds." Mol Psychiatry **11**(11): 1049-1060, 1979.

Selkoe, D. J. (2002). "Alzheimer's disease is a synaptic failure." Science **298**(5594): 789-791.

Shang, Y. C., Z. Z. Chong, et al. (2012). "Prevention of beta-amyloid degeneration of microglia by erythropoietin depends on Wnt1, the PI 3-K/mTOR pathway, Bad, and Bcl-xL." Aging (Albany NY) **4**(3): 187-201.

Sharma, A., C. A. Hoeffer, et al. (2010). "Dysregulation of mTOR signaling in fragile X syndrome." J Neurosci **30**(2): 694-702.

Shepherd, G. M. (2013). "Corticostriatal connectivity and its role in disease." Nat Rev Neurosci **14**(4): 278-291.

Skeberdis, V. A., V. Chevaleyre, et al. (2006). "Protein kinase A regulates calcium permeability of NMDA receptors." Nat Neurosci **9**(4): 501-510.

Snyder, G. L., S. Galdi, et al. (2003). "Regulation of AMPA receptor dephosphorylation by glutamate receptor agonists." Neuropharmacology **45**(6): 703-713.

Soboloff, J., B. S. Rothberg, et al. (2012). "STIM proteins: dynamic calcium signal transducers." Nat Rev Mol Cell Biol **13**(9): 549-565.

Tabancay, A. P., Jr., C. L. Gau, et al. (2003). "Identification of dominant negative mutants of Rheb GTPase and their use to implicate the involvement of human Rheb in the activation of p70S6K." J Biol Chem **278**(41): 39921-39930.

Takahashi, H., R. Hashimoto, et al. (2011). "Prepulse inhibition of startle response: recent advances in human studies of psychiatric disease." Clin Psychopharmacol Neurosci **9**(3): 102-110.

Tang, S. J. and E. M. Schuman (2002). "Protein synthesis in the dendrite." Philos Trans R Soc Lond B Biol Sci **357**(1420): 521-529.

Tarabeux, J., O. Kebir, et al. (2011). "Rare mutations in N-methyl-D-aspartate glutamate receptors in autism spectrum disorders and schizophrenia." Transl Psychiatry **1**: e55.

Tsai, P. T., C. Hull, et al. (2012). "Autistic-like behaviour and cerebellar dysfunction in Purkinje cell Tsc1 mutant mice." Nature **488**(7413): 647-651.

Varnai, P., L. Hunyady, et al. (2009). "STIM and Orai: the long-awaited constituents of store-operated calcium entry." Trends Pharmacol Sci **30**(3): 118-128.

Wang, Y., M. J. Rowan, et al. (1997). "Induction of LTD in the dentate gyrus in vitro is NMDA receptor independent, but dependent on Ca2+ influx via low-voltage-activated Ca2+ channels and release of Ca2+ from intracellular stores." J Neurophysiol **77**(2): 812-825.

Woods, N. K. and J. Padmanabhan (2012). "Neuronal calcium signaling and Alzheimer's disease." Adv Exp Med Biol **740**: 1193-1217.

Wu, J., R. S. Petralia, et al. (2011). "Arc/Arg3.1 regulates an endosomal pathway essential for activity-dependent beta-amyloid generation." Cell **147**(3): 615-628.

Wu, L., Z. Feng, et al. (2013). "Rapamycin upregulates autophagy by inhibiting the mTOR-ULK1 pathway, resulting in reduced podocyte injury." PLoS One **8**(5): e63799.

Yamagata, K., L. K. Sanders, et al. (1994). "rheb, a growth factor- and synaptic activity-regulated gene, encodes a novel Ras-related protein." J Biol Chem **269**(23): 16333-16339.

Yan, L., G. M. Findlay, et al. (2006). "Hyperactivation of mammalian target of rapamycin (mTOR) signaling by a gain-of-function mutant of the Rheb GTPase." J Biol Chem **281**(29): 19793-19797.

Yanow, S. K., F. Manseau, et al. (1998). "Biochemical pathways by which serotonin regulates translation in the nervous system of Aplysia." J Neurochem **70**(2): 572-583.

Yasuda, R. (2012). "Studying signal transduction in single dendritic spines." Cold Spring Harb Perspect Biol **4**(10).

Yates, J. W., J. T. Meij, et al. (2007). "Bimodal effect of amphetamine on motor behaviors in C57BL/6 mice." Neurosci Lett **427**(1): 66-70.

Yuan, J. P., W. Zeng, et al. (2009). "SOAR and the polybasic STIM1 domains gate and regulate Orai channels." Nat Cell Biol **11**(3): 337-343.

Zamponi, G. W. and K. P. Currie (2013). "Regulation of Ca(V)2 calcium channels by G protein coupled receptors." Biochim Biophys Acta **1828**(7): 1629-1643.

Zhang, Y., X. Gao, et al. (2003). "Rheb is a direct target of the tuberous sclerosis tumour suppressor proteins." Nat Cell Biol **5**(6): 578-581.

Zho, W. M., J. L. You, et al. (2002). "The group I metabotropic glutamate receptor agonist (S)-3,5-dihydroxyphenylglycine induces a novel form of depotentiation in the CA1 region of the hippocampus." J Neurosci **22**(20): 8838-8849.

Zoghbi, H. Y. and M. F. Bear (2012). "Synaptic dysfunction in neurodevelopmental disorders associated with autism and intellectual disabilities." Cold Spring Harb Perspect Biol **4**(3).

Zoncu, R., L. Bar-Peled, et al. (2011). "mTORC1 senses lysosomal amino acids through an inside-out mechanism that requires the vacuolar H(+)-ATPase." Science **334**(6056): 678-683.

Zou, J., L. Zhou, et al. (2011). "Rheb1 is required for mTORC1 and myelination in postnatal brain development." Dev Cell **20**(1): 97-108.

CURRICULUM VITAE

The Johns Hopkins University School of Medicine

Po Yu (Jeff) Chen 08/2013

Educational History:

Ph.D. 2013 Cellular Molecular Medicine

Johns Hopkins School of Medicine Paul Worley, MD

B.S 2004 Life Science (Chemistry)

Pennsylvania State University

Other Professional Experience:

Research Rotation 2007 Lab of Chi Dang, MD Ph.D

Johns Hopkins School of Medicine

Research Rotation 2007-08 Lab of Stephen Baylin, MD

Johns Hopkins School of Medicine

Visiting Scientist 2005-06 Stefan Jentsch, Ph.D

Max Planck Institute

Sr. Research Asst. 2004-07 Lab of Thomas Tuschl Ph.D.

Howard Hughes Medical Institute

Scholarships & Fundings:

Pollard Scholar 2009 Pollard Scholarship, CMM

Johns Hopkins School of Medicine

BSI Grant Support 800 26097

Peer-Reviewed Publications:

Zou J, Zhou L, Du XX, Ji Y, Xu J, Tian J, Jiang W, Zou Y, Yu S, Gan L, Luo M, Yang Q, Cui Y, Yang W, Xia X, Chen M, Zhao X, Shen Y, **Chen PY**, Worley PF, Xiao B. (2011) Rheb1 is Required for mTORC1 and Myelination in Postnatal Brain Development. Dev Cell. *20*. 97-108.

Landthaler M, Gaidatzis D, Rothballer A, **Chen PY**, Soll S, Dinic L, Ojo T, Hafner M, Zavolan M, Tuschl T. (2008) Molecular characterization of Human Argonaute-Containing Ribonucleoprotein Complex and their bound target mRNAs. RNA. *14*. 2580-96.

Chen PY, Weinmann L, Gaidatzis D, Pei Y, Zavolan M, Tuschl T, Meister G. (2008) Strand-specific 5'-O-methylation of siRNA duplexes controls guide strand selection and targeting specificity. RNA. *14*. 263-274.

Meister G, Landthaler M, Peters L, **Chen PY**, Urlaub H, Luhrmann R, Tuschl T. (2005) Identification of novel Argonaute-associated proteins. Current Biology. *23*. 2149-55.

Chen PY, Meister G. (2005) MicroRNA-guided posttranscriptional gene regulation. Biological Chemistry. *12*. 1205-18.

Chen PY, Manninga H, Slanchev K, Chien M, Russo JJ, Ju J, Sheridan R, John B, Marks DS, Gaidatzis D, Sander C, Zavolan M, Tuschl T. (2005). The developmental miRNA profiles of zebrafish as determined by small RNA cloning. Genes & Dev. *11*, 1288-93.

Leaman D, **Chen PY**, Fak J, Yalcin A, Pearce M, Unnerstall U, Marks DS, Sander S, Tuschl T, and Gaul U. (2005). Antisense-Mediated Depletion Reveals Essential and Specific Functions of microRNAs in *Drosophila* Development. Cell *7,* 1097-1108.

Posters, Presentations and National Meetings:

Rapamycin & mTOR signaling in the Modulation of Healthspan & Lifespan: Potential and Problems by the American Federation for Aging Research in New York 2010.

Presented "Directed Guide Strand Selection Using 5' Methoxy Modified siRNA Duplex" at the *Second Annual Meeting of the Oligonucleotide Therapeutics Society* in New York 2006.

RNAi at Cold Spring Harbor in New York 2005.

siRNA and miRNA at the Keystone Symposia in Colorado 2004.

Presented "Mass Spectrometric Screening for Polyphenolic Protein Adducts" at the *Preceedings of the 50th ASMS Conference on Mass Spectrometry and Allied Topics* in Pennsylvania 2002.

Services & Leaderships:

Research Supervisor 2008-12 3 Technicians 3 undergraduate researchers